REGULAR AND IRREGULAR MOTION

M. V. Berry
H. H. Wills Physics Laboratory
Tyndall Avenue
Bristol BS8 1TL, England

1. INTRODUCTION

The aim here is to describe some recent advances in the understanding of classical systems. As is often the case, these advances have been made with the aid of, and have led to, deep theorems in pure mathematics, couched in language unfamiliar to physicists. Concurrently, numerical experiments, extensively carried out by astronomers, have illuminated similar problems from a different point of view. Reviews bringing these approaches together are now appearing along with second-order reviews like this one. The bibliography is intended as a guide; further references may be found in the works cited and in other articles in this volume.

Over the last century attention has shifted from the computation of individual orbits towards the qualitative properties of families of orbits. For example, the question of whether a given orbit is stable can only be answered by studying the development of all orbits whose initial conditions are in some sense "close to" those of the orbit being studied. More generally, one can consider all orbits of a given system - defined by a given Hamiltonian - and inquire whether all, or "almost all" or "most" or "hardly any" are stable. More generally still, one can consider all possible Hamiltonian functions within some class, and seek the "generic" or typical behavior of its family of orbits. Finally, one can ask whether Hamiltonian systems display properties typical of the wider class of "dynamical systems" which may be dissipative and not describable by a Hamiltonian function (they do not).

One motivation for such studies is the feeling that after three hundred years we really ought to know what Newton's equations are telling us about the qualitative behavior of conservative systems with two degrees of freedom. And yet the orbits of a point mass m in the potential (fig. 1)

$$V = \frac{r^2}{2} + ar^3 \sin 3\theta$$

have only begun to be understood in detail in the last decade or so.

Another motivation is the desire to know whether the solar system, and the galaxy, are stable under the mutual perturbations of their constituents, or whether they will eventually collapse or disperse to infinity.

Another motivation is in the foundations of statistical mechanics. In that subject no attempt is made to follow the detailed motion of all the constituents of a complicated system of many inter-

ISSN: 0094-243X/78/016/$1.50

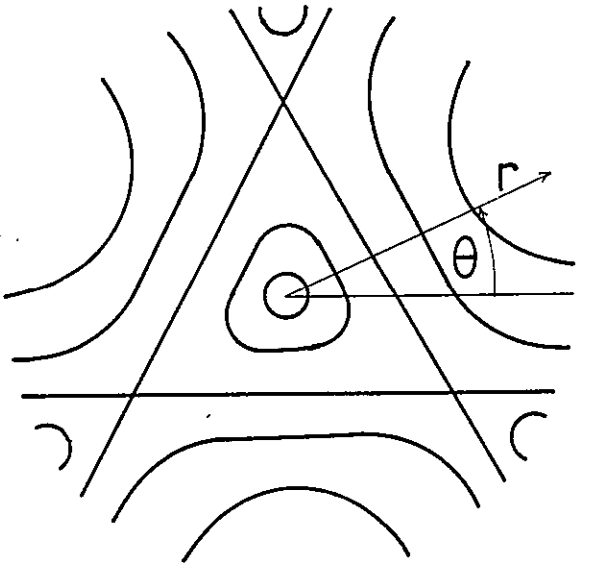

Fig. 1

acting bodies. Instead, we are content with a knowledge of the macroscopic observables, which are assumed to involve long-time averages over the motion of the bodies. Even these are too difficult to calculate, and a further assumption is made - the famous "ergodic hypothesis". This is that over the course of time the system explores the whole of the region of phase space that is energetically available to it (the "energy surface"), and eventually covers this region uniformly. Time averages can thus be replaced by averages over the energy surface in phase space, and statistical mechanics becomes a going concern.

But is the ergodic hypothesis true? No. In general it is false. It is not the case that all systems explore the whole of the available energy surface in phase space. In the standard "integrable" problems of the classical mechanics textbooks - the Kepler problem, n-dimensional harmonic oscillators, etc. - we shall see that systems explore infinitesimal fractions of the energy surfaces. Perhaps ergodic behavior appears the moment an "integrable" system is subjected to a "non-integrable" perturbation? Fermi believed this, but it too is false as we shall see. Then what systems are ergodic? This is still not known, although at last it has been shown that the system consisting of two or more interacting hard spheres is ergodic, so that statistical mechanics is valid in this case.

These results might seem somewhat meagre, justifying the theoretical physicists' traditional skepticism about the value of

"ergodic theory". But a by-product of the analysis has been the discovery of a vast realm of "stochastic" behavior between the extremes of the integrable and the ergodic and some understanding of how deterministic systems can exhibit motion which in some respects is as random as the tossing of a coin.

Yet another motivation is that some formulations of classical and quantum mechanics are so similar, any advance in classical mechanics ought to lead to advances in quantum mechanics. In particular, any transition of classical orbits from regular to random ought to be reflected in the form of the wave functions for quantum states, and in the distribution of quantum energy levels, especially in the semi-classical limit where these are densely distributed.

Proper discussion of these subjects involves topology, number theory, smooth mappings and other branches of pure mathematics. My treatment will be intuitive rather than rigorous.

2. INTEGRABLE SYSTEMS AND INVARIANT TORI*

We begin with integrable systems for which the solution of Newton's equations can be reduced to the solution of a set of simultaneous equations, followed by integrations over single variables. We restrict ourselves to (nondissipative) systems describable by a Hamiltonian function

$$H(\underline{q},\underline{p}) \ ,$$

where there are N degrees of freedom and, $\underline{q} = (q_1 \ldots q_i \ldots q_N)$ is the system's configuration and $\underline{p} = (p_1 \ldots p_N)$ is the canonical momentum vector conjugate to $\underline{q}$. Occasionally, we may allow H to have an explicit time dependence but almost always we shall treat conservative systems. The history $\underline{q}(t)$ of the system is found by solving Hamilton's equations

$$\dot{\underline{q}} = \nabla_{\underline{p}} H \qquad (2.1.a)$$

$$\dot{\underline{p}} = - \nabla_{\underline{q}} H \qquad (2.1.b)$$

with given initial conditions $\{\underline{q}(0), \underline{p}(0)\}$. Of course, the first Hamilton equation (a) can be used to obtain $\underline{p}$ when $\underline{q}$ and $\dot{\underline{q}}$ are known (eq. for a non-relativistic mass point $\underline{p}=m\dot{\underline{q}}$), so it is natural and useful to describe the system's motion in *phase space* $(\underline{q}, \underline{p})$ and from here on that is what we shall do.

A completely integrable system is one where there exist N independent analytic single-valued first integrals, that is N functions

$$F_m(\underline{q}, \underline{p}) \qquad 1 \leq m \leq N$$

---

* App. 26 of Ref. 2 and Ch. 2 of Ref. 4.

that are constant along each trajectory of the system. For a conservative system one of these can be taken as the energy - the Hamiltonian itself. For a particle acted on by central forces only, three integrals of motion are the components of angular momentum

$$\underline{L} = \underline{q} \wedge \underline{p} \,, \tag{2.2}$$

where $\underline{q}$ is measured from the centre of force.

Along any trajectory, the F_m's take constant values f_m, and the N equations

$$F_m(\underline{q}, \underline{p}) = f_m \,. \tag{2.3}$$

can be solved for $\underline{p}$ in terms of $\underline{q}$ and the f's. We can consider the F's to be the new momenta

$$\overline{\underline{p}} = \underline{F} \; (=\{F_m\})$$

in a canonical transformation to new variables $(\overline{\underline{q}}, \overline{\underline{p}})$ in phase space. Since we know the $\overline{\underline{p}}$'s to be constant, the new Hamilton equation (2.1.b) shows that the new Hamiltonian cannot depend on the new $\overline{q}$'s, so the first Hamiltonian equation gives

$$\dot{\underline{q}} = \nabla_{\underline{p}} (H(\overline{\underline{p}})) = \nabla_{\underline{f}} H(\underline{f}) = \text{const.} \tag{2.4}$$

or

$$\overline{\underline{q}}(t) = \nabla_{\underline{f}} H(\underline{f})t + \underbrace{\underline{\delta}}_{\text{constants}} \,. \tag{2.5}$$

The problem is solved if we can express $\overline{\underline{q}}$ in terms of the old coordinates $\underline{q}$. This is achieved by demanding that the transformation

$$(\underline{q}, \underline{p}) \rightarrow (\overline{\underline{q}}\, \overline{\underline{p}})$$

be canonical. This in turn can be accomplished with the generating function

$$S(\underline{q},\overline{\underline{p}}) = \int_{\underline{q}_0}^{\underline{q}} \underline{p}(\underline{q},\overline{\underline{p}})\cdot d\underline{q} = \int_{\underline{q}_0}^{\underline{q}} \underline{p}(\underline{q},\underline{f})\cdot d\underline{q} = S(\underline{q},\underline{f}) \,, \tag{2.6}$$

where $\underline{p}(\underline{q},\underline{f})$ is obtained from (2.3). Standard theory yields

$$\overline{\underline{q}} = \nabla_{\underline{f}} S(\underline{q},\underline{f}) \,, \tag{2.7}$$

thus the solution $\underline{q}(t;\underline{f},\underline{\delta})$ via (2.5) (the $\underline{f},\underline{\delta}$ are the 2n constants required to define a solution). All exactly-soluble systems in classical mechanics are integrable in this sense.

Of course, it is necessary for the constants of motion $F_m(\underline{q},\underline{p})$ to be independent and in addition the following condition must also hold:

$$\nabla_{\underline{p}} F_m \cdot \nabla_{\underline{q}} F_n - \nabla_{\underline{p}} F_n \nabla_{\underline{q}} F_m$$

$$\equiv \text{Poisson bracket } \{F_m, F_n\} = 0 \text{ for all m, n} \tag{2.8}$$

The F's are then said to be "in involution".

The existence of the N F_m's implies that each trajectory of the system can explore at most an N-dimensional manifold M in the 2N-dimensional phase space. Except for the trivial case of N=1, this is smaller than the energy surface E, which has 2N-1 dimensions. Therefore the ergodic hypothesis is false in general. A table might help here:

Number of degrees of freedom:	1	2	3	N
Dimensionality of phase space	2	4	6	2N
" E	1	3	5	2N-1
" M	1	2	3	N

It will be important to know what sort of manifold M is, and we show now that M is an N-*dimensional torus*: construct the following N vector fields V_m in *phase space*:

$$V_m \equiv (\nabla_{\underline{p}} F_m \ , \ -\nabla_{\underline{q}} F_m) \ , \tag{2.9}$$

i.e. the V_m's have 2N components.

On each M, defined by fixing the f_m's in (2.3), the V_m's are smooth and independent (because the F_m's are), and moreover the V's are *parallel* to M, since by virtue of (2.8) each V_m is perpendicular to all normals to M:

$$V_m \cdot (\nabla_{\underline{q}} F_n \ , \ \nabla_{\underline{p}} F_m) \tag{2.10}$$

$$= \{F_m, F_n\} = 0 \text{ for all m,n.}$$

We restrict ourselves to "bound" motion in which the region of accessible phase space is finite. Then M is a compact manifold. Now we make use of a theorem in topology which states that a compact

manifold "parallelizable" with N smooth independent vector fields must be an N-torus. This is intuitively obvious from Fig. 2. Q.E.D.

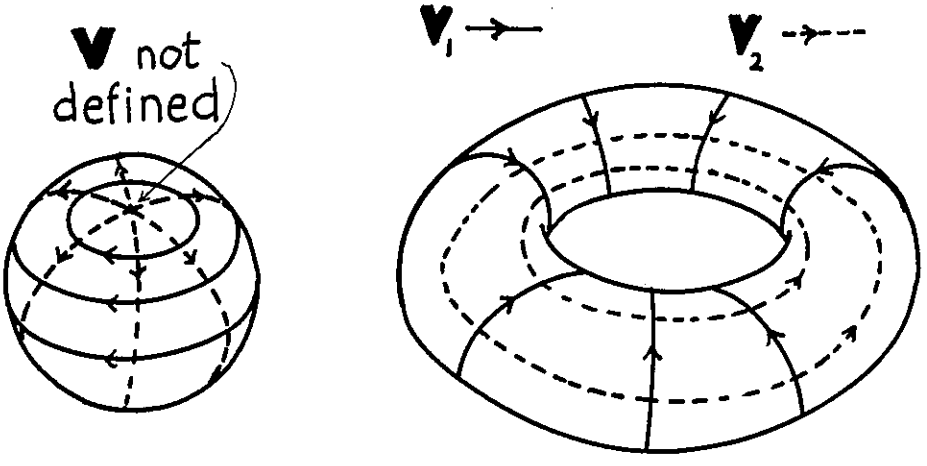

Fig. 2

(Colloquially, if M were hairy, we could comb it without singularity in N ways.)

These tori are called *invariant tori* because an orbit starting out on one remains on one forever. It is natural to coordinatize phase space using the $(\underline{q},\underline{p})$ defined earlier, since then $\underline{p} = \underline{f}$ defines which torus we are on and $\underline{q}$ are coordinates on the torus. But there are many ways of doing this, corresponding to taking not the original F_m's but any functions of them (which are still constants of motion). However, there is one standard way, that leads to the introduction of so-called *action-angle variables*. These are topologically natural, and widely employed in analytical mechanics. The variables have the following symbols:

$$\begin{aligned} \underline{\theta} &= \underline{q} = \textit{angles on torus} \\ \underline{I} &= \underline{p} = \textit{actions of torus} \end{aligned} \tag{2.11}$$

The definition is based on the observation that the generating function in (2.6), $S(\underline{q},\underline{P})$, is generally multivalued because the momenta $\underline{p}$ defined by (2.3) can be multivalued - when a system returns to a given point $\underline{q}$ it need not have the same momentum $\underline{p}$. Therefore S depends on the path $\underline{q}_0 \to \underline{q}$. But the path must certainly

lie on M since otherwise (cf. 2.3) $\underline{p}(\underline{q},\underline{f})$ is not defined. Now for different paths $\underline{q}_0 \to \underline{q}$ on M that are deformable into one another S is certainly the same, because it is the solution of a Hamilton-Jacobi equation

$$H(\underline{q},\nabla_{\underline{q}} S(\underline{q},\underline{f})) = H(\underline{f}) \ . \tag{2.12}$$

This means roughly speaking, that S is locally single-valued. It follows that for closed circuits $q_0 \to q_0$ on M that can be shrunk to zero, $S=0$. But on an N-torus there are N independent irreducible circuits γ_i that cannot be shrunk to zero, and this defines N increments ΔS that S can gain on returning to the same point $\underline{q}$. The action variables are defined by

$$I_i \equiv \frac{1}{2\pi} \int_{\gamma_i} \underline{p}\cdot d\underline{q} = \frac{1}{2\pi} \times \text{sum of areas of N projections}$$

$$\text{of } \gamma_i \text{ on planes } q_1p_1, q_2p_2, \ldots q_Np_N \tag{2.13}$$

$$= \frac{\Delta S}{2\pi} \text{ for ith circuit on } M$$

This defines the N I's in terms of the N f's and vice versa. For a conservative system the energy H is one of the f's and hence can be expressed as a function of the I's:

$$H = H(\underline{I}) \ . \tag{2.14}$$

The I's define the torus M. The coordinates *on* M are the "angles" $\underline{\Theta}$ canonically conjugate to $\underset{\sim}{I}$:

$$\underline{\Theta} \equiv \nabla_{\underline{I}} \, S(\underline{q},\underline{I}). \tag{2.15}$$

The reason for calling them angles is that Θ_i changes by 2π, and $\Theta_{i\neq j}$ do not change as we traverse circuit γ_i on M:

$$(\Delta\Theta_i)_{\gamma_i} = \Delta_{\gamma_i} \frac{\partial S}{\partial I_i}(q,I)$$

$$= \frac{\partial}{\partial I_i} \Delta_{\gamma_i} S \tag{2.16}$$

$$= \frac{\partial}{\partial I_i} 2\pi I_j = 2\pi\delta_{i,j}$$

This means that in the canonical transformation

$$\begin{Bmatrix} \underline{q} \\ \underline{p} \end{Bmatrix} \rightarrow \begin{Bmatrix} \underline{\Theta} \\ \underline{I} \end{Bmatrix} , \tag{2.17}$$

the $\underline{q}$'s and $\underline{p}$'s are *periodic* functions of $\underline{\Theta}$ with period 2π:

$$\underline{q} = \sum_{\underline{m}} \underline{q}_{\underline{m}}(\underline{I}) e^{i\underline{m}\cdot\underline{\Theta}} , \quad \underline{p} = \sum_{\underline{m}} \underline{p}_{\underline{m}}(\underline{I}) e^{i\underline{m}\cdot\underline{\Theta}} \tag{2.18}$$

where $\underline{m}$ is a N-dimensional lattice vector (i.e. integer components). Soon we shall see what a pleasant picture of the motion this gives. Meanwhile, we illustrate the formalism with a few *examples*:

Swing (fig. 3)

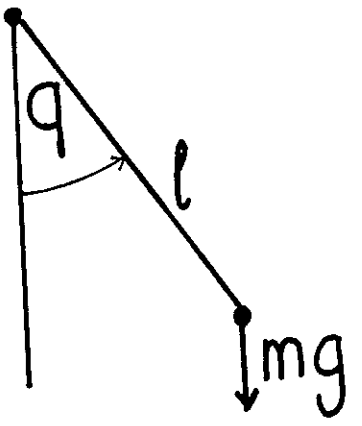

Fig. 3

The motion is one-dimensional:

$$\text{Lagrangian} \quad L = \underbrace{\frac{1}{2} m(\ell\dot{q})^2}_{KE} - \underbrace{mg\ell(-\cos q)}_{PE} , \tag{2.19}$$

$$p = \frac{\partial L}{\partial \dot{q}} = m\ell^2\dot{q} \ ;$$

$$\text{Hamiltonian} \quad H = p\dot{q} - L = \frac{p^2}{2m\ell^2} + mg\ell(-\cos q) , \tag{2.20}$$

which yields the equations of motion -

$$\dot{q} = \frac{p}{m\ell^2} \, , \quad \dot{p} = -mg\ell \sin q \, , \tag{2.21}$$

or

$$\ddot{q} = -\frac{g}{\ell} \sin q \, , \tag{2.22}$$

as is well known. There is one constant of motion, H itself (≡f). Therefore, the manifold M is

$$\frac{p^2}{2m\ell^2} - mg\ell \cos q = f \, ,$$

$$\text{i.e.} \quad p(q,f) = \sqrt{2m\ell^2(f+mg\ell \cos q)} \, . \tag{2.23}$$

All these curves M (1-dimensional) in phase space are closed because $q+2\pi \leftrightarrow q$ so that phase space is really cylindrical (fig. 4).

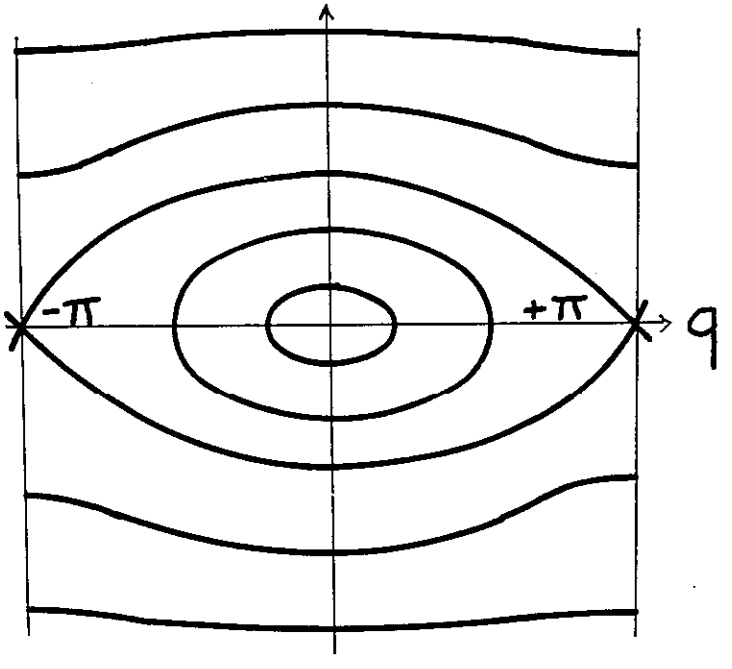

Fig. 4

The closed curves are the tori. These are of two kinds:

"librations" between fixed limits of q, for f < mgℓ (fig. 5)

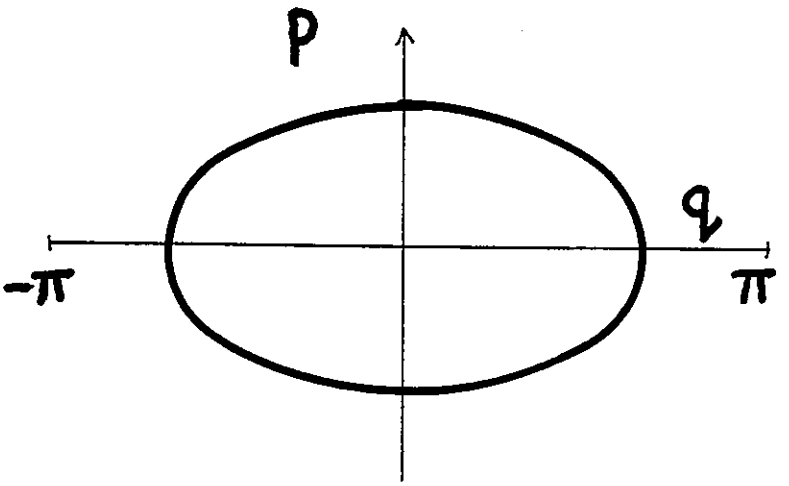

Fig. 5

and "rotations" with q increasing or decreasing forever for f > mgℓ (fig. 6)

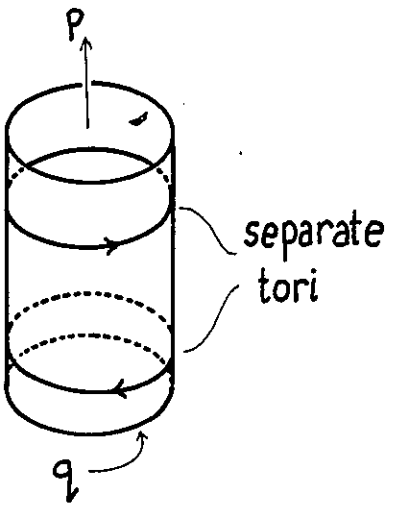

Fig. 6

These are separated by a self crossing curve (fig. 7) corresponding to $f = mg\ell$.

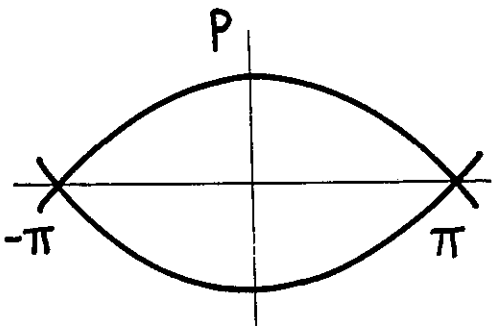

Fig. 7

The action is

$$I \equiv \frac{1}{2\pi} \oint \underline{p} \cdot d\underline{q} = \frac{Re}{\pi} \int_0 \sqrt{2m\ell^2 (f + mg\ell \cos q)} \quad , \qquad (2.24)$$

which implicitly defines the "action" Hamiltonian (fig. 8).

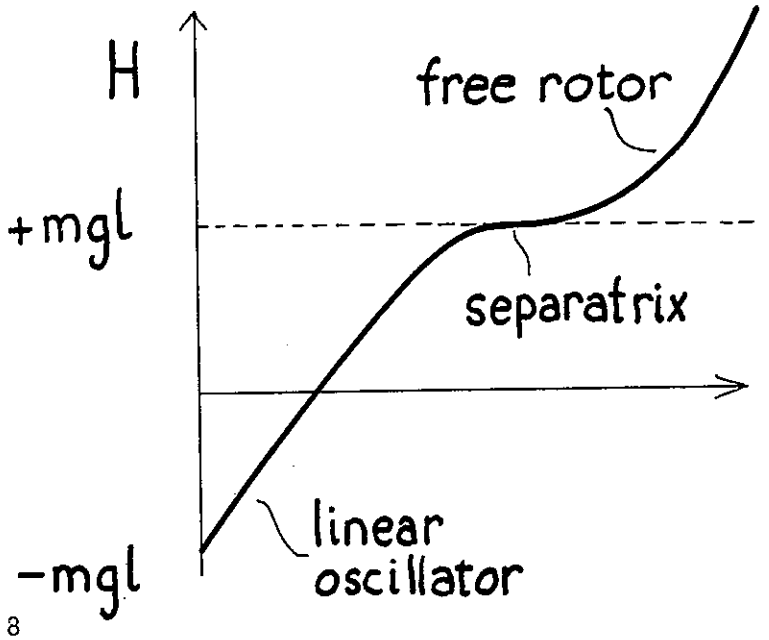

Fig. 8

2-D HARMONIC OSCILLATOR

Here,

$$H(\underline{q},\underline{p}) = \frac{p_1^2}{2} + \frac{p_2^2}{2} + \frac{\omega_1^2 q_1^2}{2} + \frac{\omega_2^2 q_2^2}{2} \quad . \tag{2.25}$$

The two constants of motion are (energy in each mode)

$$F_1 = \frac{p_1^2}{2} + \frac{\omega_1^2 q_1^2}{2} \quad , \quad F_2 = \frac{p_2^2}{2} + \frac{\omega_2^2 q_2^2}{2} \quad . \tag{2.26}$$

The q_1 and q_2 motions are uncoupled, hence these give the irreducible circuits γ_1 and γ_2, and (fig. 9):

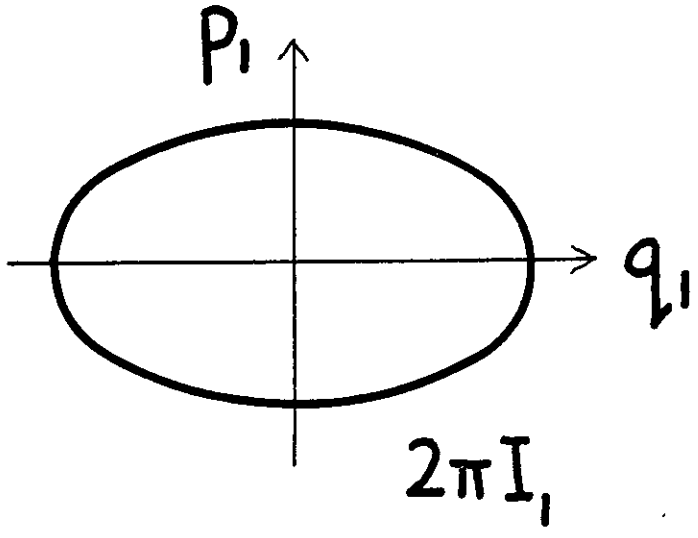

Fig. 9

$$I_1 = \frac{1}{2\pi} \int_{\gamma_1} p_1 dq_1 = \frac{1}{2\pi} \oint \sqrt{2(F_1 - \tfrac{1}{2}\omega_1^2 q_1^2)}\, dq_1$$

$$= \frac{1}{2\pi} \times \text{area of ellipse}$$

$$= \frac{1}{2} \sqrt{2F} \sqrt{\frac{2F}{\omega_1^2}} = \frac{F_1}{\omega_1} \quad , \quad I_2 = \frac{F_2}{\omega_2} \quad . \tag{2.27}$$

Therefore, the Hamiltonian in action variables is

$$H(\underline{I}) = F_1 + F_2 = I_1\omega_1 + I_2\omega_2 \qquad (2.28)$$

and I_1 and I_2 are related as in Fig. 10.

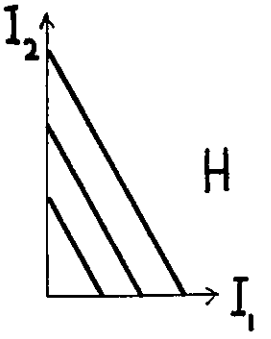

Fig. 10

PLANE MOTION UNDER CENTRAL FORCE

The Hamiltonian is

$$H = \frac{p_r^2}{2m} + \frac{p_\Theta^2}{2mr^2} + V(r) \ , \qquad (2.29)$$

for the geometry of Fig. 11 and the potential of Fig. 12.

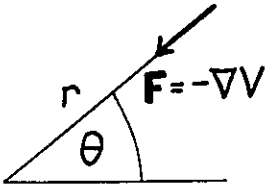

Fig. 11

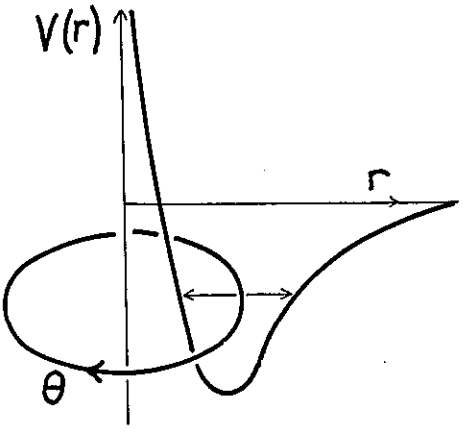

Fig. 12

Constants of motion:

$$F_1 = H, \; F_2 = p_\theta (= mr^2\dot{\theta}) \; . \tag{2.30}$$

Irreducible circuits are libration in r and rotation in θ.

$$I_2 = \frac{1}{2\pi\gamma_2} \int p_\theta \, d\theta = \frac{F_2}{2\pi} \int_0^{2\pi} d\theta = F_2 \; , \tag{2.31}$$

$$\begin{aligned} I_1 &= \frac{1}{2\pi} \oint p_r \, dr \\ &= \frac{Re}{\pi} \int_0^{\infty} [2m(F_1 - \frac{I_2^2}{2mr^2} - V(r))]^{1/2} \, dr \; , \end{aligned} \tag{2.32}$$

which defines the Hamiltonian (fig. 13) as

$$H(I_1, I_2) = F_1(I_1, I_2) \; . \tag{2.33}$$

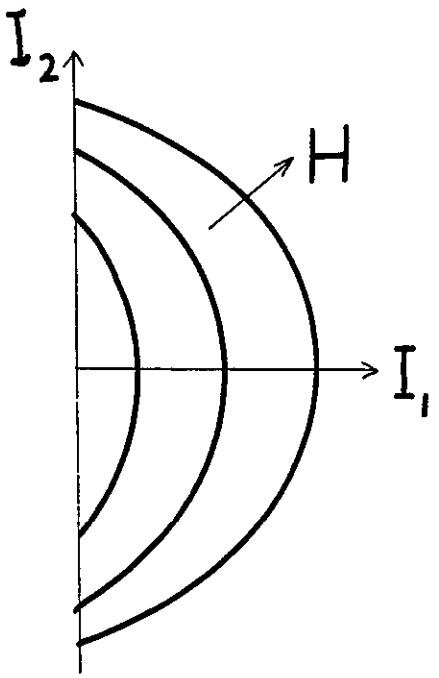

Fig. 13

In terms of general action-angle theory, the Hamiltonian (2.14) yields the equations of motion

$$\underline{I} = \text{const.}, \ \dot{\underline{\Theta}} = \nabla_{\underline{I}} H(I) = \text{const.} \ , \tag{2.34}$$

or

$$\underline{\Theta}(t) = \underline{\omega}(\underline{I})t + \underline{\delta} \ , \tag{2.35}$$

where $\underline{\delta}$ represents N constants and

$$\underline{\omega}(\underline{I}) \equiv \nabla_{\underline{I}} H(\underline{I}) \text{ (the frequency vector on the torus } \underline{I}) \ . \tag{2.36}$$

Thus (2.18) gives the motion as

$$\begin{aligned} \underline{q}(t) &= \sum_{\underline{m}} \underline{q}_{\underline{m}}(\underline{I}) e^{i(\underline{m}\cdot\underline{\omega}t + \underline{m}\cdot\underline{\delta})} \\ \underline{p}(t) &= \sum_{\underline{m}} \underline{p}_{\underline{m}}(\underline{I}) e^{i(\underline{m}\cdot\underline{\omega}t + \underline{m}\cdot\underline{\delta})} \end{aligned} \tag{2.37}$$

This shows that the system's orbit on M is *multiply periodic* with the N periods

$$T_i = \frac{2\pi}{\omega_i} \ . \tag{2.38}$$

for a circuit round Θ_i.

If the orbit on M is *closed*, i.e. if for some τ

$$\underline{\Theta}(\tau) = \underline{\Theta}(0) + 2\pi N \ , \tag{2.39}$$

then it does not fill M but only occupies a one-dimensional region on M (fig. 14).

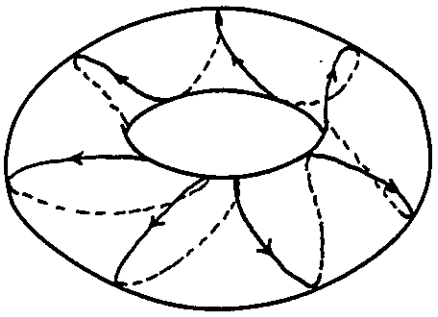

Fig. 14

If the orbit *never closes*, it traverses a helix on M which covers it densely after infinite time (fig. 15). This is "ergodicity on M" though not on the energy surface, and not of any stochastic character.

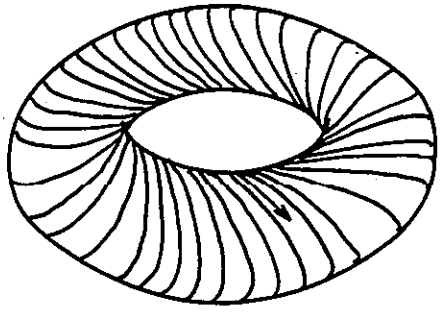

Fig. 15

Now which of these situations is typical? To get closure, the frequencies $\underline{\omega}$ must be commensurable; this condition can be written in either of the following ways:

$$\left.\begin{array}{l} \underline{\omega} = \underline{N}\,\omega_b \quad (\underline{N} \text{ is a vector with integer components}) \\ \text{or } N\text{-}1 \text{ relations } \underline{\omega}\cdot\underline{m} = 0 \text{ hold } (\underline{m} \text{ a finite non-zero vector} \\ \text{with integer components}). \end{array}\right\} \quad (2.40)$$

In general, closure occurs after N_1 circuits of Θ_1, N_2 circuits of $\Theta_2 \ldots N_N$ circuits of Θ_N, with period

$$\tau = \frac{2\pi}{\omega_b} = \frac{2\pi N_i}{\omega_i} = \frac{N_i}{T_i} \,. \quad (2.41)$$

From number theory (as we shall see later) commensurability is the exception rather than the rule and (2.40) holds only for a set of $\underline{\omega}$'s, i.e. tori $\underline{I}$, of zero measure. (If s relations $\underline{\omega}\cdot\underline{m} = 0$ hold, where $s<N-1$, the orbit is not closed but inhabits a submanifold of dimensionality $N-s$ on M. The exceptional tori form a (dense) set of measure zero on which the tori are closed or partially closed.)

3. CANONICAL PERTURBATION THEORY FOR NONINTEGRABLE SYSTEMS*

Is integrability the rule or the exception? If all systems were integrable, the constants of motion $F_m(\underline{q},\underline{p})$ would always exist, and our inability to determine them for all but the simplest

*Some of this material is covered in: Ch. 9 of Ref. 5, Ch. 4 of Ref. 4, Ch. 1 of Ref. 1, Sec. 2-3d of Ref. 17, and Ref. 9.

problems would merely reflect our lack of analytical ingenuity. But it might be that integrable Hamiltonians form a very small set (possibly of zero measure), and the slightest perturbation of such a Hamiltonian would render the F_m non-existent (except the energy for conservative cases) and destroy the tori M so that each system trajectory would in the course of time fill a region in phase space of dimensionality greater than M (of course if the perturbation were small, the system, if started on or near an unperturbed torus M, would stay near M for a very long time).

Astronomers realized long ago that it is possible to devise a formal perturbation theory for modified tori M starting from an "unperturbed" torus M_0. This theory is of practical usefulness in celestial mechanics for calculating the orbits of heavenly bodies over *long but finite periods of time*. In the case of a planetary orbit, for example, the unperturbed system consists of the two-body problem of that planet moving in the Sun's field. This is the easily integrable Kepler problem. The perturbations come from the attractions of the other planets, principally Jupiter. If we "switch on" the mass M_J of Jupiter, and ignore the effect on Jupiter's orbit of the planet (say the earth ⊕) being considered (i.e. regard ⊕ as a "test body"), then we have the simplest case of the "plane restricted three body problem", with M_J as the perturbation away from integrability. We shall study this in more detail later.

But these methods only ensure the existence of tori M if the perturbation series converge *for infinite time*, and we shall see that the convergence is a very delicate matter indeed. Most physicists, when they thought about the matter, have tended to feel, with Fermi, that the slightest perturbation of an integrable system would destroy the tori - i.e. the series for M would diverge. Confirmation of this opinion would go a long way towards validating the ergodic hypothesis and hence statistical mechanics. Landau, however, thought that all systems are in principle integrable - i.e. phase space is filled with tori M. In fact, what happens is that "most" tori persist under perturbation, albeit in distorted form. Some are destroyed, however, and these form not a "set of measure zero" but a finite set which grows with the perturbation. The destroyed tori are distributed among those which are preserved, in a pathological manner. These assertions were rigorously proved by Moser and Arnol'd in 1962, on the basis of suggestions by Kolmogorov in 1954. They form what has become known as the "KAM theorem" which is one of the few certain statements in this subject. The proof is long, intricate and subtle, but the ideas on which it is based are most instructive and we shall concentrate on them.

Suppose that we have an integrable system. Then its phase space can be coordinatized by action-angle variables $\underline{I}$, $\underline{\Theta}$ and the Hamiltonian is a function $H_0(\underline{I})$ of $\underline{I}$ only. We illustrate this with another example to recall the theory: a particle in a two-dimensional box with sides a, b (fig. 16).

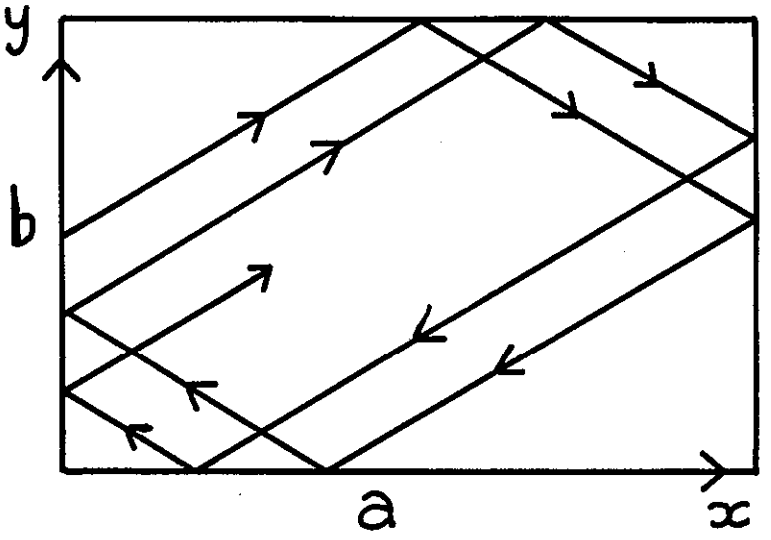

Fig. 16

The constants of motion are the x and y *speeds* $|v_x|$, $|v_y|$ which are unaffected by collisions. The actions are

$$I_1 = \frac{1}{2\pi}\oint p_x dx = \frac{1}{2\pi} \times m\,|v_x| \times 2a\ ,$$

$$|v_x| = (\pi/ma)I_1,\ |v_y| = (\pi/mb)I_2\ ,$$

and

$$H_0 = \frac{m}{2}\left(|v_x|^2 + |v_y|^2\right) = \frac{\pi^2}{2m}\left(\frac{I_1^2}{a^2} + \frac{I_2^2}{b^2}\right). \qquad (3.1)$$

The frequencies $\underline{\omega}$ are

$$\omega_1 = \frac{\partial H}{\partial I_1} = (\pi^2/ma^2)I_1,\ \omega_2 = (\pi^2/mb^2)I_2\ . \qquad (3.2)$$

The coordinates are given in terms of $\underline{\Theta}$ by

$$\begin{pmatrix}\underline{q}\\ \underline{p}\end{pmatrix} = \sum_{\underline{m}} \begin{pmatrix}\underline{q}_{\underline{m}}(\underline{I})\\ \underline{p}_{\underline{m}}(\underline{I})\end{pmatrix} e^{i\underline{m}\cdot\underline{\Theta}}\ , \qquad (3.3)$$

where q_m and p_m follow readily from a Fourier analysis of the motion, which in this case is as shown in Fig. 17.

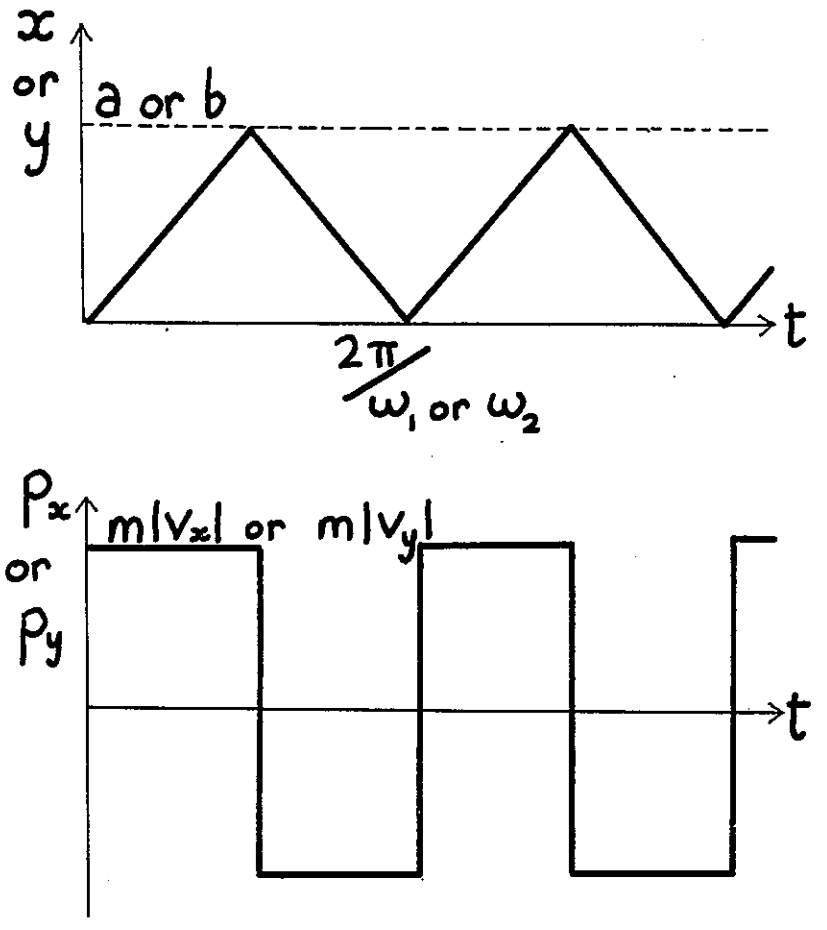

Fig. 17

Perturb the system H_0 with a nonintegrable perturbation $\varepsilon H_1(\underline{I},\underline{\Theta})$. For example, we could give the box a curved floor by making H_1 an extra force

$$H_1 = x^2y^2 = (\sum_{\underline{m}} x_{\underline{m}}(\underline{I})e^{i\underline{m}\cdot\underline{\Theta}})^2 \quad (\sum_{\underline{m}} y_{\underline{m}}(\underline{I})e^{i\underline{m}\cdot\underline{\Theta}})^2 . \tag{3.4}$$

In the new system,

$$H(\underline{I},\underline{\Theta}) = H_0(\underline{I}) + \varepsilon H_1(\underline{I},\underline{\Theta}) , \tag{3.5}$$

$\underline{I}$ and $\underline{\Theta}$ are perfectly good canonical coordinates but they are no longer action-angle variables because $\underline{\Theta}$ appears in H, so the $\underline{I}$ are not constants of the motion.

If tori exist in this system, there must be new action-angle variables $\underline{I}'$, $\underline{\Theta}'$ such that

$$H(\underline{I},\underline{\Theta}) = H'(\underline{I}') , \tag{3.6}$$

and the new variables must be related to the old by a canonical transformation generated by a function $S(\underline{\Theta},\underline{I}')$,

i.e.

$$\begin{pmatrix}\underline{I}\\ \underline{\Theta}\end{pmatrix} \quad \leftarrow \begin{pmatrix}\underline{I} = \nabla_{\underline{\Theta}}S\\ \nabla_{\underline{I}'}S = \underline{\Theta}'\end{pmatrix} \rightarrow \quad \begin{pmatrix}\underline{I}'\\ \underline{\Theta}'\end{pmatrix} . \tag{3.7}$$

Substitution in (3.6) for $\underline{I}$ gives

$$H(\nabla_{\underline{\Theta}}S(\underline{\Theta},\underline{I}'), \underline{\Theta}) = H'(\underline{I}') \tag{3.8}$$

as the condition S must satisfy. Thus the question of the continuing existence of tori reduces to the question of whether (3.8) can be solved.

It is natural to seek a solution S in powers of the perturbation parameter ε, and the "zeroth-order" term must be $\underline{\Theta}\cdot\underline{I}'$. This generates the identity ($\underline{\Theta}' = \underline{\Theta}$; $\underline{I}' = I$). Thus we write

$$S = \underline{\Theta}\cdot\underline{I}' + \varepsilon S_1(\underline{\Theta},\underline{I}') + \ldots . \tag{3.9}$$

We must substitute this into (3.8), where H is given by (3.5):

$$H_0(\underline{I}' + \varepsilon\nabla_{\Theta}S_1 + \ldots) + \varepsilon H_1(\underline{I}' + \ldots, \underline{\Theta}) = H'(E') , \tag{3.10}$$

or (to first order in ε)

$$H_0(\underline{I}') + \varepsilon(\nabla_{I'} H_0(\underline{I}')\cdot\nabla_{\underline{\Theta}} S_1 + H_1(\underline{I}',\underline{\Theta})) = H'(\underline{I}') \ . \quad (3.11)$$

Now we note that

$$\nabla_{I'} H_0(\underline{I}') = \underline{\omega}_0(\underline{I}') = \text{frequency vector of unperturbed motions,} \quad (3.12)$$

and

$$H_1(\underline{I},\underline{\Theta}) = \sum_{\underline{m}} H_{1\underline{m}}(\underline{I}) e^{i\underline{m}\cdot\underline{\Theta}} \ , \quad (3.13)$$

since H_1 is a function of $\underline{p}$ and $\underline{q}$ and these are periodic in $\underline{\Theta}$, and also S_1 is periodic in $\underline{\theta}$ with an arbitrary constant term that we set equal to zero. Hence,

$$S_1(\underline{\Theta},\underline{I}') = \sum_{\underline{m}\neq 0} S_{1\underline{m}}(\underline{I}') e^{i\underline{m}\cdot\underline{\Theta}} \ . \quad (3.14)$$

Thus, we equate Fourier coefficients and obtain

$$(\underline{m}=0) \qquad H'(\underline{I}') = H_0(\underline{I}') + \varepsilon H_{1\underline{0}}(I') + \ldots \text{ (the new H)} \quad (3.15)$$

$$(\underline{m}\neq 0) \qquad S_{1\underline{m}}(\underline{I}') = + \frac{iH_{1\underline{m}}(\underline{I}')}{\underline{m}\cdot\underline{\omega}_0(\underline{I}')} + \ldots \ . \quad (3.16)$$

The generator of the new tori is therefore

$$S(\underline{\Theta},\underline{I}') = \underline{\Theta}\cdot\underline{I}' + \varepsilon i \sum_{\underline{m}\neq 0} \frac{H_{1\underline{m}}(\underline{I}')}{\underline{m}\cdot\underline{\omega}_0(\underline{I}')} e^{i\underline{m}\cdot\underline{\Theta}} + \ldots \ . \quad (3.17)$$

It looks as if we are in business - just continue this process to infinite order in ε, and we are left with S and hence the tori. But this is hopelessly naive! The flies in the ointment are the quantities $\underline{m}\cdot\underline{\omega}_0$. If the frequencies $\underline{\omega}_0$ of motion on the unperturbed torus are commensurable - i.e. if the orbits are *closed* and the fundamental frequencies are in *resonance* - then there are always terms $\underline{m}$ for which (cf 2.40)

$$\underline{\omega}_0\cdot\underline{m} = 0 \ . \quad (3.18)$$

For these $\underline{m}$, the terms in (3.17) are infinite and the series diverges. Worse still, even for incommensurable $\underline{\omega}_0$ it is always possible to find $\underline{m}$'s for which $\underline{\omega}_0 \cdot \underline{m}$ is as small as we like (fig. 18). For ever larger $\underline{m}$'s in the sums in the series (3.17), we must occasionally encounter even smaller $\underline{m} \cdot \underline{\omega}_0$ terms. This makes us doubt whether (3.17) *ever* converges. There are really two doubts: the convergence of the sums $\sum_{\underline{m}}$ and of the series in powers of ε. This is the notorious "problem of small divisors" that plagued celestial mechanics. It does not arise for systems with one degree of freedom.

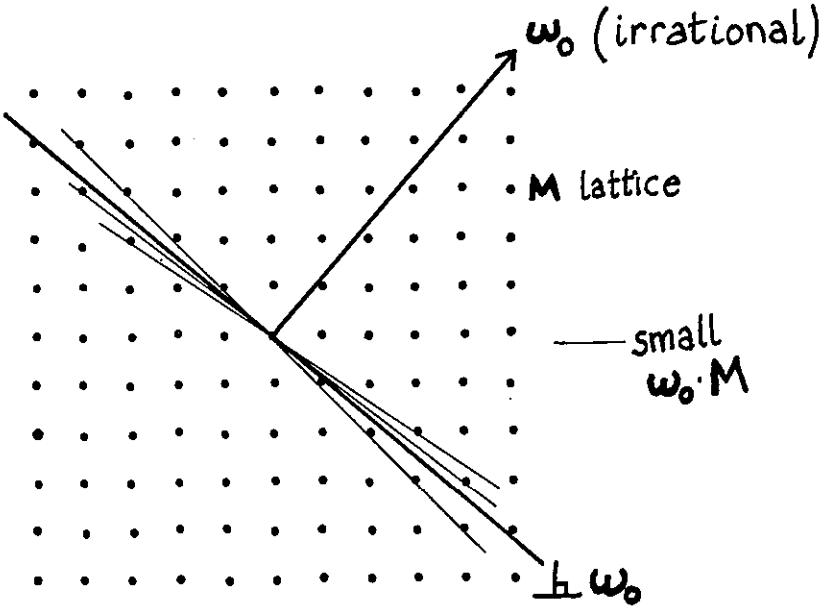

Fig. 18

In astronomical practice the unperturbed motions of interest often lie on tori that are not close to low-order commensurable ones (although there are also astonishing commensurabilities as we shall see later). - i.e. $\underline{\omega}_0 \cdot \underline{m}$ is only small for very large $\underline{m}$ (this means that when considering the Earth's motion, say, we use the fact that its frequency is 11.86 times that of its principal perturber, Jupiter). For these large $\underline{m}$ the Fourier coefficients $H_{l\underline{m}}$ of the perturbation are very small, so that if we cut off the sums before these $\underline{m}$'s are reached, and work to only a few terms in ε, the motion can in practice be predicted for a long time. But the success of these predictions in no way bears on the question of whether tori exist, since this concerns motion over *infinite* times. (For the molecular motions of interest in statistical mechanics, one second corresponds to 10^{13} collisions ("cycles") which for a planetary system would take 1000 times the age of the universe.)

Although perturbation series like (3.17) are familiar to most physicists they are a very crude tool for studying the delicate problems arising from the small denominators. The central feature of KAM's technique is the replacement of (3.17) by a series of successive approximations to the suspected new torus that has a vastly improved convergence. We shall not delve deeply into these technicalities, but only illustrate them with the following example:

Finding the zero of a function

Suppose we want the position x of the zero of a function f(x) (fig. 19).

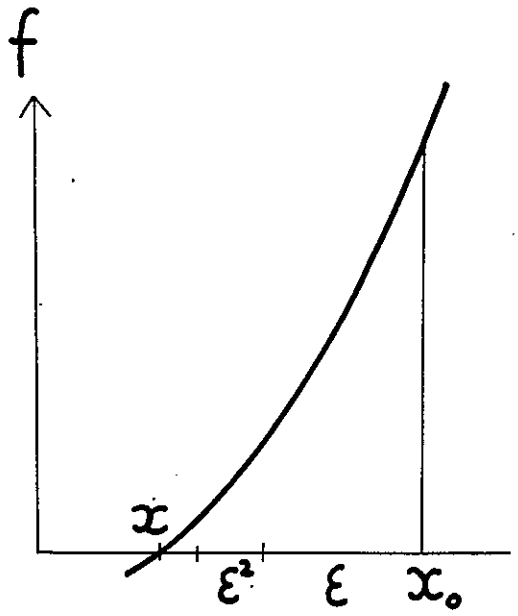

Fig. 19

We start with a guess: the zero is at x_0 - the "unperturbed" value- and proceed to refine the guess. First we use perturbation theory, analogous to (3.17). Write

$$f(x) = 0, \text{ i.e. } f(x_0 + (x-x_0)) = \sum_{n=0}^{\infty} f_n \frac{(x-x_0)^n}{n!} = 0, \quad (3.19)$$

where f_n is the n-th derivative of f at x_0. Rearranging, we get

$$(x-x_0) + \frac{(x-x_0)^2}{2}\frac{f_2}{f_1} + \frac{(x-x_0)^3}{6} + \ldots = \frac{-f_0}{f_1} \equiv \varepsilon \ . \quad (3.20)$$

By standard "reversion of series" we can get the deviation $x-x_0$ from the zero in terms of the "perturbation" ε:

$$x-x_0 = \varepsilon + \varepsilon^2 \left(\frac{-f_2}{2f_1}\right) + \varepsilon^3 \left(2\left(\frac{f_2}{2f_1}\right)^2 - \frac{f_3}{6f_1}\right) + \ldots \ . \quad (3.21)$$

This is the analogue of (3.17) for the mechanical problem.

It is also a pretty silly way to find a zero. Much better is *Newton's method* based on iteration (fig. 20).

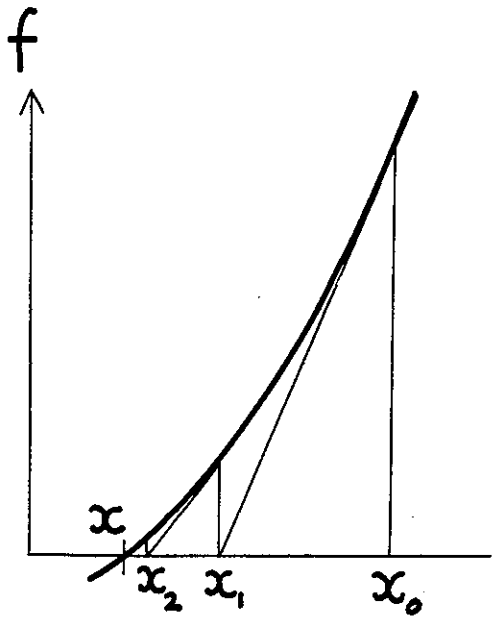

Fig. 20

Starting at x_0, we obtain the next approximation x_1 from

$$f(x) = f(x_0+x-x_0) \sim f(x_0)+(x_1-x_0)f'(x_0) = 0 \tag{3.22}$$

i.e.

$$\varepsilon_1 \equiv (x_1-x_0) = \frac{-f(x_0)}{f'(x_0)} = \varepsilon \text{ of (3.20)},$$

and the next as

$$\begin{aligned} \varepsilon_2 &\equiv (x_2-x_1) = \frac{-f(x_1)}{f'(x_1)} \ , \\ &\vdots \\ \varepsilon_n &\equiv x_n-x_{n-1} = -\frac{f(x_{n-1})}{f'(x_{n-1})} \ . \end{aligned} \tag{3.23}$$

etc.

How quickly does this converge? We can estimate ε_{n+1} in terms of ε_n by

$$\varepsilon_{n+1} = \frac{-f(x_n)}{f'(x_n)} \simeq \frac{-[f(x_{n-1})+\varepsilon_n f'(x_{n-1})+\frac{1}{2}\varepsilon_n^2 f''(x_{n-1})]}{f'(x_{n-1})+\varepsilon_n f''(x_{n-1})} \tag{3.24}$$

$$\simeq -\frac{1}{2}\varepsilon_n^2\left[\frac{f''(x_{n-1})}{f'(x_{n-1})}\right] = O(\varepsilon_n^2) \ .$$

$$\therefore \quad \varepsilon_1 = \varepsilon, \ \varepsilon_2 = O(\varepsilon^2), \varepsilon_3 = O(\varepsilon^4), \varepsilon_4 = O(\varepsilon^8), \ldots \ \varepsilon_n = O(\varepsilon^{2^{n-1}}) \ , \tag{3.25}$$

so that instead of (3.21) we have

$$x-x_0 = \sum_1^\infty \varepsilon_n = \varepsilon + O(\varepsilon^2) + O(\varepsilon^4) + O(\varepsilon^8) + O(\varepsilon^{16}) + \ldots \tag{3.26}$$

whose astonishing convergence beats almost any pathology of the approximated function f.

It is amusing to show this by numerical example. Let

$$f(x) = \tan x - 1, \quad \text{so } x = \frac{\pi}{4} = .785398164 \ . \tag{3.27}$$

We take $x_0 = 1$. Then the two methods give

	Perturbation			Newton		
n	x_n	$x_n - x_\infty$	ε^{n+1}	x_n	$x_n - x_\infty$	ε^{n^2}
0	1	.214602	.214602	1	.214602	.214602
1	.837277868	.051880	.0461	.837277868	.051880	.0461
2	.796040059	.010642	.0099	.788180293	.002782	.0021
3	.787025592	.001627	.0021	.785405918	.000008	.000004
∞	.785398164	0	0	.785398164	0	0

The reason for this astonishing "quadratic convergence" is that at each stage f is evaluated at the current approximation x_n rather than at the zero-order approximation x_0 as in the perturbation series (3.21).

Precisely the same device is employed by KAM in the mechanical problem. Each new torus generated by the previous approximation is itself made the basis of the next approximation, rather than (as in 3.17) expressing all approximations in terms of the unperturbed torus $(\underline{I},\underline{\theta})$ with Hamiltonian $H_0(\underline{I})$. The accelerated convergence thus obtained was subjected to a searching analysis by KAM.

Their central result is that the process of generating "perturbed" tori does in fact converge, for small but finite ε, almost always. Therefore, most trajections continue *for all time* on the tori M of dimensionality N, and do not explore the whole 2N-1 dimensional energy surface. How then can ergodicity come about? What of statistical mechanics? The answer lies in the qualifications "almost always" and "most". For it turns out that unperturbed tori in the neighborhood of those on which orbits are *closed* (or partially closed) are almost all destroyed. These orbits lie on tori with commensurable frequencies, i.e. those for which

$$\underline{\omega}_0 \cdot \underline{m} = 0 \text{ for some } \underline{m}, \text{ or } \underline{\omega}_0 = \underline{N}\omega_b \ . \qquad (3.28)$$

These "destroyed" tori are those giving rise to the small denominators in (3.17). But we have already seen that for *any* $\underline{\omega}_0$ there are, infinitely close by, "rational" tori satisfying (3.28). So, are we any better off? Surely after destroying all rational tori (3.28) and those near them, there are none left at all? Not so. To understand this, and KAM's specification of the "width" of the destroyed regions, we must learn a little of the mathematics of rational and irrational numbers. Then we shall give some striking astronomical illustrations of the KAM theorem, and describe numeri-

cal experiments that show what happens in the "gaps" where tori have been destroyed. Finally we attempt to explain how *stochastic* features enter into the motion in these gaps, which therefore provide the gateway to statistical mechnaics, growing with ε and eventually filling the whole phase space.

4. THE ARITHMETIC OF TORUS DESTRUCTION[14]

Consider (3.28) for two degrees of freedom (the simplest non-trivial case). The second of the equations gives the frequency ratio σ of the tori bearing closed orbits as

$$\frac{\omega_{01}}{\omega_{02}} \equiv \sigma = \frac{N_1}{N_2} = \frac{r}{s} \qquad (r \text{ and } s \text{ are integers}) \ . \tag{4.1}$$

Thus σ is a rational number (r,s is simply a more convenient notation for N_1,N_2). A torus with incommensurable frequencies has irrational σ and cannot be written in the form (4.1). But it can be approximated *arbitrarily closely* by rational σ's. Take $\sigma=\pi$, for instance. Then a series of approximations can be generated by successive truncations of the decimal expansion:

$$\sigma=\pi = 3.141592654 \ldots \approx r/s = \frac{3}{1} \ , \ \frac{31}{10} \ , \ \frac{314}{100} \ , \ \frac{3142}{1000} \ , \ \frac{31416}{10000} \ , \ \ldots . \tag{4.2}$$

The better approximations have larger values of r and s. In fact for these decimal expansions

$$\left|\sigma - \frac{r}{s}\right| < \frac{1}{s} \ . \tag{4.3}$$

Actually it is possible to do better; to approximate irrational tori much more closely by rationals. The point is that decimals, while useful for computation, are very "impure" representations of numbers σ, in that the arithmetic nature of σ is contaminated with the special properties of the base 10, and the same holds for any other base. The best representation for arithmetic purposes is the *continued fraction* for σ, written as

$$\sigma = a_0 + \cfrac{1}{a_1 + \cfrac{1}{a_2 + \cfrac{1}{a_3 + \ldots}}} \qquad \begin{array}{l} (a_0 \text{ integer } (-\infty \ldots -1, 0, +1 \ldots) \\ a_1, a_2 \ldots \text{natural numbers} \\ \qquad (1,2,3,\ldots) \end{array} \tag{4.5}$$

This is unique, and can be derived by subtracting the integral part a_0 of σ, reciprocating, subtracting the integral part a_1 of the number

thus obtained, reciprocating, ...a_2 ..... etc. For π we obtain

$$\pi = 3 + \cfrac{1}{7 + \cfrac{1}{15 + \cfrac{1}{293 + \ldots.}}} \tag{4.6}$$

The successive approximants of the continued fraction, namely,

$$\sigma_n \equiv \frac{r_n}{s_n} = a_0 + \cfrac{1}{a_1 + \cfrac{1}{a_2 + \ddots \cfrac{1}{a_n}}} , \tag{4.7}$$

define a sequence r_n/s_n of rational approximations to σ. It can be shown that these are *best* approximations in the sense that no rational r/s with $s \leq s_n$ is closer to σ than r_n/s_n. Simple algebra based on (4.7) shows that the sequence always converges to σ, and that the successive r_n/s_n are alternately greater and less than σ (fig. 21).

Moreover,

$$\left|\sigma - \frac{r_n}{s_n}\right| < \frac{1}{s_n s_{n-1}} , \tag{4.8}$$

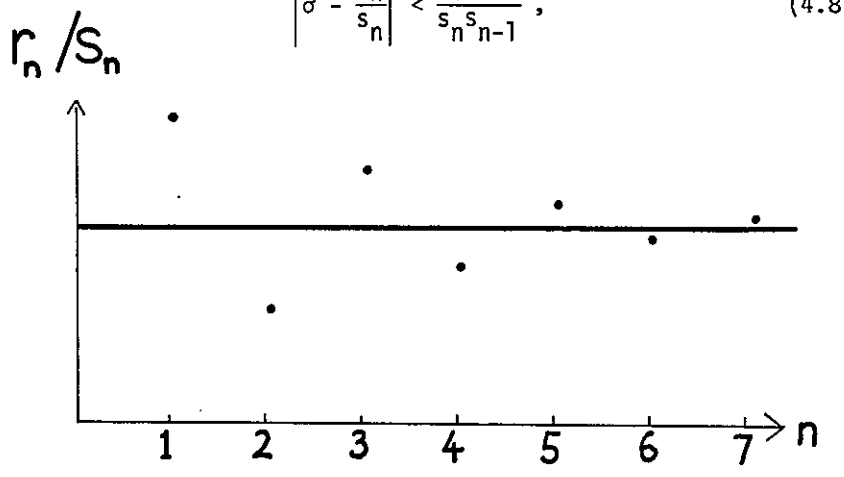

which is much better than (4.3). To illustrate this, we get for π

$$\frac{r_0}{s_0} = 3, \quad \frac{r_1}{s_1} = \frac{22}{7} = 3.1429 \ldots \quad \frac{r_2}{s_2} = \frac{333}{106} = 3.14151$$
$$\text{(2 places)} \qquad \text{(3 places)} \qquad (4.9)$$
$$\frac{r_3}{s_3} = \frac{355}{113} = 3.1415929$$
$$\text{(6 places)}$$

The last result was known to Lao-Tze (604-531BC).

Two digressions: (1) obviously the continued fraction for υ converges faster if the sequence $a_0\ a_1 \ldots$ diverges faster, and vice versa. Thus, the sequence for π, which soon contains the large integer $a_4 = 293$, converges very fast indeed (see 4.9) and the *slowest* convergence, corresponding to the irrational σ worst approximated by rationals, is given by the number

$$\sigma = \cfrac{1}{1 + \cfrac{1}{1 + \cfrac{1}{\ddots}}} = 0\ .618033989 \ldots = \frac{\sqrt{5}-1}{2} = \text{golden mean} \qquad (4.10)$$

(2) Much of the theory of continued fractions was developed in the 17th and 18th centuries in connection with orrery technology. An orrery is a mechanical model of the solar system: turn a handle and a system of gearwheels moves the planets around at the correct proportionate speeds. The problem was that the frequency ratios are not all rational (or, to experimental accuracy, very high-order rational), so that a theoretically perfect gearing would involve inordinate numbers of teeth (tooth ratio ω_1/ω_2 for two planets with frequencies ω_1 and ω_2). The approximants of the continued fraction for ω_1/ω_2 give a "best" sequence of gear rations.

Equation (4.8), then, tells us that for *any* σ whatever it is possible to find rationals r/s differing from σ by less than a quantity of orders s^{-2}. For *particular classes* of σ, sharper bounds exist (i.e. $|\sigma - r/s| < O(1/s^3)$ or $(\sigma - r/s) < O(e^{-s})$, etc.), but (4.8) is the best that can be achieved for *all* σ.

Now, KAM prove convergence of the accelerated iteration-perturbation scheme for the torus generator S for all initial tori whose frequency ratio is sufficiently irrational for the following relation to hold (in the two-dimensional case):

$$\left|\frac{\omega_{01}}{\omega_{02}} - \frac{r}{s}\right| > \frac{K(\varepsilon)}{s^{2.5}} \text{ , for all integers } r \text{ and } s \text{ ,} \qquad (4.11)$$

where K is a number, independent of r and s, that tends to zero with the perturbation ε. The tori excluded by (4.11), which are mostly destroyed, are those satisfying

$$\left|\frac{\omega_{01}}{\omega_{02}} - \frac{r}{s}\right| < \frac{K(\varepsilon)}{s^{2.5}} \text{ , for some } r \text{ and } s \text{ .} \qquad (4.12)$$

This is a more restrictive condition than (4.8) (which applies for all $\sigma = \omega_{01}/\omega_{02}$) and we can expect therefore that after these tori are destroyed there will still be some left.

We can quite easily show that this is in fact the case. Without loss of generality, we can consider all initial tori whose frequency ratios lie in a range of size unity, and moreover take this to be the range $0 \leq \omega_{10}/\omega_{20} < 1$. We delete from this line all segments satisfying (4.12):

$$0 \quad \underset{K/55.9}{1/5} \quad \underset{K/32}{1/4} \quad \underset{K/15.6}{1/3} \quad \underset{K/55.9}{2/5} \quad \underset{K/5.7}{1/2} \quad \underset{K/55.9}{3/5} \quad \underset{K/15.6}{2/3} \quad \underset{K/32}{3/4} \quad \underset{K/55.9}{4/5} \quad 1 \rightarrow \frac{\omega_{01}}{\omega_{02}} \text{ .}$$

Thus we delete $K/s^{2.5}$ about each rational r/s on the range 0 to 1. The total length deleted is thus

$$\sum_{s=1}^{\infty} \frac{K}{s^{2.5}} s = K \sum_{s=1}^{\infty} \frac{1}{s^{1.5}} \simeq K \qquad (4.13)$$

(s is the number of r-values with r/s on 0 to 1)

which tends to zero with K and hence with ε. This is actually an over-estimate of the "measure" of the destroyed tori, because we have included separately rationals r/s whose deleted neighborhoods overlap. The destroyed tori would still have finite measure if (4.11) were less sharp. More precisely, $K/s^{2.5}$ could be replaced by K/s^{μ} where $\mu > 2$. Analogous results were proved by KAM for all degrees of freedom N. The precise value of K is not determined by KAM, nor is it proved what happens to motion in the gaps.

We repeat the main result: in a perturbed system, most orbits lie on tori in phase space. Those that do not, form a small but finite set pathologically distributed in phase space near each unperturbed torus that supported closed or partially closed orbits. From a physical point of view the motion in high-order "gaps" (large s) is hard to study, because these gaps are very narrow

$(0(s^{-2.5}))$, and random *further* perturbations (which must always be present in view of the fact that no real system can be isolated) will probably push the system out of the gap and onto a nearby torus. But the low-order gaps, resulting from low-order resonances among the unperturbed frequencies, are relatively wide and give rise to observable and computable effects as we shall now see.

5. ASTRONOMY OF THE GAPS BETWEEN TORI[11,15,16]

Let us apply the KAM theory to the simplest case of the "plane, circular, restricted three-body problem". Consider three bodies moving under their mutual gravitation: the "attractor" A with mass M, the "perturber" P with mass m and the "test body" T with mass μ (fig. 22).

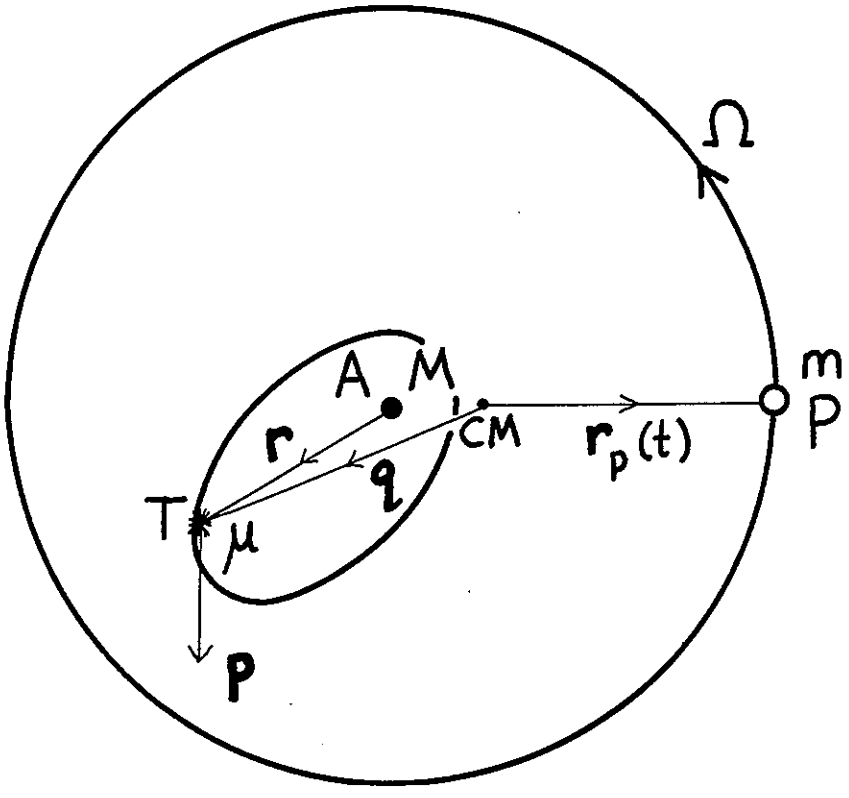

Fig. 22

The "restricted" problem has $\mu \ll m$ and $\mu \ll M$, so that the effect of T on the motion of A and P can be neglected. The two-body motion of A and P is easily solved, and we have to find the motion of T in the known field of A and P. We consider only the case of where A, T, P move in a fixed *plane*, and we let P move about its center of mass with A in a *circle* rather than the more general ellipse. Finally we consider P to be a perturbation on T, i.e. $m \ll M$, so that T's motion is dominated by A. When m=0, T moves in a Kepler ellipse about A. What happens to T when we switch on P? This is the simplest nonintegrable problem in celestial mechanics, and Poincaré realized it to be of crucial importance for theoretical dynamics.

The Hamiltonian for T is

$$H(\underline{q},\underline{p},t) = \frac{|\underline{p}|^2}{2\mu} - \frac{GM\mu}{r} - \frac{Gm\mu}{|\underline{q}-\underline{r}_p(t)|} \quad . \qquad (5.1)$$

The coordinate $\underline{q}$ (measured from the center of mass of A and P) has two components because T moves in a plane. $\underline{r}_p(t)$ is the known moving position of the perturbator P (also measured from the center of mass), and $\underline{r}$ is the vector from A to T. It is very awkward to work with this time dependent Hamiltonian, and we can make the system conservative by viewing T's motion from a frame rotating with the angular velocity, $\underline{\Omega}$, of P; in this frame P is at rest (fig. 23). The new Hamiltonian can be shown by elementary methods to be

$$H(\underline{q},\underline{p}) = \frac{|\underline{p}|^2}{2\mu} - \underline{p}\cdot(\underline{\Omega}\times\underline{q}) - \frac{GM\mu}{\underline{r}} - \frac{Gm\mu}{|\underline{q}-\underline{r}_p|} \quad . \qquad (5.2)$$

The last term is the non-integrable perturbation H_1, with P's mass m playing the role of the small parameter ε.

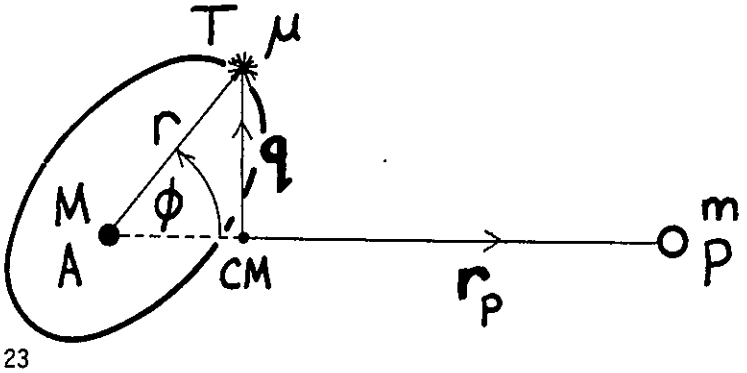

Fig. 23

In polar coordinates r, ϕ, p_r,p_ϕ, the unperturbed Hamiltonian is

$$H_0(\underline{q},\underline{p}) = \frac{p_r^2 + \frac{p_\phi^2}{r^2}}{2\mu} - \Omega P_\phi - \frac{GM\mu}{r} \quad . \tag{5.3}$$

(We have used the fact that $q \to r$ as $m \to 0$.) Neither t nor ϕ appears in this, so the two constants of motion are p_ϕ and H_0 itself. Specifying both of these defines a torus M. The actions I_ϕ and I_r of M expressed in terms of p_ϕ and H_0 are as follows

$$I_\phi = \frac{1}{2\pi} \int_0^{2\pi} p_\phi \, d\phi = P_\phi$$

$$I_r = \frac{1}{2\pi} \oint p_r dr = \frac{R_e}{\pi} \int_0^{\infty} dr \sqrt{2m(H_0 + I\Omega_\phi + \frac{\mu GM}{r}) - \frac{I_\phi^2}{r^2}} \tag{5.4}$$

$$= -I_\phi + \frac{GM\mu^2}{\sqrt{-2\,(H_0+\Omega I_\phi)}} . \tag{5.6}$$

The Hamiltonian H_0 in action variables for this rotating frame is therefore

$$H_0\,(\underline{I}) = -\frac{\mu^3 M^2 G^2}{2(I_r+I_\phi)^2} - \Omega I_\phi \ . \tag{5.7}$$

The unperturbed frequencies $\nabla_{\underline{I}} H_0$ are

$$\omega_{0\phi} = -\Omega + \frac{\mu^3 G^2 M^2}{(I_r+I_\phi)^3} \ , \ \omega_{0r} = \frac{\mu^3 G^2 M^2}{(I_r+I_\phi)^3} \ . \tag{5.8}$$

This is easily interpreted, since

$$\frac{\mu^3 G^2 M^2}{(I_r+I_\phi)^3} \equiv \omega_T \tag{5.9}$$

is the unperturbed frequency of T's Kepler motion in the *non*-rotating frame, in which both r and ϕ motions have the same frequency

because of the well-known degeneracy of motion in the inverse-square law force in which all orbits are closed. Therefore (5.8) can be written in the obvious form

$$\omega_{0\phi} = -\Omega + \omega_T, \quad \omega_{0r} = \omega_T \ , \tag{5.10}$$

and the frequency ratio is

$$\frac{\omega_{0\phi}}{\omega_{0r}} = 1 - \frac{\Omega}{\omega_T} \ . \tag{5.11}$$

The KAM theorem can be applied to Hamiltonian (5.2) with m as perturbation. It shows that the motion of T continues to lie on an invariant torus in almost all cases if $m \ll M$. But are destroyed tori near motions of T with rational $\omega_{0\phi}/\omega_{0r}$ or, from (5.11), with rational Ω/ω_T, corresponding to *resonance* between the periods of P and T. In the solar system there are two near-continuous distributions of test bodies T where the gaps between tori are observed.

The first case is the *asteroid belt* between Mars and Jupiter. The attractor is the Sun, the perturber is Jupiter and the test mass is any asteroid. According to (5.11) and KAM, we should expect gaps in the asteroid belt at distances from the Sun where T's unperturbed frequency ω is commensurable with Jupiter's frequency ω_J. These gaps were indeed observed by Kirkwood in 1866. Modern data show them very clearly (fig. 24).

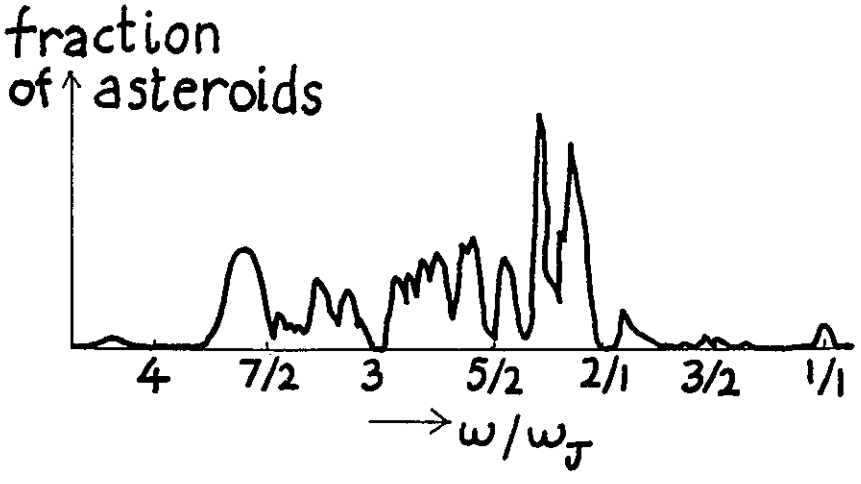

Fig. 24

The early stages of orbit instability beginning as unperturbed circles near the resonance $\omega/\omega_J = 2$ are shown clearly in computations by Franklin in 1973: the orbit turns into an ellipse whose semimajor axis a oscillates in length (fig. 25).

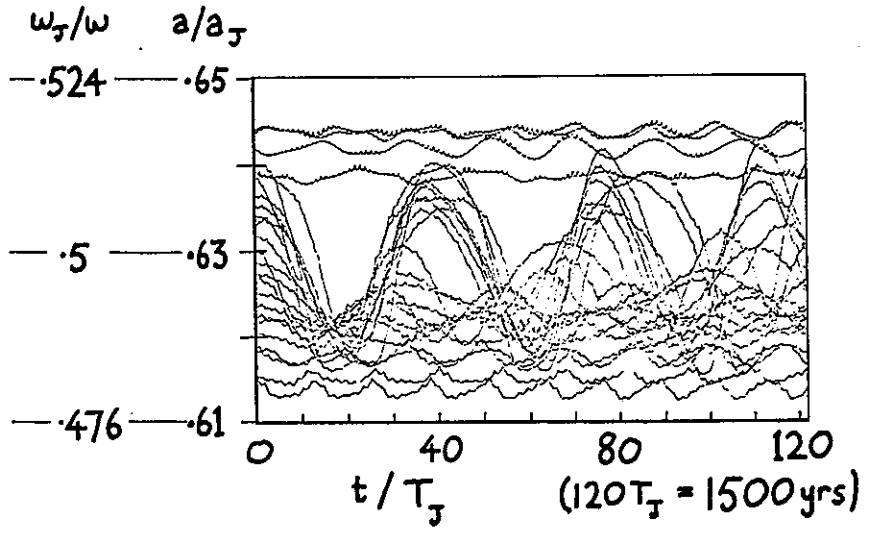

Fig. 25

The oscillations near resonance look as though they are diverging, but 1500 years is far too short a time to show anything conclusive.

The only apparent violation of KAM's prediction of gaps is the lowest resonance of all: 1:1. But this is not a violation at all, because these asteroids - the Trojan group, about 15 of them (the first discovered in 1906) - do not cover a torus in phase space but are clustered at two points on Jupiter's orbit, forming equilateral triangles with Jupiter and the Sun (fig. 26). The possibility of such a triangle was first appreciated in 1772 by Lagrange as (he thought) a mathematical curiosity in the 3 body problem: *any* 3 masses can move stably in a rigid equilateral triangle with angular velocity (fig. 27)

$$\Omega = \sqrt{\frac{G}{r^3}(M + m + \mu)} \approx \omega_J \quad \text{(in our case)} , \qquad (5.12)$$

where r is now the side length (Ω refers to rotation about the center of mass).

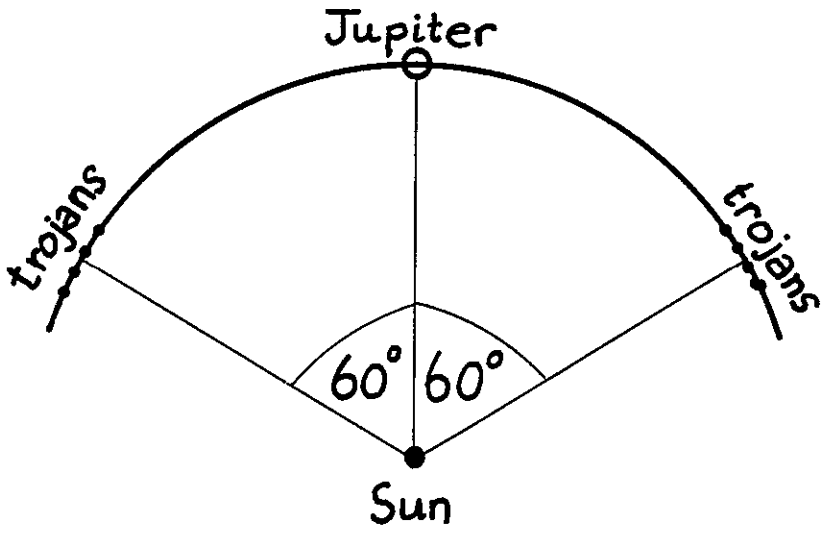
Jupiter
trojans
trojans
60°
60°
Sun

Fig. 26

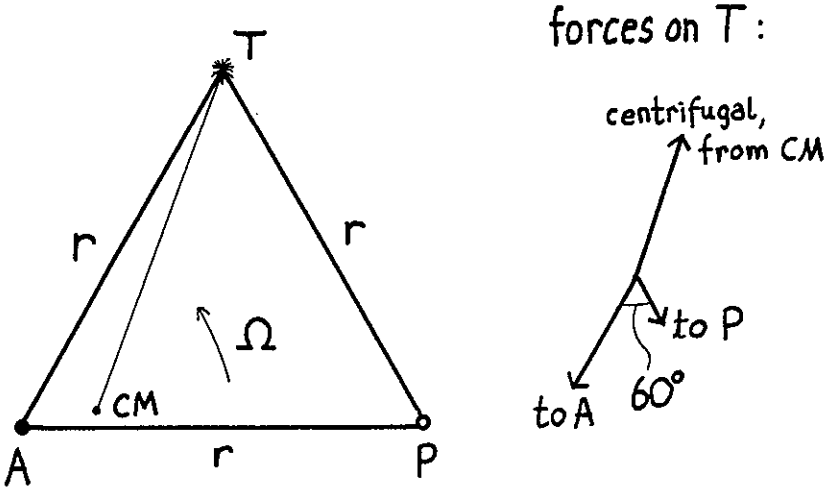
T
r
r
Ω
CM
A
r
P
forces on T :
centrifugal,
from CM
to P
to A
60°

Fig. 27

These "Lagrangian points" on Jupiter's orbit correspond not to a torus'-worth of orbits but to two *isolated* closed orbits.

The second set of solar-system gaps occurs in the *rings of Saturn* (fig. 28). In this system, Saturn is the attractor, the perturber is any of the inner satellites, principally Mimas, and the test masses are ring particles (Maxwell showed that a rigid ring, or a liquid ring with viscous stresses, would be unstable, so the particles are essentially independent, moving in circular orbits and not colliding.)

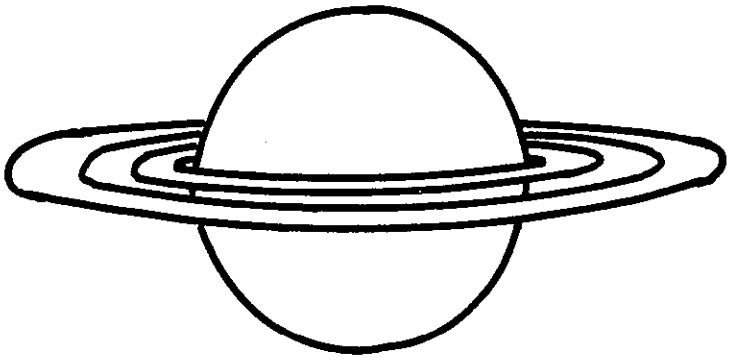

Fig. 28

Why should there be rings at all? Roche showed that any large body so close to Saturn would be disrupted by Saturn's gravity (or not form in the first place). Disruption occurs (fig. 29) if the attraction between two elements of the body is less than the tidal force from Saturn. Take the elements to be spheres in contact (radius a). The tidal force is the difference between Saturn's force on the two elements. Hence, disruption occurs if

$$\frac{Gm^2}{(2a)^2} < \frac{2GMm}{r^3}(2a) \ , \quad \text{or} \ \frac{16M}{mr^3}a^3 > 1 \ . \tag{5.13}$$

If the densities of Saturn and the hypothetical satellite are assumed equal, this gives ($m \propto a^3$, $M \propto R^3$)

$$r < 16^{1/3} R = 2.52R, \tag{5.14}$$

$$= 152{,}300 \text{ km} \ .$$

Janus, the tiny innermost satellite of Saturn (discovered in 1967) just makes it; its distance is r = 156,800 km!

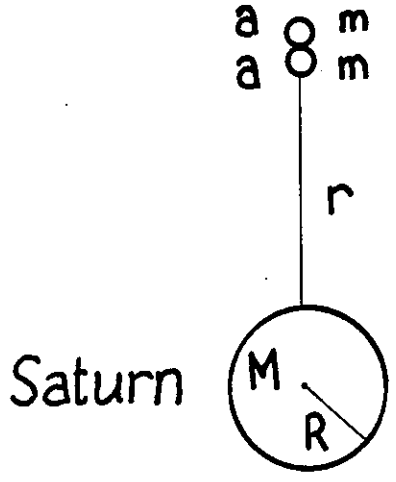

Fig. 29

The ring system lies wholly within the Roche limit, and has the structure shown in Figure 30.

The "3ω mimas" resonance is very close to the gap between ring B and the crepe ring, but "$2\omega_{\text{mimas}}$" and "$3\omega_{\text{enceladus}}$" lie just inside the "Cassini division" between the main A and B rings. However, Frankin has shown (1973) that the effect of the mass in ring B moves both these resonances right into the gap (roughly, it is as if Saturn were a bit heavier).

A present-day theoretical physicist might naturally think of making a computer model of the rings. This leads to difficulties, however, well expressed by Franklin:

"I began with the naive hope that all one had to do was to take a planet, put a large number of massless ring particles around it, introduce the inner satellites.... turn on a machine and after a while discover that the satellite perturbations, particularly ones near resonance, had sculptured the ring. I was set to lease the movie rights....to watch a nice uniform ring quickly being sculptured into Saturn's ring. Well, the movie has yet to be made... The problem is simply that things happen on an enormously slow time scale, not slow cosmologically, but very slow when it comes to the allowances made by administrators of computing facilities".

I want to digress a bit now, to discuss something that confused me while I was checking these Saturnian ring gaps. If one considers Tethys, the next satellite beyond Enceladus, one obtains almost *precisely* the same ring gaps as those from Mimas. The reason is

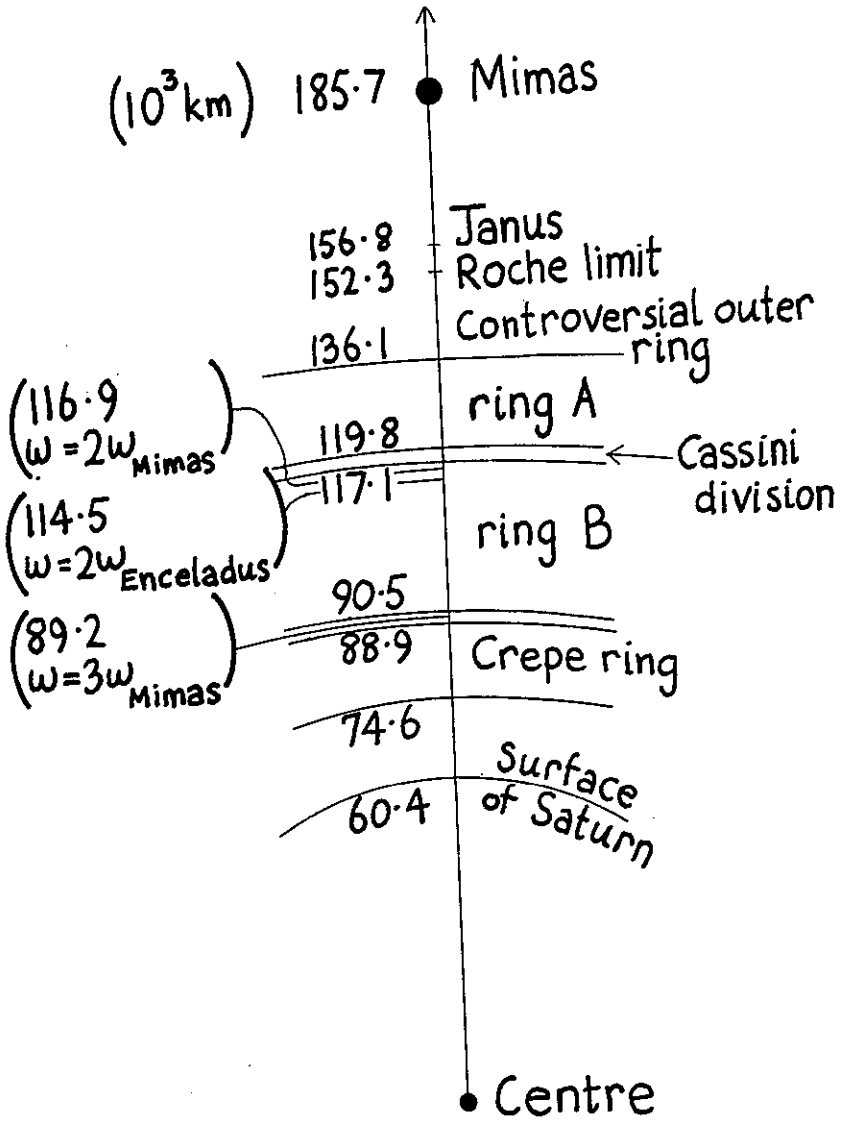
(10^3km)
185·7
Mimas
156·8
Janus
152·3
Roche limit
Controversial outer ring
136·1
ring A
119·8
Cassini division
117·1
ring B
90·5
88·9
Crepe ring
74·6
Surface of Saturn
60·4
Centre
(116·9 ω = 2ω Mimas
(114·5 ω = 2ω Enceladus
(89·2 ω = 3ω Mimas

Fig. 30

that, to one part in 10^3, $\omega_{Mimas} = 2\omega_{Tethys}$. This seems precisely to contradict the KAM theorem, which as we have seen eliminates tori made up of closed orbits. In reality however, such commensurabilities do not contradict the theorem, for at least two reasons. Firstly, the Mimas-Tethys system is *interactive* rather than perturbative - each body affects the other - whereas in the Mimas-ring system and the Tethys-ring system the ring particles are passive test masses, responding to the satellites' field but not affecting it. Secondly, the KAM theorem does *not* show that closed orbits are destroyed, but only that the tori composed of them are destroyed - *isolated* closed orbits can and do exist (cf. the Trojan asteroids).

Nevertheless, it does seem surprising that of all possible orbits, most of which are unclosed and lie on undestroyed tori, Mimas and Tethys should choose a closed orbit. One's surprise is increased by the recent discovery that commensurability is apparently the rule rather than the exception in the solar system! Careful analysis by Roy and Ovenden in the 1950's and Molchanov in 1966 is claimed to show that this cannot be due to chance. It seems that a *complete* set of commensurabilities $\underline{\omega}\cdot M=0$ exists for each of the following four systems: Saturns' satellites, Jupiter's satellites, Uranus's satellites, and the planets themselves.

Let us examine this for the nine planets: I(Mercury)-IX(Pluto). Then, to a close approximation

$$M_{rn}\omega_n = 0 \qquad (r = 1 \text{ to } 8,\ n = 1 \text{ to } 9)\ ,$$

where

$$M_{rn} = \begin{pmatrix} 1 & -1 & -2 & -1 & 0 & 0 & 0 & 0 & 0 \\ 0 & 1 & 0 & -3 & 0 & -1 & 0 & 0 & 0 \\ 0 & 0 & 1 & -2 & 1 & 1 & 1 & 0 & 0 \\ 0 & 0 & 0 & 1 & -6 & 0 & -2 & 0 & 0 \\ 0 & 0 & 0 & 0 & 2 & -5 & 0 & 0 & 0 \\ 0 & 0 & 0 & 0 & 1 & 0 & -7 & 0 & 0 \\ 0 & 0 & 0 & 0 & 0 & 0 & 1 & -2 & 0 \\ 0 & 0 & 0 & 0 & 0 & 0 & 1 & 0 & -3 \end{pmatrix} \qquad (5.15)$$

The error is measured by $\Delta\omega_n/\omega_n$, where ωn is the planet's measured frequency and $\Delta\omega_n$ the deviation when (5.15) is used to calculate the frequency, taking (say) Jupiter's frequency (ω_v) as the standard. Then:

Planet n	$\Delta\omega_n/\omega_n$
I	.0004
II	.0015
III	.0031
IV	.0031
V	0
VI	.0068
VII	-.0118
VIII	.0075
IX	-.0025

It all seems pretty accurate - the commensurability integers in (5.15) are all small (≤ 7) and so are the errors. Perhaps the whole solar system is in resonance! From a historical viewpoint, this discovery discredits the Bode-Titius law, namely:

distance of planet from Sun is

$$\alpha\ 3x2^n + 4,\ (n = -\infty,1,2,\ldots) \quad (5.16)$$

and supports Pythagoras' theory of planetary harmony, namely volume of "crystal sphere"

$$\alpha(\text{distance})^3\ \alpha(\text{period})^2 \text{ with } \alpha \text{ an integer .} \quad (5.17)$$

Suppose this is correct. Then we must ask why is the solar system in a state which seems to have zero a priori probability (closed orbit for the whole motion)? The beautiful theory has been elaborated by Molchanov and Goldreich that the *non-Hamiltonian effects* of viscous dissipation and tidal friction would slowly *pull into resonance* a system started out with random multiply periodic initial conditions (i.e. on some surviving incommensurable KAM torus). The "short" term motion is accurately Hamiltonian, but over cosmological times the system would drift across tori (the "constants" $\underline{I}$ would vary) and into a periodic state as a result of the dissipation. Most of the dissipation is thought to have occured in the early stages of the solar system's evolution as a result of friction from the then relatively dense interplanetary gas. This has now largely condensed, so that the system is almost entirely Hamiltonian but with a motion that was selected by non-Hamiltonian processes. (Dissipation violates Liouville's theorem, so that an ensemble of plane solar systems distributed uniformly over an energy surface in the 9x2x2 = 36 dimensional phase space can eventually all become concentrated on the small set of periodic orbits.)

But all of this is controversial. It may be that as an indication of resonance the equations (5.15) are deceptive. For one thing, only nine frequencies ω_i are involved, even though mutual perturbations break the Kepler degeneracy and lead to two frequencies per planet instead of one. More seriously, a little arithmetic shows that (5.15) implies that all ω_n are integer multiples of a basic frequency

$$\omega_b = \frac{\omega_V}{210} = \frac{\omega_{\text{Jupiter}}}{210}\ , \quad (5.18)$$

so that the resonant period of the solar system is $210T_{\text{Jupiter}} \sim$

2500 years. After this time the planets should have returned to their original configuration. But the errors $\Delta\omega/\omega$ will spoil this prediction, to the extent that the Earth (say) will be about 7 revolutions out of phase after one of these so-called resonant periods. In other words, the commensurability that seemed so close is in reality so poor that the resonance loses phase coherence before one "revolution"! Another criticism of the "goodness of resonance" is based on the claim that almost *any* nine randomly-chosen frequencies can be made to satisfy a low-order resonance equation like (5.5) to comparable accuracy, but this claim is controversial.

6. SURFACES OF SECTION AND AREA PRESERVING MAPPINGS[2,10,13]

Now we describe an important technique, originally suggested by Poincaré, for studying the breakdown of integrability and the motion in gaps between destroyed tori. The method best suits two dimensional problems and we consider only three dimensions here. Then the phase space $\underline{q},\underline{p}$ is four-dimensional and the energy "surface" E (i.e. the "surface" $H=E$) is three-dimensional. (It is a mistake to think of this as being like ordinary three-dimensional position space, because it is non-Euclidean, closed, and may be multiply-connected (cf., two-dimensional surfaces in three-dimensional space).)

The x surface of section S_x is the intersection of E with $y=0$, and has (p_x,x) as coordinates. Then specifying the position of a system on S_x completely specifies its state, apart from a sign, because p_x,x and y (=0) are specified, and for the usual Hamiltonians quadratic in p_i the value of p_y is determined by the condition $H(x,y=0,p_x,p_y)=E$ up to a sign. We define this sign to be positive. (The y surface of section S_y is defined in a precisely analogous manner).

A system started out on S_x will subsequently cross it repeatedly, because in a bound system y will repeatedly oscillate through zero and half these zeros will have positive p_y. Thus an initial point $X_0 \equiv (x_0 p_{x0})$ on S_x will subsequently cross S_x at $X_1 \equiv (x_1 p_{x1})$, $X_2, X_3 \ldots$ (fig. 31).

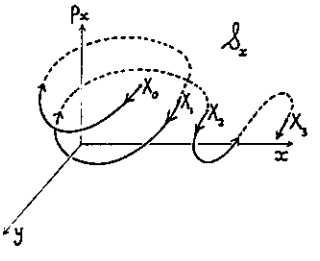

Fig. 31

At each new crossing the whole plane S_x is mapped onto itself, because every point X_0 maps onto some new point X_1. (The time taken for each iteration is different for each point X, but this is irrelevant for our purposes.) Call the mapping T: $X_1 \equiv T(X_0)$ (fig. 32).

An important property of the mapping of S_x is that it is *area-preserving*:

$$\frac{|d\underline{X}_1|}{|d\underline{X}_0|} \quad \frac{|dp_{x1}dx_1|}{|dp_{x0}dx_0|} = 1 \ . \tag{6.1}$$

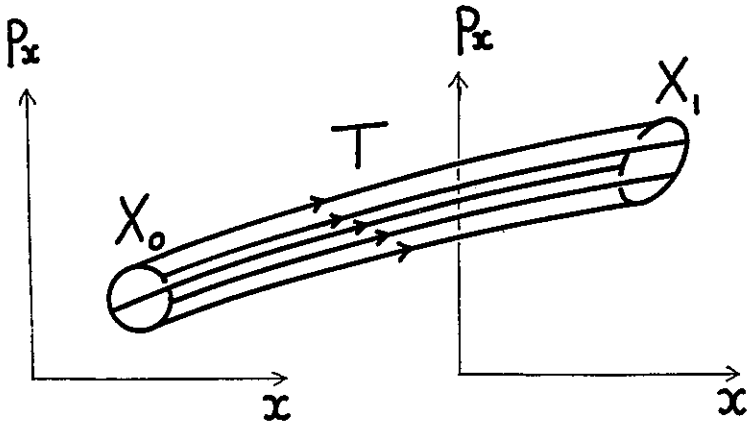

Fig. 32

This follows from the Hamiltonian character of the dynamics between "collisions" with S_x: during the motion, $\underline{q}$ and $\underline{p}$ remain canonical. Therefore, the system's state $(\underline{q}_1, \underline{p}_1)$ at time t, can be obtained from its state $(\underline{q}_0\underline{p}_0)$ at t_0 by a canonical transformation - the motion itself can be thought of as the unfolding of a (time-dependent) canonical transformation with generator S:

$$\left.\begin{aligned} &(\underline{q}_0\underline{p}_0) \overset{t_0}{\leftarrow} S(\underline{q}_0, \underline{p}_1 \ , \ t_0, \ t_1) \overset{t_1}{\rightarrow} (\underline{q}_1, \ \underline{p}_1), \\ &\underline{p}_0 = \nabla_{\underline{q}_0} S \ , \\ &\underline{q}_1 = \nabla_{\underline{p}_1} S \ . \end{aligned}\right\} \tag{6.2}$$

In particular,

$$p_{x0} = \frac{\partial S}{\partial x_0}\ ,\ x_1 = \frac{\partial S}{\partial p_{x1}}\ ,\ \frac{\partial p_{x0}}{\partial p_{x1}} = \frac{\partial x_1}{\partial x_0} = \frac{\partial^2 S}{\partial p_{x1}\partial x_0}\ , \qquad (6.3)$$

from which (6.1) follows immediately.

The usefulness of these surfaces of section lies in the fact that the iterates $X_1, X_2 \ldots$ of an initial point X_0 reveal whether or not the motion is *integrable*. If it is the system does not explore all of E but only a 2-torus M. This torus intersects S_x in a smooth closed curve C (fig. 33). All iterates X_j must lie on C, and after sufficiently many iterations the form of C usually becomes apparent.

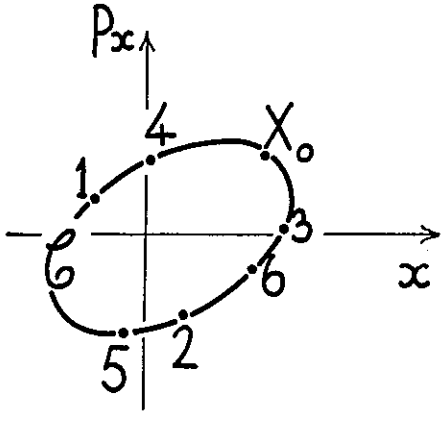

Fig. 33

If the motion is periodic - i.e. the orbit is closed - then some iterate X_n will coincide with X_0 (n depends on the order of commensurability of the frequencies ω_1 and ω_2). Thus X_0 is a *fixed point* of the mapping T^n. In integrable cases there is a torus-full of these closed orbits, so that the whole curve C is made up of these fixed points. Most curves C are, however, sections of irrational tori, and are generated by all the iterates of *any* point X_0. The curves C are *invariant curves* of the mapping, because T maps them onto themselves:

$$T(C) = C \qquad (6.4)$$

For *non-integrable* motion, tori do not exist, so that the system explores a three-dimensional region of E. Therefore its crossings of S_x cover not a curve but a *two-dimensional region* of S_x (Fig. 34).

Then,

$$H = \frac{1}{2}(p_1^2 + p_2^2 + p_3^2) + e^{-(Q_1-Q_3)} + e^{-(Q_2-Q_1)} + e^{-(Q_3-Q_2)} - 3. \qquad (6.5)$$

This is really a two-dimensional problem, since $p_1+p_2+p_3$ is a constant of the motion, that reflects our freedom to add an extra rigid translation to any motion. It is possible to make a (non-intuitive) change of variables (canonical transformation) to make the problem mathematically identical to a particle moving in a two-dimensional potential:

$$H(\underline{q},\underline{p}) = \frac{p_x^2 + p_y^2}{2} + \frac{1}{24}\left[e^{2y + 2\sqrt{3}x} + e^{2y-2\sqrt{3}x} + e^{-4y}\right] - \frac{1}{8}. \qquad (6.6)$$

The equations of motion of trajectories for fixed E were studied by Ford and his collaborators, who presented their results as "x=0" surfaces of section S_y. The perturbation parameter can be thought of as E itself in this case, since for small E the particle can explore only the xy region near the origin, where H is an integrable system - the isotropic harmonic oscillator:

$$H(\underline{q},\underline{p}) \overset{\underline{q}\to 0}{\to} \frac{p_x^2 + p_y^2 + x^2 + y^2}{2} . \qquad (6.7)$$

Figure 36 shows the equipotential contours.

For the oscillator, the Hamiltonian is integrable. It was thought that as E increased, and more and more of the nonquadratic regions of the well become accessible, more and more "rational" tori would be observed to break up - on the surface of section the "orbits" $X_0, X_1 \ldots$ of initial points X_0 would no longer be on smooth curves C. But this behavior was not found. Instead the iterates stayed firmly on smooth curves for E=1, E=256 (fig. 37), and all E up to the computer's limit of 56000!

It looks as though the system is behaving like an integrable system! The above pictures do not show the individual intersections of the curves C by the orbit $X_0 \ldots$, but the curves themselves. These curves are identical with computer-calculated "analytic" curves obtained by a perturbation theory analogous to that employed in Chapter 2. Analogous, but not the same, because the "unperturbed" Hamiltonian in this case is an equal-frequency oscillator, for which *all* orbits are closed. But a special perturbation theory can be devised to deal with this single massive degeneracy (it is enormously elaborate) and there is a corresponding variant of the KAM

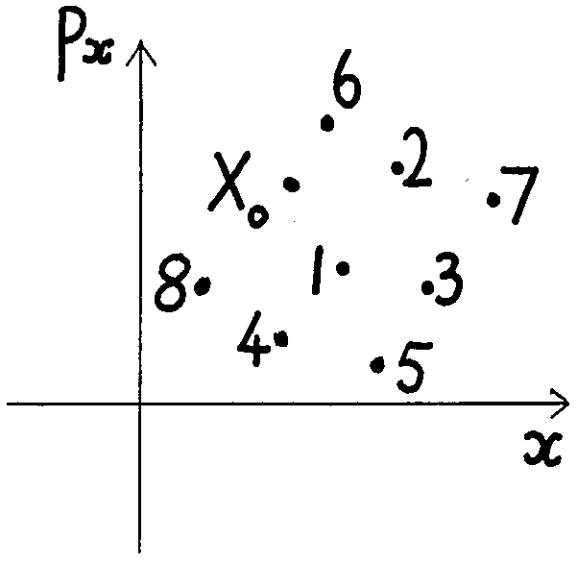

Fig. 34

This will become more and more apparent as the number of iterations increases.

With computers, many iterations of T can be carried out for a range of starting-points X_0 on S_x. Such experiments can never yield proofs of the existence or nonexistence of invariant curves C, because it is always conceivable that high order iterates X_n might diverge from a curve suggested by early iterates, or that iterates apparently randomly filling a part of S_x might really all lie on some definite but complicated curve C. However, when interpreted in the light of the KAM theorem and some further analysis that we shall discuss later, the experiments are extremely instructive.

The first example, that led to a surprise, is the *three-particle Toda lattice*. This is perhaps the simplest non trivial "solid". Three particles move on a "ring with exponential forces" (fig. 35).

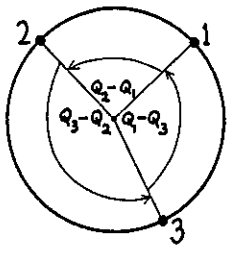

Fig. 35

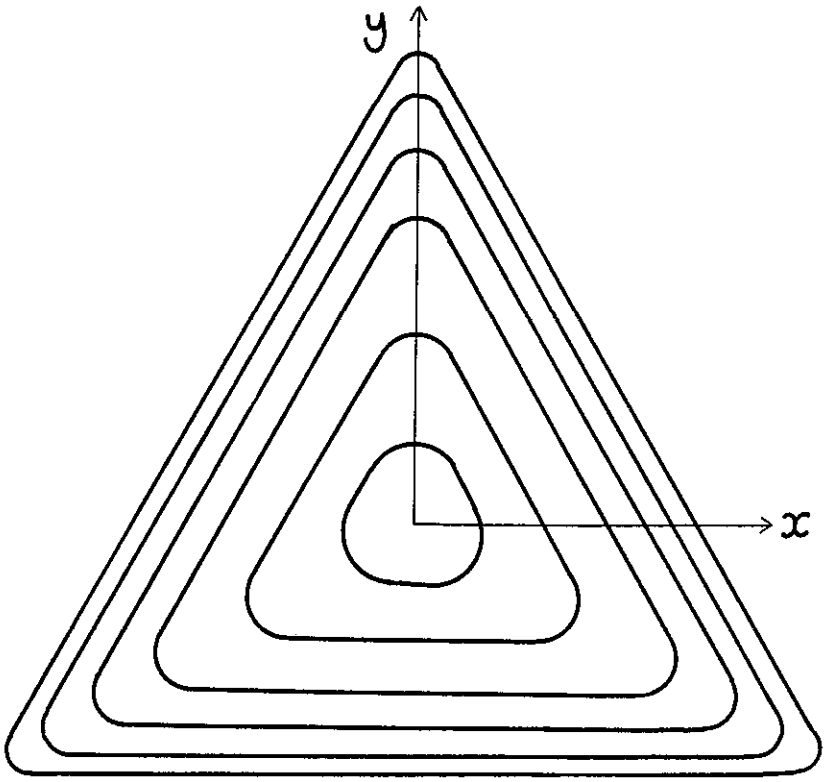

Fig. 36

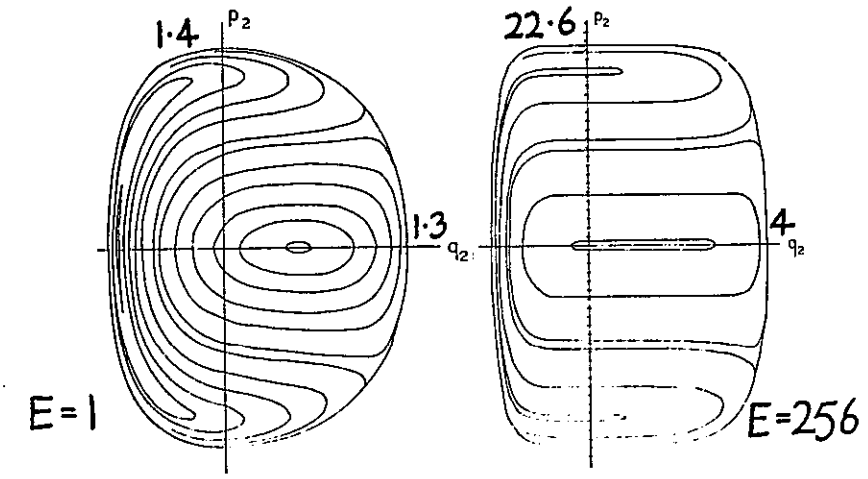

Fig. 37

theory: "most" perturbed orbits will still lie on tori. The perturbation theory gives a series for an extra constant of the motion $F(\underline{p},\underline{q})$, additional to H. It was calculated through eighth-order terms in the p's and q's. These trajectory computations suggest that the series converges - i.e. that F exists.

And indeed it does; Hénon found the following analytic form for it:

$$F(\underline{p},\underline{q}) = 8p_x(p_x^2 - 3p_y^2) + (p_x + \sqrt{3}p_y)\, e^{2y-2\sqrt{3}x} + (p_x - \sqrt{3}p_y)\, e^{2y+2\sqrt{3}x} - 2p_x\, e^{-4y}, \qquad (6.8)$$

$$\underline{p},\underline{q}\to 0 \qquad 12(yp_x - xp_y) \quad .$$

Therefore this constant "evolves" out of the angular momentum which is conserved for small E. The invariant curves could have been computed much more easily simply by using (6.6) and (6.8) with x=0, eliminating p_x in terms of E and finding $p_y(y)$ in terms of E and F.

Now comes the surprise. Instead of Toda's Hamiltonian (6.6), look at the *Hénon-Heiles potential*, which is its truncation after third-order terms:

$$H(\underline{q},\underline{p}) = \frac{p_x^2 + p_y^2 + x^2 + y^2}{2} + x^2 y - \frac{y^3}{3} . \qquad (6.9)$$

This is the system whose potential contours were sketched on fig. 1. It has been employed as a simulation of a three-atom solid, a vibrating triatomic molecule - which is really the same thing - and the "Hartree" averaged field seen by a star moving in the galaxy.

This system differs from Toda's in that it has a "dissociation energy" E=1/6, above which the energy surface is unbounded. Therefore we can "perturb" the oscillator (E=0) only with energies from 0 to 1/6. Bearing in mind, however, the integrability discovered for the Toda lattice for vast E's and the identity of the Hamiltonian's through cubic order, we do not expect very different behavior in the Hénon-Heiles case.

But we do get different behavior. On fig. 38, the left hand column shows the eighth-order-perturbation-theory-generated surfaces of section for various energies computed by Gustavson. Orbits would seem to lie on smooth invariant curves as a result of the new constant of the motion given by the perturbation theory. The right-hand column shows the "exact" trajectories through the surfaces of section. For E=1/24 and E=1/12 the mapping plane is covered with invariant curves identical with those given by perturbation theory.

Above E ≃ 1/9, however, Hénon and Heiles found that there are some orbits that do not seem to lie on invariant curves - the tori have been destroyed! The difference in behavior is dramatic: *all* the random looking dots on each of the E=1/8 and E=1/6 pictures were generated by one trajectory as it crossed S_y while wandering ergodically through *E*. At the same time, some tori persist, even up to (and actually above) the dissociation energy.

The kind of behavior is what the KAM theorem led us to expect. To begin to understand the destruction of tori in more detail, however, we must learn a bit more about mappings.

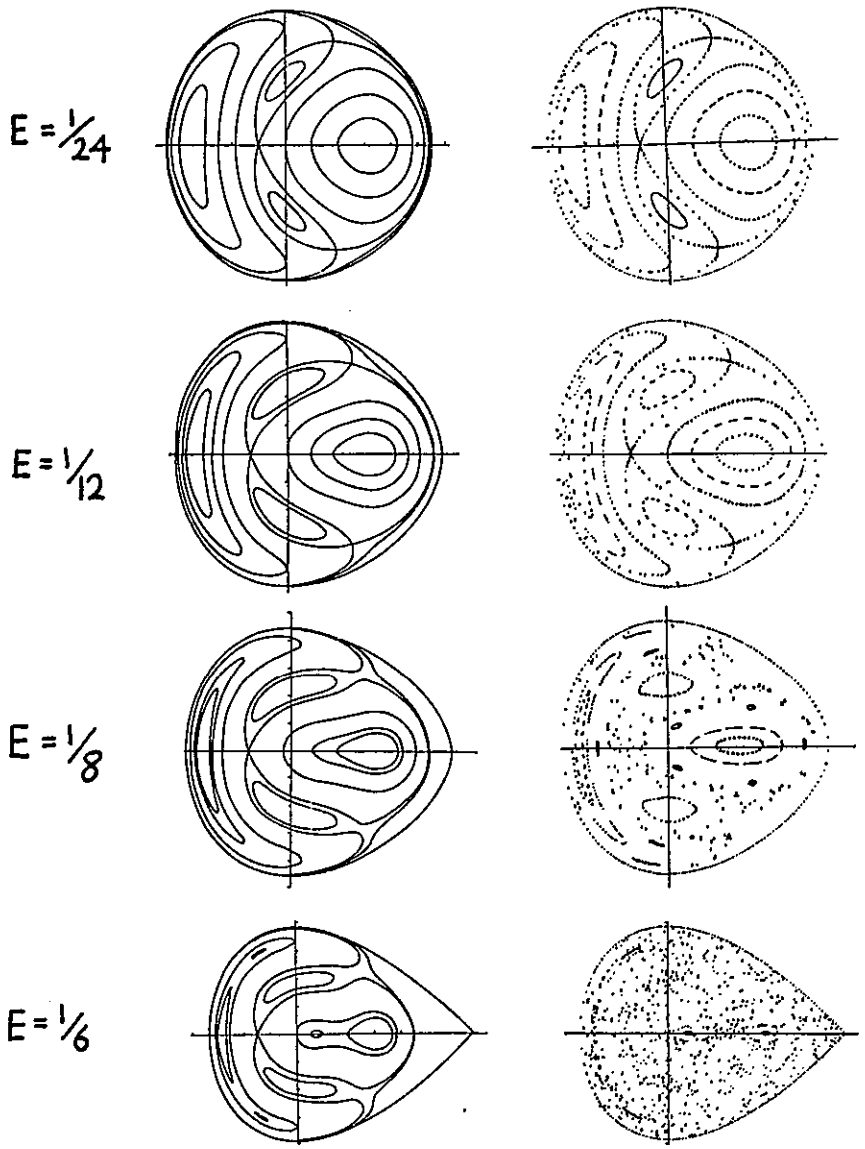

Fig. 38

7. TWIST MAPPINGS, FIXED POINTS, IRREGULARITY*

The tori of integrable systems intersect the surface of section S_x in concentric curves which in the simplest case are closed. It is natural to employ action-angle variables I_x, Θ on S_x, (fig. 39). Then $\rho \equiv \sqrt{2I_x}$ and Θ are polar coordinates on S_x. This is consistent, since the area of the S_x section of the torus I_x is (cf. 2.13).

$$\oint \underline{p}\, \underline{dq} = \oint p_x d_x = \pi \rho^2 = 2\pi I_x \,. \tag{7.1}$$

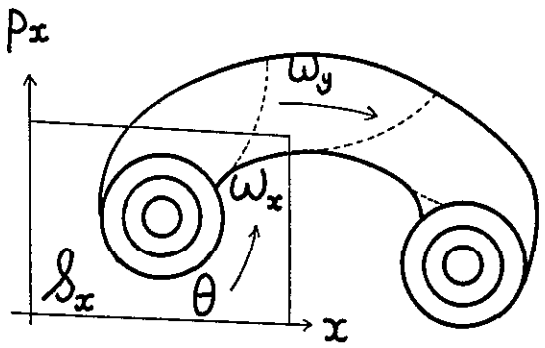

Fig. 39

The invariant curves are now circles on S_x (fig. 40).

The mapping of any trajectory conserves ρ (i.e. I_x) but changes Θ. If $t = 2\pi/\omega_y$ is the interval between crossings of S_x, then the angle Θ_1 at which a trajectory next intersects S_x if its initial angle was Θ_0 is

$$\Theta_0 = \Theta_1 + \omega_x t = \Theta_1 + 2\pi \frac{\omega_x}{\omega_y} \,. \tag{7.2}$$

Now

$$\frac{\omega_x}{\omega_y} \equiv \alpha(\rho) \tag{7.3}$$

* For reference, see Sec. 20 and App. 27 of Ref. 2, Secs. II.4 and III.6 of Ref. 17, Sec. 5 of Ref. 10.

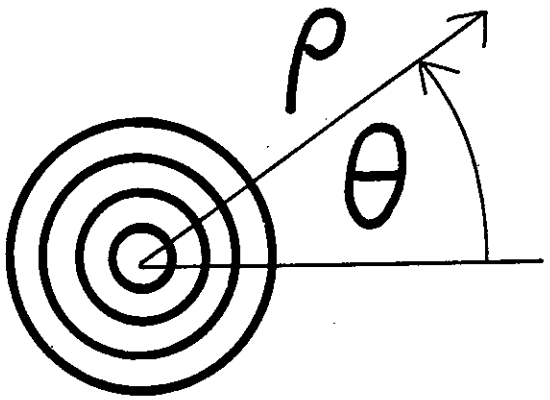

Fig. 40

is the frequency ratio on the torus considered. We have written α as a function of ρ only, because we are working at fixed E, so that specifying ρ (i.e. I_x) also determines the other action I_y. Thus, we have reduced an integrable system to the following "twist mapping" T

$$\left.\begin{aligned} \rho_1 &= \rho_0 \\ \theta_1 &= \theta_0 + 2\pi\alpha(\rho_0) \end{aligned}\right\} \begin{pmatrix}\rho_1\\ \theta_1\end{pmatrix} = T \begin{pmatrix}\rho\\ \theta\end{pmatrix} . \qquad (7.4)$$

$\alpha(\rho)$ is known as the "rotation number". We assume it to be a smooth function of ρ. Circles map to circles, radii to curved arcs through the origin O (fig. 41).

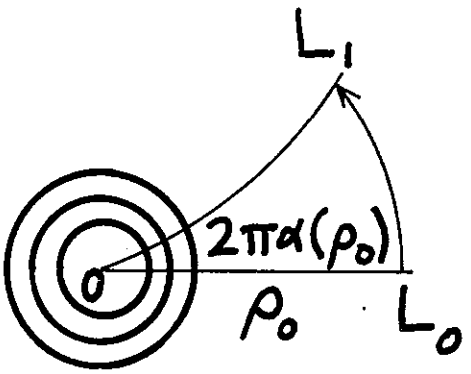

Fig. 41

Obviously T is area-preserving.

So far we have just restated known facts about integrable systems, but in a new language. Likewise, the KAM theorem can be restated: Perturb T into a new mapping T_ε, defined as

$$\left.\begin{aligned}\rho_1 &= \rho_0 + \varepsilon f(\rho_0,\theta_0)\\ \theta_1 &= \theta_0 + 2\pi\alpha(\rho_0) + \varepsilon g(\rho_0,\theta_0)\end{aligned}\right\} \begin{pmatrix}\rho_1\\ \theta_1\end{pmatrix} = T_\varepsilon \begin{pmatrix}\rho\\ \theta\end{pmatrix}, \tag{7.5}$$

where f and g have period 2π in θ_0, are so related as to preserve area, and have f=g=0 at ρ_0=0 so that 0 remains a fixed point. Then most points in S_x lie on smooth invariant curves (sections of tori) of T, that are distortions of the invariant circles of T. The only possible exceptions are near "commensurable" tori on which $\alpha(\rho_0)$ was rational. This is more restricted than our earlier statement of the KAM theorem (it applies only to 2 dimensions) and also more general in that T and T_ε can be *any* area-preserving mappings that need not originate in a Hamiltonian, and α, f and g need not be analytic but only smooth in the first 333 derivatives (this number has been reduced since the first proof by Moser).

The advantage of stating the problem in the geometric language of mappings is that it enables us to understand a little more about what happens in the "gaps" where commensurable tori (closed orbits) existed. Consider a "rational" unperturbed circle C,

$$\alpha(\rho_0) = \frac{r}{s} \qquad (r,\ s \text{ integers}). \tag{7.6}$$

Every point on C is a fixed point of T^s, since

$$T^s \begin{pmatrix}\rho_0\\ \theta_0\end{pmatrix} = \begin{pmatrix}\rho_0\\ \theta_0 + 2\pi s\ \alpha(\rho_0)\end{pmatrix} = \begin{pmatrix}\rho_0\\ \theta_0 + 2\pi r\end{pmatrix} = \begin{pmatrix}\rho_0\\ \theta_0\end{pmatrix}. \tag{7.7}$$

KAM tells us nothing about what happens to this circle of fixed points under T_ε. We might expect them all to be destroyed. This is not the case; in general, an even multiple of s, i.e. 2ks (k=1, 2,3 ...), fixed points remain under perturbation. This is the *Poincaré-Birkhoff fixed point theorem*, which we now prove.

Consider two circles C_+ and C_- between which lies the circle C on which α=r/s. On C_+, $\alpha > r/s$, and on C_-, $\alpha < r/s$. Therefore, T^s maps C_+ anti-clockwise, C_- clockwise, and C not at all (fig. 42).

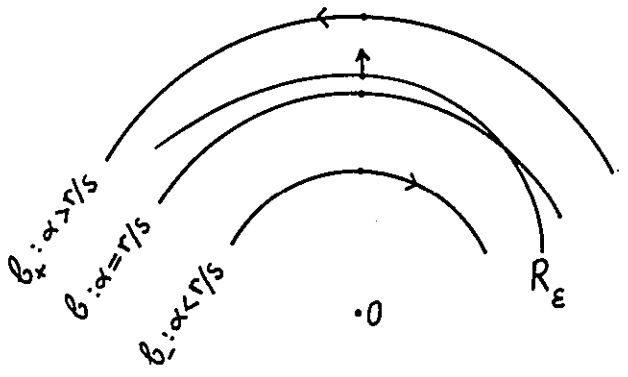

Fig. 42

Under the perturbed mapping T_ε^s these relative twists are preserved if ε is small enough. Thus, on any radius from 0 there must be one point whose angular coordinate is unchanged by T_ε^s. These "radially mapped" points make up a curve R_ε, close to C. Any of the sought-for fixed points of T_ε^s must lie on R_ε. Applying T_ε^s to R_ε generates another curve $T_\varepsilon^s R_\varepsilon$ (fig. 43). This image curve *must intersect* R_ε, because it must have the same area as R_ε and also enclose 0. Ignoring degenerate

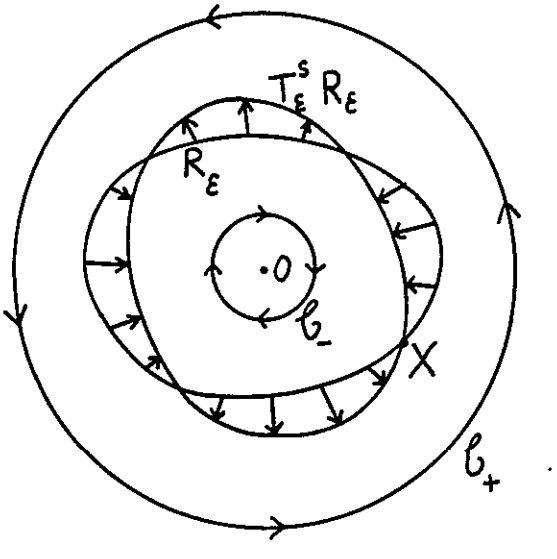

Fig. 43

cases of measure zero in which R_ε touches $T_\varepsilon^s R_\varepsilon$, we find that there must be an *even number* of these intersections.

Each intersection X is a fixed point of T_ε^s. However the orbit of X under T_ε consists of points

$$X,\ T_\varepsilon X,\quad T_\varepsilon^2 X \ldots T_\varepsilon^s X = X,\ T_\varepsilon^{s+1} X = T_\varepsilon X,\ \ldots \tag{7.8}$$

so that *all* the points on this orbit are fixed points of T_ε^s. The orbit has s distinct points on it, so that the number of intersections must be an even multiple of s: There are *2ks fixed points of* T_ε^s.

Therefore, some fixed points are preserved under perturbation. It is obvious from the method of proof that in general not all will be preserved - all but a finite number will be destroyed, so that formal techniques for calculating perturbed invariant curves (tori) must diverge. This can be rigorously proved for polynomial mappings, where TX is a polynomial function of the coordinates x_0 and y_0 of X. Then the fixed point equation for T^s, namely

$$T^s X = X, \tag{7.9}$$

consists of two polynomial equations in x and y, which by a theorem of Bézout have only a finite number of roots (fixed points).

The fixed points we have found are of two basic types, and we now examine these. The type of a fixed point is defined by the form of the nearby invariant curves. To examine these it is sufficient to *linearize* the mapping equations near the fixed point. Without loss of generality we can take the fixed point as the origin O of the mapping plane (q,p). Then the linearized mapping T must take the form

$$\begin{pmatrix} q_1 \\ p_1 \end{pmatrix} = \begin{pmatrix} T_{11}q_0 + T_{12}p_0 \\ T_{21}q_0 + T_{22}p_0 \end{pmatrix} \equiv (T) \begin{pmatrix} q_0 \\ p_0 \end{pmatrix}. \tag{7.10}$$

The nature of O is determined by the eigenvalues λ_1, λ_2 of the matrix T, which are given by

$$\det \begin{vmatrix} T_{11}-\lambda & T_{12} \\ T_{21} & T_{22}-\lambda \end{vmatrix} = 0\ . \tag{7.11}$$

Because the mapping is area preserving, det T is unity and

$$\lambda_2 = \lambda_1^{-1} . \tag{7.12}$$

Thus the eigenvalues are either *real numbers*, λ and λ^{-1}, or *complex conjugates on the unit circle* (because T is a real mapping); we examine these cases separately.

If λ_1 and λ_2 are *complex*, we can write

$$\lambda_1 = e^{i\alpha} , \quad \lambda_2 = e^{-i\alpha} , \tag{7.13}$$

and T can always be reduced, by a linear change of coordinates, to the form

$$\begin{pmatrix} q_1 \\ p_1 \end{pmatrix} = \begin{pmatrix} q_0 \cos \alpha - p_0 \sin \alpha \\ q_0 \sin \alpha + p_0 \cos \alpha \end{pmatrix} . \tag{7.14}$$

This is just a simple rotation by constant angle α, an obvious special case of the twist mapping (7.4); the invariant curves are circles. In the general case where the λ's are complex, the invariant curves are ellipses (fig. 44), and the fixed point 0 is said to be of *elliptic type*.

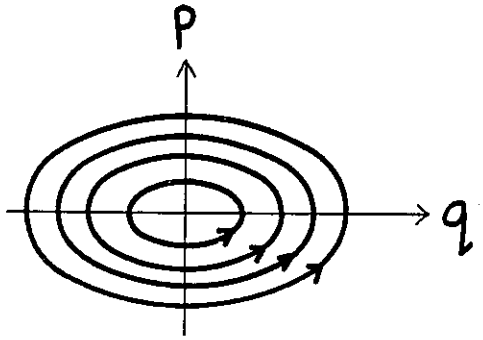

Fig. 44

Elliptic fixed points are *stable*, because any point ("orbit") near to 0 will remain near 0 after arbitrarily many iterations of T.

If the eigenvalues are *real numbers* λ (where $|\lambda|>1$) and λ^{-1}, the effect of T can always be reduced to

$$\begin{pmatrix} q_1 \\ p_1 \end{pmatrix} = \begin{pmatrix} \lambda q_0 \\ \frac{1}{\lambda} p_0 \end{pmatrix} \tag{7.15}$$

in which the invariant curves are hyperbolae p = const./q (fig. 45). Thus, this kind of fixed point is said to be of *hyperbolic type.* Actually there are two sorts of hyperbolic fixed point: the *ordinary hyperbolic point,* where $\lambda>0$ and the iterates of any point remain on one branch:

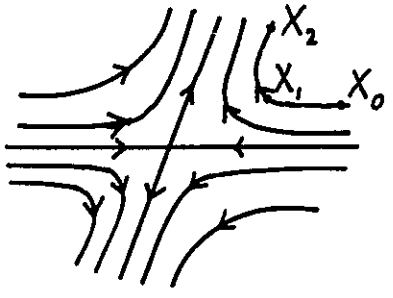

Fig. 45

And the *hyperbolic fixed point with reflection,* where $\lambda<0$ and the iterates jump back and forth between opposite branches (fig. 46).

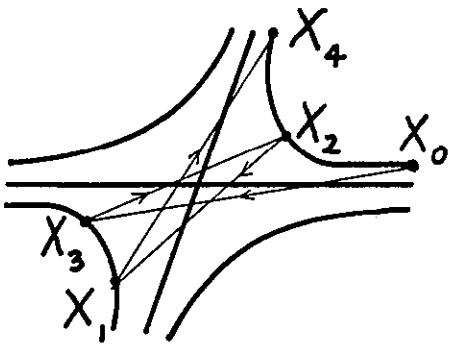

Fig. 46

We shall concern ourselves primarily with ordinary hyperbolic fixed points. Obviously, hyperbolic fixed points are *unstable,* because any point near to 0 but not at 0 will eventually map far away from 0.

Simple examples of elliptic and hyperbolic fixed points occurred in Section 2. The phase plane for the swing, for example, contains elliptic fixed points at p=0, $q=2n\pi$, and hyperbolic fixed points at p=0, $q=(2n+1)\pi$ (fig. 47). Another interesting case is that of plane motion under central force specified by a potential V(r). We take the surface of section as the "radial" plane (r,p_r) through the angle $\theta=0$. For fixed energy E, the orbit of the moving mass is restricted by the constancy of angular momentum I_2 (Eq. 2.31) to lie on the invariant curves

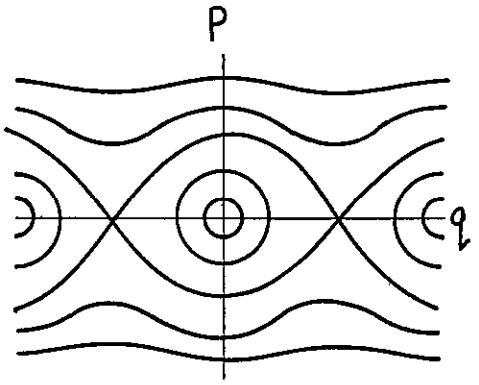

Fig. 47

$$p_r = \pm \left[2m(E-V(r) - \frac{I_2^2}{2mr^2} \right]^{1/2} \tag{7.16}$$

(cf. 2.33). The form of these curves is determined by

$$V_{eff}(r) = V(r) - \frac{I_2^2}{2mr^2} , \tag{7.17}$$

and of course by V(r), which we take to be of "Lennard-Jones" type (fig. 48). The system of invariant curves depends on E (fig. 49). The hyperbolic point corresponds to so-called *orbiting*, i.e. positive-energy spiral scattering.

Between the elliptic and parabolic cases lie the special, non-generic, set-of-measure-zero, infinitely-improbable-unless-you-deliberately-set-out-to-create-them *parabolic fixed points*, where $\lambda_1=\lambda_2=\pm 1$; we consider only the "ordinary" type, where $\lambda=+1$. Then T can always be reduced to

$$\begin{pmatrix} q_1 \\ p_1 \end{pmatrix} = \begin{pmatrix} q_0 + Cp_0 \\ p_0 \end{pmatrix} \tag{7.18}$$

where C is any constant. The invariant curves are straight lines (fig. 50). In the language of fluid mechanics, the parabolic case corresponds to simple shear flow, the elliptic case to a flow with vorticity-dominated stagnation point (the limiting case being a centre of pure rotation), and the hyperbolic case to a strain-rate-dominated flow (the limiting case being pure shear).

In the parabolic case there can actually be a *line* of fixed points (p=0 in fig. 50) . This is familiar! It occurs

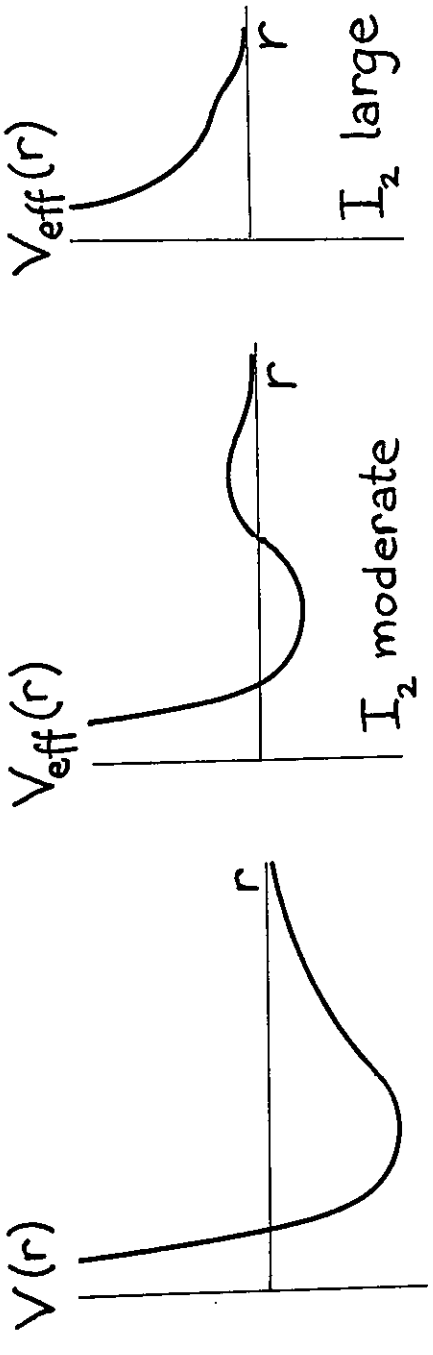

Fig. 48

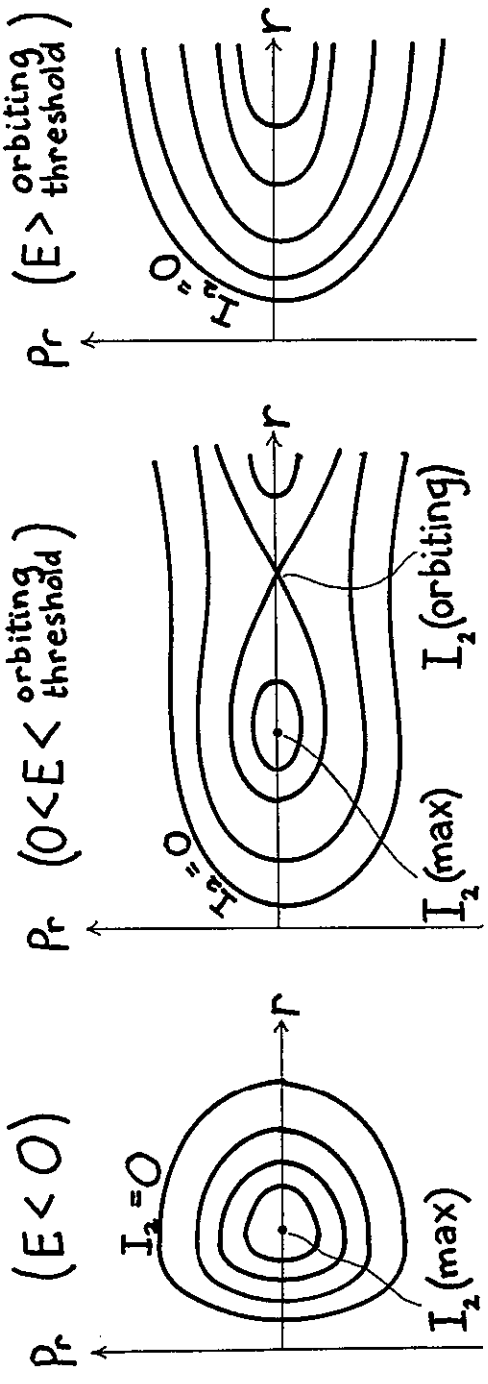
(E > orbiting threshold)
r
$I_2 = 0$
P_r
(0 < E < orbiting threshold)
r
$I_2 = 0$
I_2(orbiting)
I_2(max)
P_r
(E < 0)
r
$I_2 = 0$
I_2(max)
P_r

Fig. 49

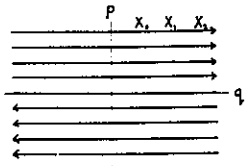

Fig. 50

in the unperturbed twist mapping (7.4) for every curve C whose rotation number is rational. This observation makes the Poincaré-Birkhoff fixed point theorem look rather inevitable, because under perturbation the curve C of parabolic fixed points "generifies" into a finite set of hyperbolic and elliptic fixed points whose eigenvalues λ are close to, but not exactly equal to unity. Hyperbolic *and* elliptic? Yes, and, moreover, in equal numbers. It is obvious from the continuity of arrows in the figure on fig. 43 that the fixed points on R_ε are alternately elliptic and hyperbolic (fig. 51). Because λ is close to unity, the hyperbolic points are *ordinary*. Therefore, we can now add something to the fixed point theorem: *of the 2ks fixed points of T_ε^s that remain after the break-up of the curve with rotation number r/s, precisely ks are elliptic, and ks hyperbolic, the two types forming an alternating sequence.*

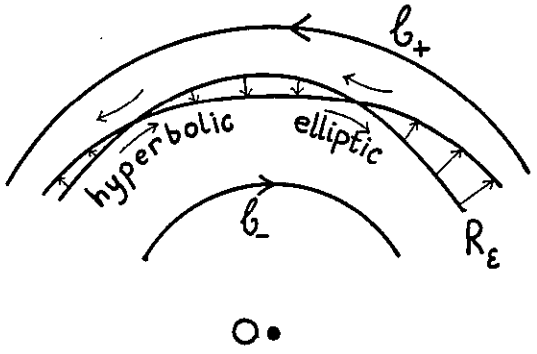

Fig. 51

We have not yet arrived at the point where the full structure of a perturbed twist mapping - i.e. a perturbed integrable system - is apparent. There are two further steps. The first concerns the *elliptic fixed points*, and follows from a *simultaneous* application of the KAM and Poincaré-Birkhoff theorems. These apply to *every* elliptic fixed point, in whose neighborhood there are closed invariant irrational curves. Where the rational curves used to be, a new structure of fixed points, half of which are elliptic, and in whose neighborhood there are closed invariant irrational curves, surrounded by *more* elliptic fixed points, and so on. Each elliptic fixed point is a microcosm of the whole, down to arbitrarily small scales. Schematically, this is shown on Fig. 52.

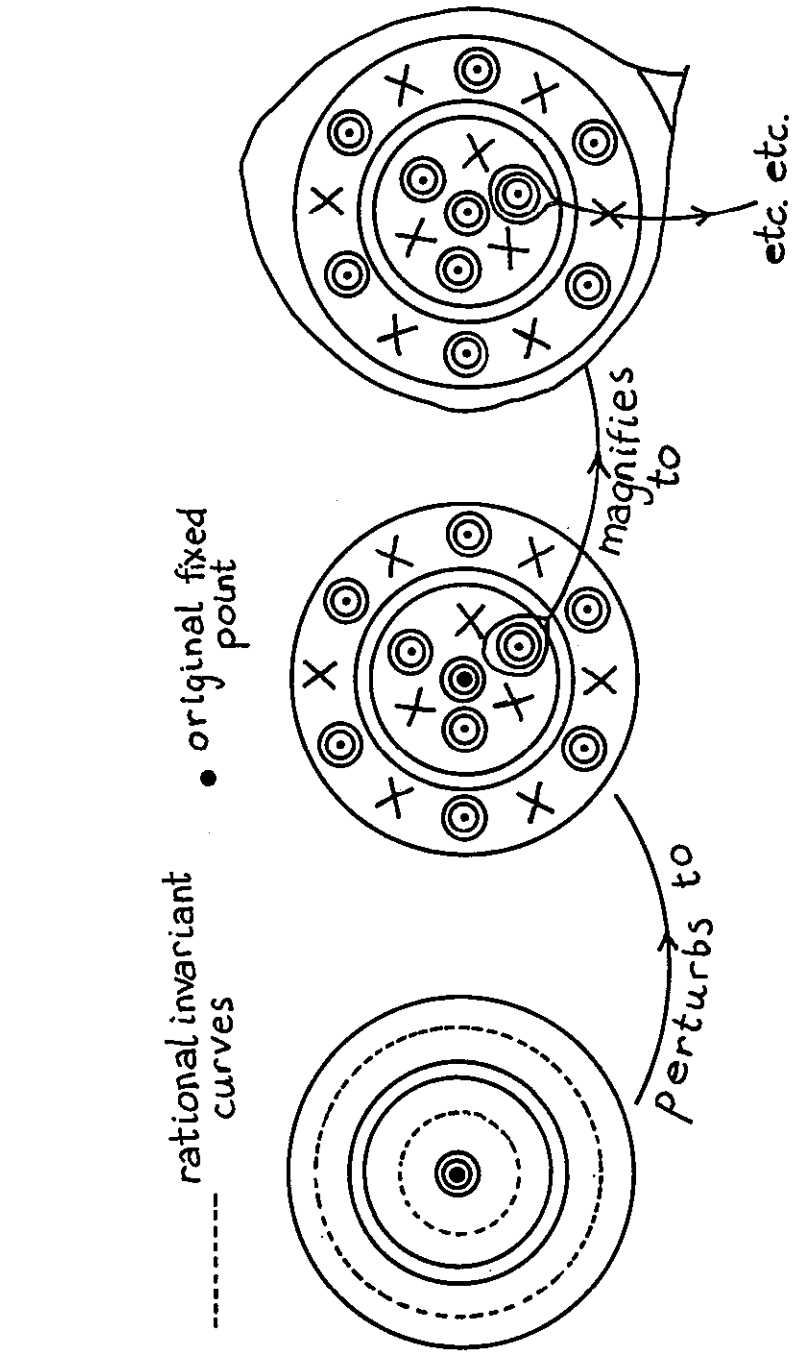
rational invariant curves
original fixed point
perturbs to
magnifies to
etc. etc.

Fig. 52

This is still not a complete picture: we have left gaps around the *hyperbolic fixed points*. Treatment of this region constitutes the second and final step in understanding the generic structure of these perturbed systems. At any hyperbolic point H, four invariant curves meet (fig. 53).

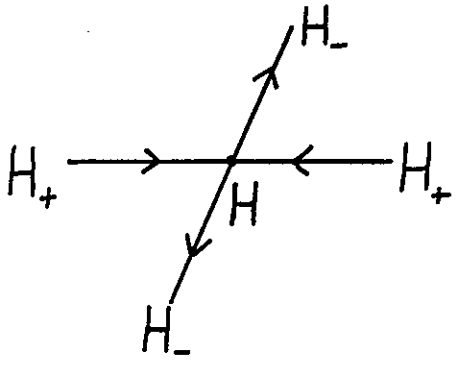

Fig. 53

Two of these are *ingoing* curves H_+, and the other two are *outgoing* curves H_-. A point X lies on H_+ if it arrives at H after infinitely many iterations of T, i.e.

$$T^s X \to H \text{ as } s \to \infty \text{ , if X is on } H_+ \text{ .} \tag{7.19}$$

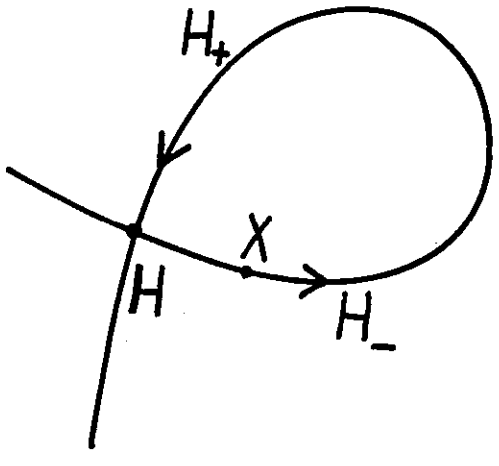

Fig. 54

Similarly, a point X is on H_- if it was at H infinitely many iterations ago, i.e.

$$T^{-s}X \to H \text{ as } s\to\infty \text{ , if X is on } H_- \text{ .} \tag{7.20}$$

Points on H_+ approach H infinitely slowly as $s\to\infty$, and points on H_- receded from H infinitely slowly at $s=-\infty$, as can be seen from the "standard form" (7.15) where H_+ was the axis p and H_- the axis q: as $s\to+\infty$ a point with $q_0=0$ maps onto

$$q_s = 0 \text{ ,} \qquad p_s = p_0/\lambda^s = p_0 e^{-s\ell n\lambda} \to 0 \text{ .} \tag{7.21}$$

What happens as we follow the arcs H_+ and H_- away from H? For integrable systems the arcs join smoothly, as on figs. 47 and 49. Any point X on this invariant curve (fig. 54) can be thought of as having started out at H, mapped out along H_- and homed in back to H along H_+ after a double infinity of iterations of T. More generally, when H is a fixed point of T^s rather than T, H is one member of a set of s hyperbolic fixed points corresponding to an unstable closed orbit, and the outgoing curve H_- from H joins smoothly with the ingoing curve H_+ belonging to one of H's neighboring hyperbolic points (fig. 55).

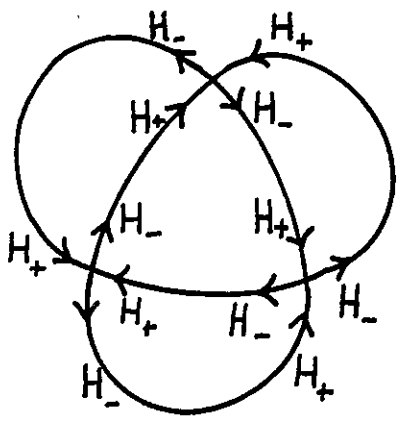

Fig. 55

But it is intuitively obvious (though hard to prove!) that this smooth joining is exceptional, nongeneric. So what happens generically? One thing that cannot happen is for any arc, say H_+, to intersect itself. For if such an intersection could occur, at X, say, then its image TX, and the image TX' of a neighboring point X', must lie close together (fig. 56). But the image TX" of the point X" shown on the sketch, cannot lie near to TX or TX', because it must be preceded by the image of the whole arc X" X'. This contradicts the continuity of the mapping (nearby points map to nearby points) and hence is impossible. Q.E.D.

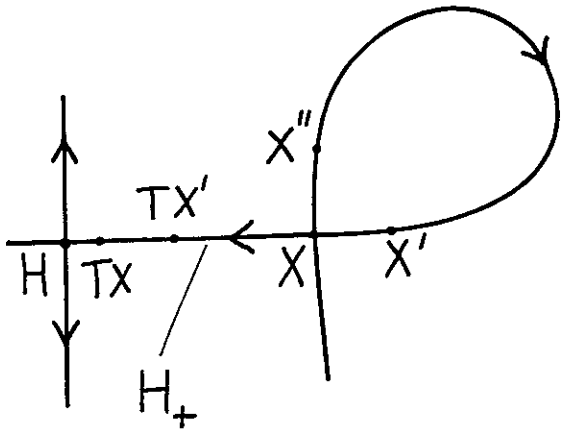

Fig. 56

However, it can and does happen that the arcs H_+ and H_- intersect *one another*. Points X where this occurs are called *homoclinic* if the arcs belong to the same fixed point H or to different points of the same unstable closed orbit, and *heteroclinic* if the arcs belong to two fixed points not associated with the same closed orbit. We consider only homoclinic points.

Consider a homoclinic point X. How do the curves $H_\pm$ continue beyond X? To answer this we must consider the iterates T^s ($-\infty < s < +\infty$) of the neighborhood of X. By continuity, these iterated neighborhoods must all resemble one another, and in particular the neighborhood of X. Therefore H_+ and H_- must cross in all these neighborhoods: just one homoclinic point is impossible, and the *existence of one implies an infinity of others!* Thus H_+ forms a series of loops intersecting H_-, and vice versa (fig. 58). More than this is true. *Every point* of the arc of H_- between two intersections 1 and 2 of H_+ is a further intersection. This follows from the area-preserving property of T: without further inter-

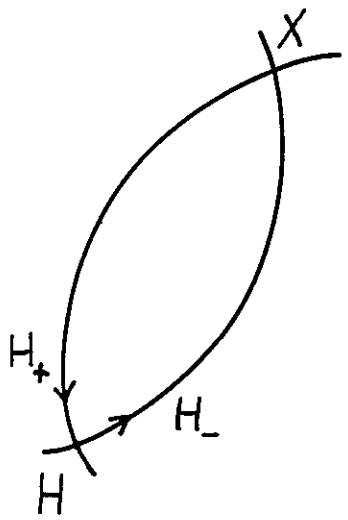

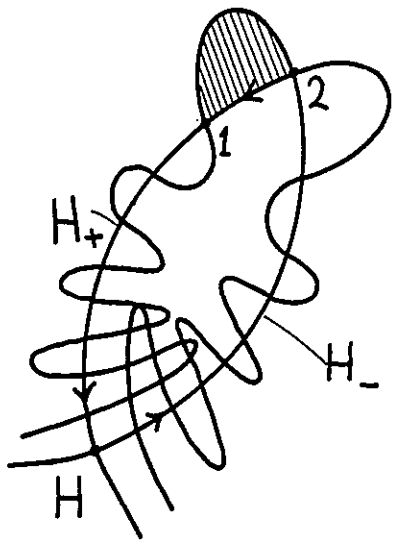

Fig. 57

Fig. 58

sections the shaded area would be mapped onto each succeeding loop without change of area, and this could not happen infinitely many times in a finite region. All this was known to Poincaré, who wrote:

"The intersections form a kind of lattice, web or network with infinitely tight loops; neither of the two curves (H_+ and H_-) must ever intersect itself, but it must bend in such a complex fashion that it intersects all the loops of the network infinitely many times.

One is struck by the complexity of this figure which I am not even attempting to draw. Nothing can give us a better idea of the compexity of the three-body problem and of all problems in dynamics where there is no holomorphic integral and (the canonical perturbation) series diverge".

If we do try to draw what happens (following Arnol'd, Moser and others) the result is Fig. 59.

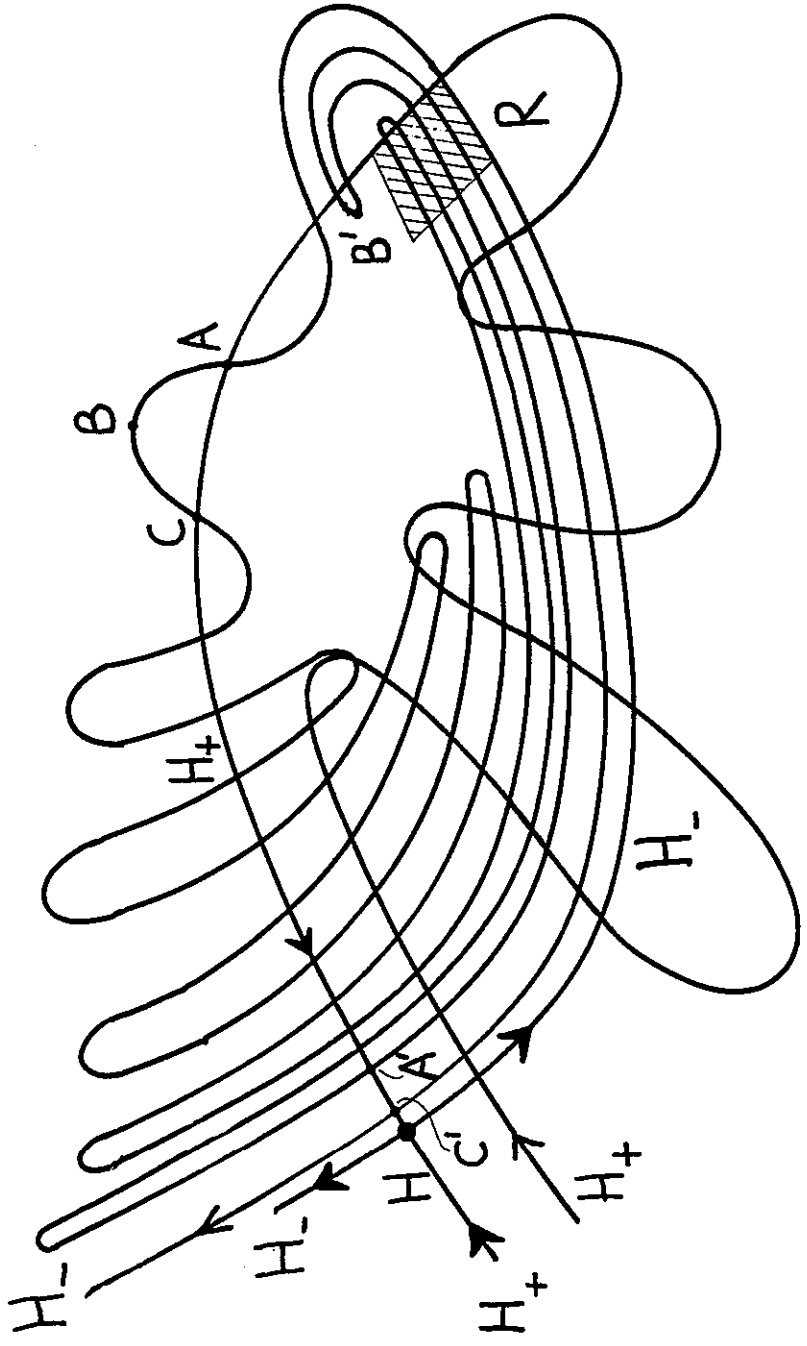

Fig. 59 (After Moser)

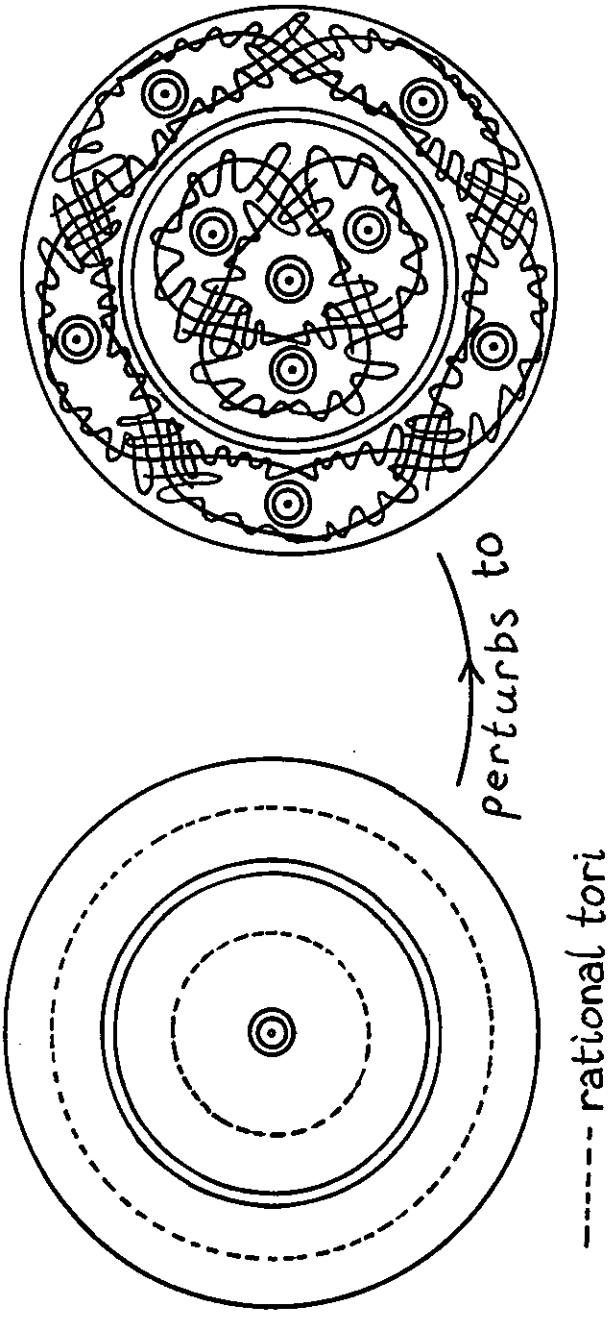

Fig. 60

This revelation of the marvelous complexity of behavior near a generic hyperbolic fixed point marks the entry of a new *stochastic* element into our discussion. For each point on an "early" loop (eg. the loop ABC of H_-)maps onto "late" loops that are ever more convoluted (eg. A'B'C') and wander over ever more extensive regions of the surface of section S. Indeed these invariant curves are in a sense *area-filling;* this follows from the "infinitely many intersections" property. Therefore a point X will eventually map arbitrarily close to any other point in the region considered. Smooth invariant curves do not exist in this region of S. Tori do not exist in this region of phase space! We shall return to these stochastic regions, generated by hyperbolic fixed points, in the last section. Meanwhile we complete the description of generically perturbed integrable systems.

The pictures on Fig. 52 had gaps near the hyperbolic fixed points. Now we can fill them in, at least roughly (fig. 60): they are dense with homoclinic points.

I do not know who first drew this astonishing picture; but even the detail shown is a woefully inadequate approximation to the true situation. What a wonderful hierarchy! Near each rational invariant curve there are hyperbolic fixed points with associated chaotically wandering curves, and elliptic fixed points surrounded with invariant curves which repeat the whole structure ad infinitum (or ad $\hbar$ - see Section 9) - a lacework of intimate intermixing of integrable and stochastic motions.

It must be emphasized that all this is in no sense pathological. It is the *generic situation* for solutions of Hamilton's equations. (For systems that are not both classical and Hamiltonian, however - e.g. dissipative or quantal systems - some of this richness of structure is smoothed away.)

There is a great deal of numerical evidence for the correctness of the picture of motion that we have been describing. The studies by Hénon and Heiles of the Hamiltonian (6.9) are a good example. On the E=1/12 section there are three hyperbolic fixed points. On the E=1/8 section these have all disappeared, and their neighborhood is filled by an irregular trajectory. At the limit of computer accuracy, one of the invariant curves surrounding the rightmost elliptic point has broken into a chain of five "islands"- that is, five elliptic points representing fixed points of T^5, each surrounded by *their* invariant curves.

To study details of the convoluted invariant arcs near hyperbolic fixed points is difficult, because it requires a whole curve to be mapped, not a single point. *Any* arc joining two (or the same) hyperbolic points (fig. 61) must eventually map onto an invariant curve joining them (fig. 62). Contopoulos has used this technique on a problem similar to that of Hénon-Heiles. There is a closed unstable orbit of T^5 with hyperbolic fixed points $X_0 \ldots X_4$ (fig. 63). He starts with a straight arc $X_0 \rightarrow X_1$, and then iterates.

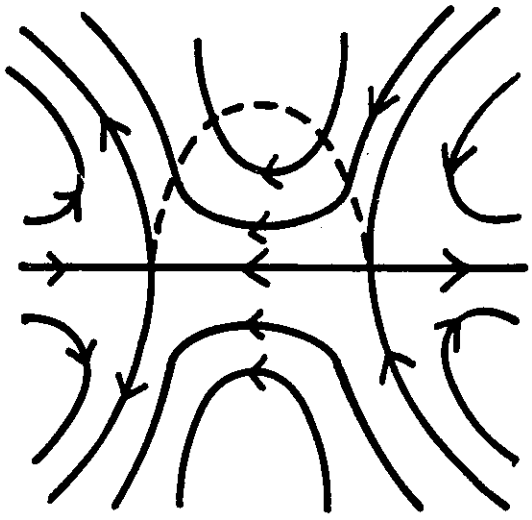

Fig. 61

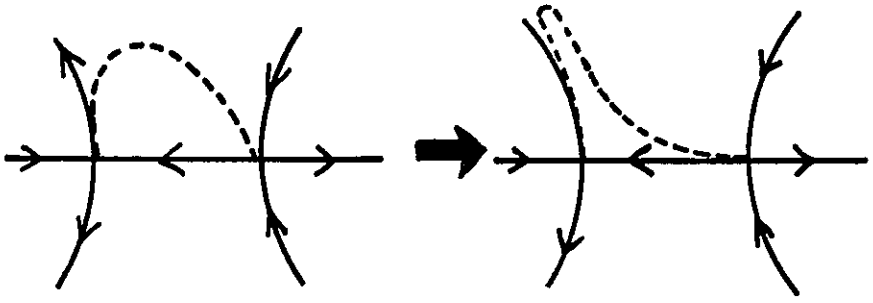

Fig. 62

The complicated outcome, even after just one cycle of iteration, is fully apparent. (Some invariant curves around elliptic fixed points are shown dotted.)

To study the hierarchy of elliptic fixed points is very time-consuming if the twist mapping is generated via a Hamiltonian, because the system's trajectory between intersections with S_x must be determined by solving the equations of motion. It is much easier to employ an *algebraic mapping*, where TX_0 is a simple explicit function of X_0. The simplest perturbed twist mapping is a quadratic addition to a rotation, and Hénon showed that no essential generality is lost by taking T as the following area-preserving mapping:

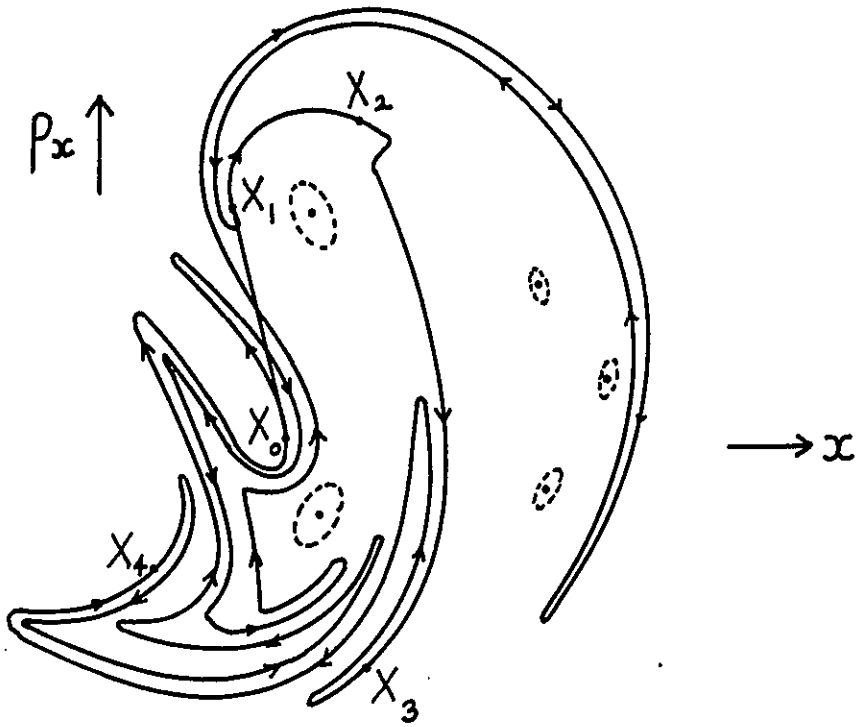

Fig. 63 (after Contopoulos)

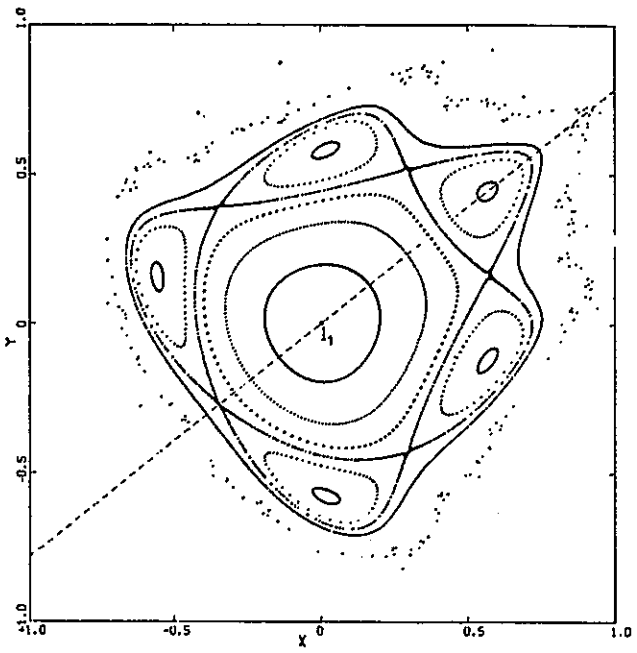

Fig. 64a

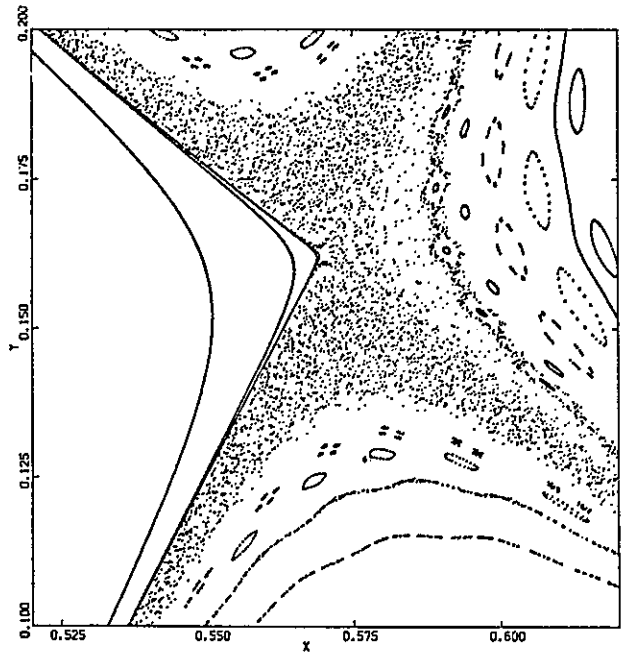

Fig. 64b

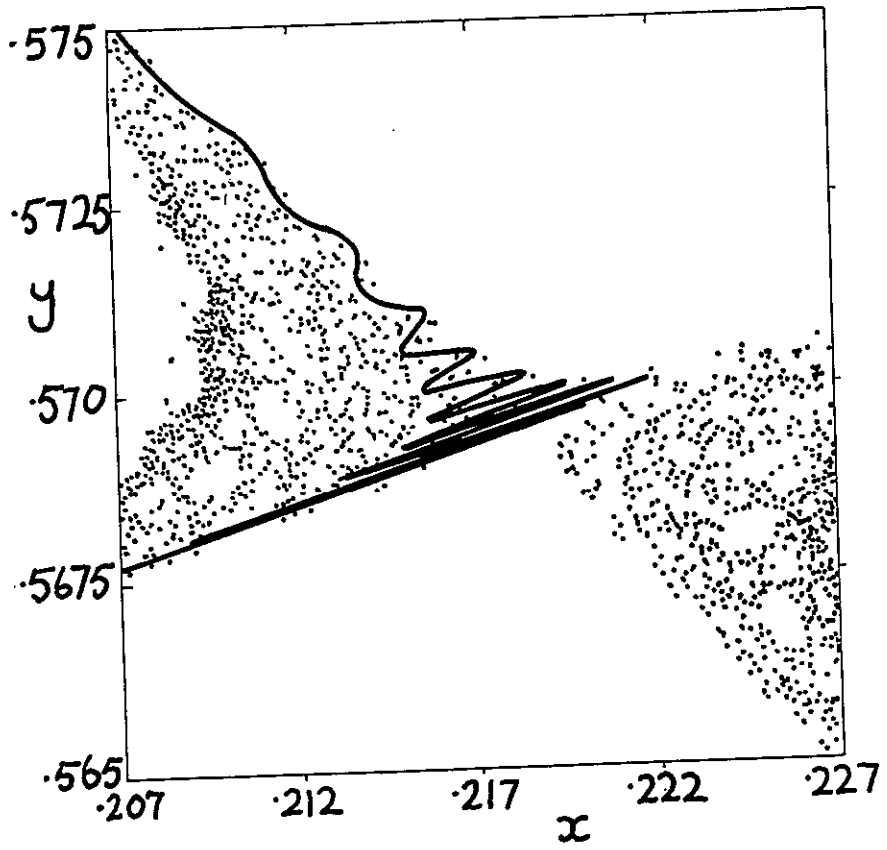

Fig. 65

$$\begin{pmatrix} x_1 \\ p_1 \end{pmatrix} = T \begin{pmatrix} x_0 \\ p_0 \end{pmatrix} = \begin{pmatrix} x_0 \cos\alpha - (p_0 - x_0^2)\sin\alpha \\ p_0 \sin\alpha + (p_0 - x_0^2)\cos\alpha \end{pmatrix}. \qquad (7.22)$$

This astonishingly simple transformation shows all the complexity we have been discussing. The angle α is fixed - it is a parameter of the mapping. The perturbation terms in x_0^2 are small near the origin 0, which is an elliptic fixed point of the unperturbed mapping. According to the KAM theorem, the perturbed mapping will also have closed invariant curves near 0. Far from 0 the perturbation is large and it is not hard to show that all points X escape exponentially fast to infinity under iterations of T.

The interesting region lies at moderate distances from 0. Fig. 64a shows Hénon's calculation of the mapping plane for $\alpha = 76.11^0$. Within the non-escaping region there is a chain of 5 elliptic islands around 0, interlaced with 5 hyperbolic points, all these being fixed points of T^5, exemplifying the Poincaré-Birkhoff theorem. The hyperbolic fixed points, which we expect to be the nuclei of irregular motion, look a bit fuzzy. Fig. 64b is Hénon's magnification of the region near the right most hyperbolic point. Not only is "area-exlporing" chaos nearly visible (the dots are 50,000 iterations of a single point!), but several stages of the hierarchy of islands can be seen as well. If the central fixed point is taken as zero-order, then first-, second-, and third-order islands can be seen in these beautiful pictures.

The Hénon mapping (7.22) also displays convoluted invariant curves in the irregular regions near hyperbolic fixed points. Using $\alpha = 66.42^0$ Cuthill (unpublished) mapped a short line segment emanating from one of the six hyperbolic points. After 146 iterations the line stretched into the irregular region near the next hyperbolic point and had begun to oscillate, as fig. 65 shows. (The line segment was of length 0.012 and it was necessary to include 55000 points on it in order for the line not to separate into dots when stretched by the mapping. The distance between neighboring hyperbolic points is about 0.5.)

We end this section with a few disconnected remarks. After introducing hyperbolic points with reflection (in whose neighborhoods iterates of a point zig-zag between opposite invariant curves), we never mentioned them again. They can arise for large perturbations by the "conversion" of elliptic fixed points with rotation angles near π (i.e. eigenvalues near -1), and give rise to strongly irregular behavior in generic cases.

Likewise, we have not considered heteroclinic points (intersections of invariant curves through fixed points of different closed orbits). These must always occur along with the homoclinic points that we found to be the source of irregular behavior, because there were infinitely many other rational tori within the destroyed zone near a low-order rational torus. In fact Chirikov has analyzed ir-

regularity in physical terms precisely by considering these "overlapping resonances" and the associated heteroclinic points.

Next, here is an imperfect analogy that might help in understanding the structure in phase space whose sections the perturbed twist mappings represent. Imagine winding a cable starting from a "primary" single loop of thin wire (fig. 66). Cover it with concentric sheaths of plastic (tori). Interrupt this sheathing to find

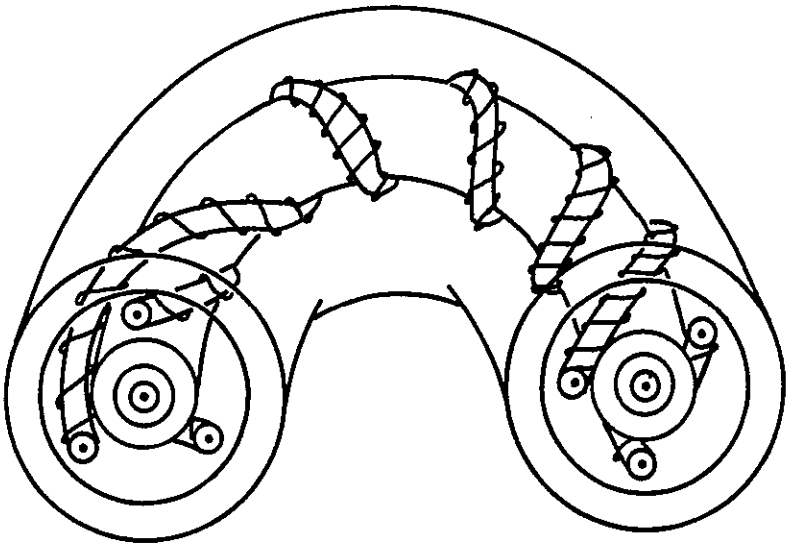

Fig. 66

a secondary sheathed loop in a spiral about the primary, to close after a few windings. On this secondary loop are tertiary, quaternary, ... windings. Continue the interrupted primary sheathings to surround the secondaries. Repeat ad infinitum. When this process has been completed, there will be some vacant spaces. Fill each with an infinitely long, tangled wire. Mathematicians have recently begun to study such structures, called, not surprisingly, "solenoids".

Finally, remember that the last two sections have dealt in detail only with systems with two degrees of freedom. These have a special property: the (two dimensional) tori stratify the (three-dimensional) energy surface E. Therefore the irregular orbits, which wander through regions where rational tori have been destroyed, are trapped between remaining irrational tori, and can explore a region of E which, while three-dimensional, is nevertheless restricted, and in particular, disconnected from other irregular regions in E (fig. 67). For more degrees of freedom, however, the tori do not stratify E. When N=3, for example, the tori are three-dimen-

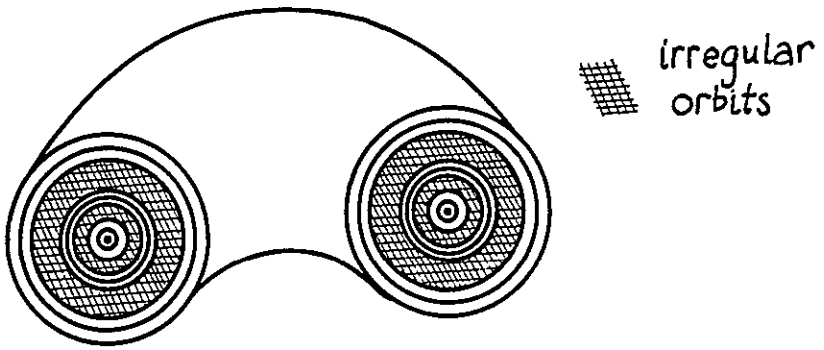

Fig. 67

sional while E is five-dimensional. Then the gaps form one single connected region, and it is conceivable, although unproven, that one single irregular orbit might cover them all. The tori are then a bit like lines in three dimensions (fig. 68). The possibility of so-called "Arnol'd diffusion" of the irregular orbits means that for N>2 the existence of invariant tori for perturbed motion is no guarantee of stability of motion, since irregular wandering orbits, that are not trapped, exist arbitrarily close to tori.

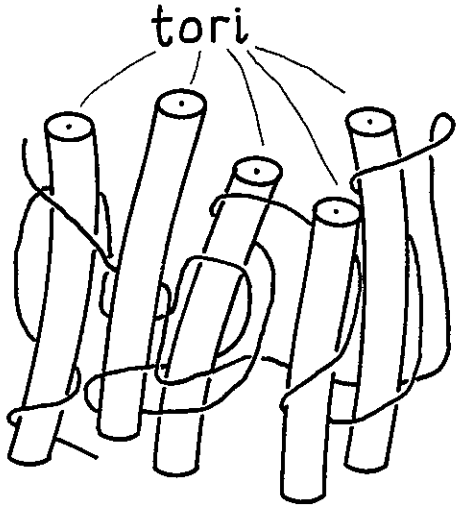

Fig. 68

8. STRONGLY IRREGULAR MOTION*

We have traced the origin of irregular motion in dynamical systems to hyperbolic fixed points of associated area-preserving mappings. If, therefore, we want models for strongly irregular motion, it is obviously sensible to try to find mappings *all* of whose fixed points are hyperbolic. (Clearly such mappings will not be perturbed twist mappings, and the corresponding dynamical systems will not be close to integrable.)

One such example is *Arnol'd's cat map* on the unit 2-torus (fig. 69).

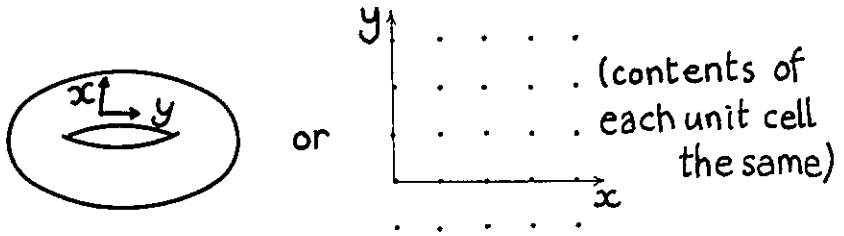

Fig. 69

The map is

$$\begin{pmatrix} x_1 \\ y_1 \end{pmatrix} = \begin{pmatrix} 1 & 1 \\ 1 & 2 \end{pmatrix} \begin{pmatrix} x_0 \\ y_0 \end{pmatrix} \equiv (T) \begin{pmatrix} x_0 \\ y_0 \end{pmatrix} . \qquad (8.1)$$

This is a special case of "rational linear automorphisms of the torus", where the matrix can have any integral coefficients. The eigenvalues of T^n and λ^n and λ^{-n}, where

$$\lambda = (3 + \sqrt{5})/2 , \qquad (8.2)$$

so that any fixed points of T^n (closed orbits) must be of hyperbolic type. Any point on the torus for which x_0 and y_0 are rational fractions is a fixed point of T^n for some n - the n's becoming larger with the denominators of the fractions - and these rationals are the *only* fixed points (because T has integer coefficients). Thus (0,0) is the fixed point of T, and (2/3, 1/5) and (3/5, 4/5) are fixed points of T^2.

* See also Sec. 3 of Ref. 10, Ch. 3 of Ref. 17, and Ch. 1-3 of Refs. 2, 6 and 7.

The mapping (8.1) shears each unit cell as shown in fig. 70.

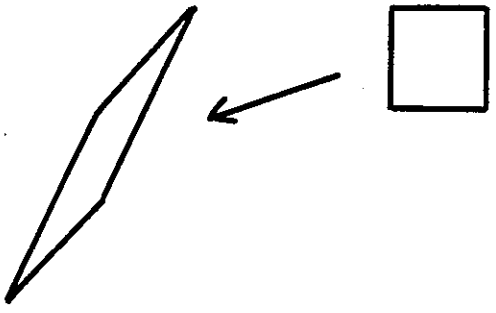

Fig. 70

What this does to a cat on the torus is shown in fig. 71. After just two iterations, the cat is wound around the torus in complicated filaments. Any small area element will ultimately (after T^{∞}) wrap densely round the torus, because its behavior under T repeats in microcosm that of the unit cell: it stretched by λ in one direction, and contracts by λ in a perpendicular direction (the angle, 58.3^{0}, made by the stretch axis with Ox, has the golden section $(\sqrt{5}+1)/2$ as its tangent). The disintegration of the cat arises from the unstable, hyperbolic, nature of T, which causes initially close points to map far apart.

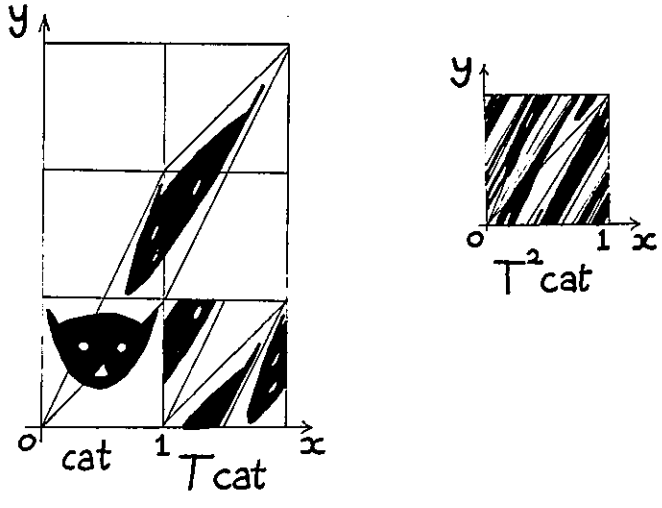

Fig. 71 (After Arnol'd and Avez).

Arnol'ds cat map has *homoclinic points* - intersections of the ingoing and outgoing curves H_+ and H_- for a hyperbolic fixed point - and we found earlier that these are associated with irregular behavior. To find the homoclinic points of the fixed point (0,0) of T, simply draw the axes of stretch (H_-) and compression (H_+) from (0,0). These are irrational directions and so wrap densely round the torus (fig. 72), never intersecting themselves but intersecting one another infinitely often. They also intersect the invariant curves of the other fixed points (of $T^{n\neq 1}$) in densely distributed *heteroclinic* points.

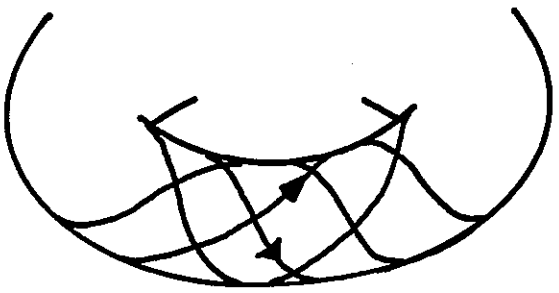

Fig. 72

This behavior under $T^{n\to\infty}$ is clearly *ergodic*: "time" averages over the iterates of any point (x_0,y_0) equal "space" averages over the torus, since any set of iterates eventually covers the torus. However, the cat map has a stronger property: *mixing*. This means that after T^{∞} not only does the entire past of a point cover the space, but so also does the present of any neighborhood of the original point. In other words, the area elements get ever more drawn out and eventually cover the space. Mixing implies ergodicity, but ergodicity does not imply mixing. For an example of this, recall the phase-space tori of Section 2, on which integrable systems live. If the frequencies are incommensurable, any orbit densely fills the torus - the orbit is ergodic on the torus (though not on the whole energy surface!). However, the (continuous) mapping of any point on the torus (eq. 2.35) is such as to *translate* the whole torus rather than distort it, so that neighboring points map together and this system is non-mixing (fig. 73).

It is not only mappings of the plane that exhibit mixing; "real" dynamical systems show it too. Perhaps the most important

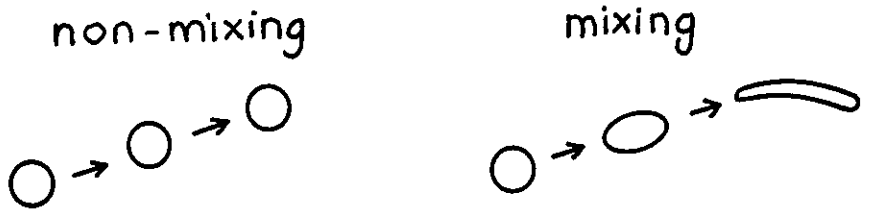

Fig. 73

of these is the *hard-sphere fluid*, whose mixing was finally rigorously established by Sinai about ten years ago. Because of the infinite contact potential this is obviously not a perturbation of any simpler system (e.g. non-interacting particles). As with Arnol'd's cat, the mixing arises from the unstable nature of the motion, and in this case the instability is the result of collisions between the spheres' convex surfaces.

The instability is well illustrated by a calculation due to Chirikov, which also shows how unpredictable these mixing systems are, *even in principle*. No hard-sphere fluid is isolated, for it is impossible to screen out at least gravitational perturbations. Therefore let the fluid (sphere radius r, mean separation ℓ, mean particle speed V) be perturbed by a mass M a distance D away (fig. 74).

Consider a molecule 1 moving to collide with 2. Both 1 and 2 will fall towards M, but at different rates, and the tidal (i.e. relative) acceleration will be (order of magnitude)

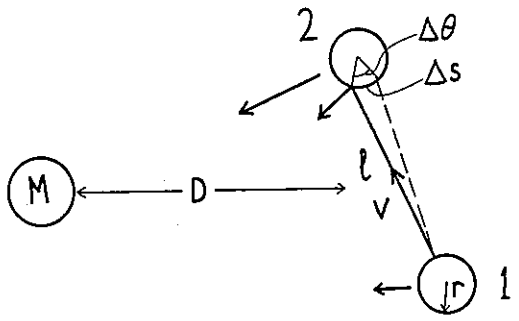

Fig. 74

$$a \sim \frac{GM\ell}{D^3} . \qquad (8.3)$$

This will render 1's position of impact on 2 uncertain by

$$\Delta S \sim \frac{a\ell^2}{V^2} , \qquad (8.4)$$

and its angle of reflection uncertain by

$$\Delta\Theta \sim \frac{\Delta s}{r} = \frac{GM\ell^3}{D^3V^2r} . \qquad (8.5)$$

This in turn will render the reflection angle after succeeding collisions uncertain by $(\ell/r)\ \Delta\Theta$, $(\ell/r)^2\ \Delta\Theta$, $(\ell/r)^3\ \Delta\Theta$ ..., so that the number, n, of collisions after which the determinacy is lost (angle uncertain by 1 radian) is

$$n \sim \frac{\ell n(1/\Delta\Theta)}{\ell n\ \ell/r} = \frac{\ell n\ (\frac{D^3V^2r}{GM\ell^3})}{\ell n\ \ell/r} . \qquad (8.6)$$

Now let the fluid be oxygen at NTP and let M be an electron at the limit of the observable universe, i.e. $D\sim10^{10}$ light years. Then we get n~56! If the spheres are billiard balls (r~3cm,ρ~30cm, $V\sim1ms^{-1}$) and M is someone in the billiard-room (M~50kg, D~1m), then we get n~9! Unstable indeed! It would be amusing to work out the effects of these perturbations on the electrons in computers doing molecular dynamics calculations. (The uncertainty arising from quantum mechanics gives n=0 for oxygen - i.e. even the first collision cannot be accurately "aimed" - and n=15 for billiard balls.)

It is worth emphasizing that Sinai's proof that hard spheres form a mixing system is valid not only in the "thermodynamic limit" (exceeding one!). The simplest case is two discs, moving on a closed two-dimensional surface with Euclidean metric; this has to have the topology of a torus. Even if one disc is fixed (a hole in the torus) the motion of the other is mixing (fig. 75).

Another mixing system is a mass point moving on a geodesic on a closed surface whose Gaussian curvature (product of two principal curvatures) is negative everywhere. (This is rather unimaginable in that a closed negatively-curved surface cannot be embedded in a Euclidean 3-space, but in its four-dimensional form it may have cosmological implications.) The essential point is that on such a surface two geodesics that are close and parallel at some point will separate exponentially for past and future times (fig. 76): this

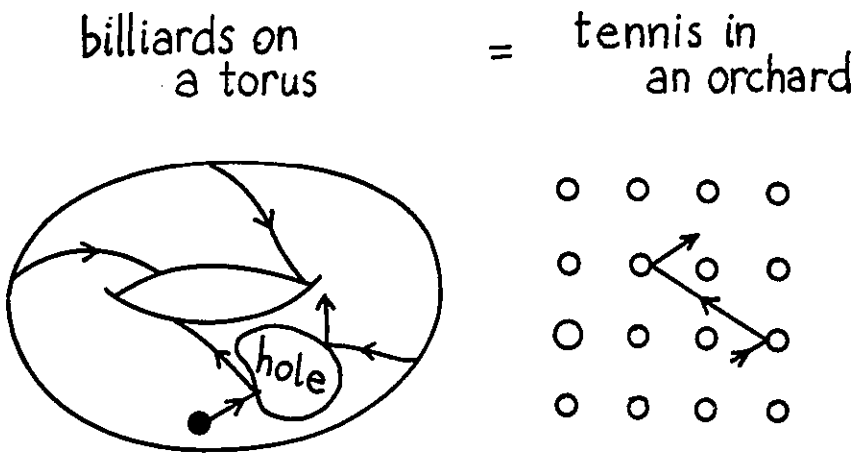

Fig. 75

contrasts with the convergence that occurs on positively-curved surfaces, e.g. spheres. This behavior can be derived from the fact that a geodesic is a space curve, lying in the surface, whose principal normal always coincides with the surface normal. The "torus billiard table" is actually a special case of this negative-curvature system.

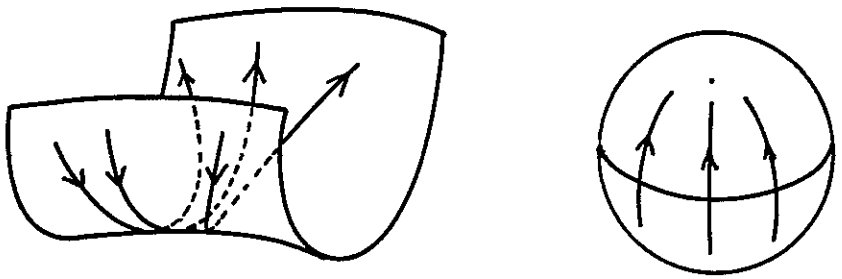

Fig. 76

Now we understand, at least in outline, how ergodicity, mixing and loss of determinacy arise. We have yet to consider the *approach*

to equilibrium, and *randomness*. As a model for these two kinds of behavior, we now discuss the *Baker's transformation*. This is the following area-preserving map on the unit square (x,y):

$$\left.\begin{aligned}\begin{pmatrix}x_1\\y_1\end{pmatrix} &= \begin{pmatrix}2x_0\\y_0/2\end{pmatrix} \quad \text{if } 0 \le x_0 < 1/2\\ &= \begin{pmatrix}2x_0-1\\\dfrac{y_0+1}{2}\end{pmatrix} \quad \text{if } 1/2 \le x_0 < 1\end{aligned}\right\} . \tag{8.7}$$

Pictorially, the map transforms as shown on fig. 77.

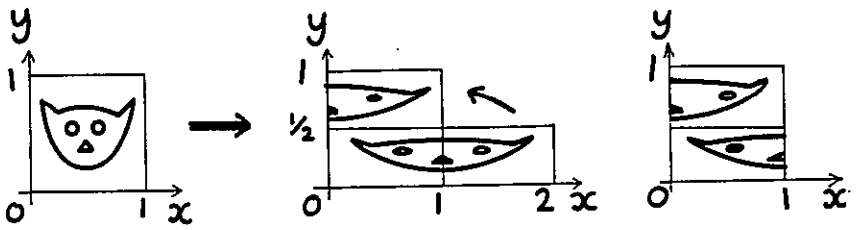

Fig. 77

The process resembles the rolling-out of dough; hence the name. Any area element will ultimately stretch into a long horizontal filament crossing the square many times. Therefore the map is mixing and hence ergodic.

The Baker's transformation is perfectly deterministic and reversible (time-reversal gives a similar mapping with stretching along y instead of x). To demonstrate the inexorable approach to equilibrium it is necessary first to define a distribution function $f_n(x,y)$ after n iterations. The "Liouville" equation of motion for $f_n(x,y)$ is, from (8.7),

$$\begin{aligned}f_n(x,y) &= f_{n-1}\left(\frac{x}{2}\,,\ 2y\right) \quad \text{if } 0 \le y < 1/2\\ &= f_{n-1}\left(\frac{x+1}{2}\,,\ 2y-1\right) \quad \text{if } 1/2 \le y < 1\,.\end{aligned} \tag{8.8}$$

Next we must coarse-grain f_n to remove some of its fine-scale information. We do this by defining

$$W_n(x) \equiv \int_0^1 dy\ f_n(x,y) \ . \tag{8.9}$$

This corresponds to integrating out uninteresting phase-space variables in a mechanical problem. From (8.8) we get W's equation of motion:

$$W_n(x) = \int_0^{1/2} dy\ f_{n-1}(\tfrac{x}{2},\ 2y) + \int_{1/2}^1 dy\ f_{n-1}\ (\tfrac{x+1}{2},\ 2y-1) \ , \tag{8.10}$$

i.e.

$$W_n(x) = 1/2\ [W_{n-1}(\tfrac{x}{2}) + W_{n-1}(\tfrac{x+1}{2})] \ . \tag{8.11}$$

If $f_n(x,y)$ is normalized to unity, so is $W_n(x)$, and this equation preserves that normalization under iteration.

The "equilibrium" solution $W_n(x)=1$ obviously satisfies (8.11). Moreover, *any* initial $W_0(x)$ will tend to unity after an infinity of iterations, since one iteration replaces the value of W at x by the mean of its values at two points (x/2 and x+1/2) surrounding x - i.e. the mapping has a smoothing effect. It is amusing to verify this by showing how iteration must destroy all Fourier components $e^{2\pi i \ell x}$ (ℓ=1,2,3...) describing the variation of $W_0(x)$. From (8.11),

$$e^{2\pi i \ell x} \to \frac{(1+e^{\frac{2\pi i \ell}{2}})e^{\frac{2\pi i \ell x}{2}}}{2} \to \frac{(1+e^{\frac{2\pi i \ell}{2}})}{2}\frac{(1+e^{\frac{2\pi i \ell}{4}})}{2} e^{\frac{2\pi i \ell x}{4}} \to \tag{8.12}$$

$$\ldots \prod_{n=1}^{\infty} [\frac{1+e^{\frac{2\pi i \ell}{2^n}}}{2}] \ .$$

A bracket n in this product must always vanish, since this requires

$$\frac{2\pi\ell}{2^n} = (2m+1)\pi \ , \text{ i.e. } \ell = 2^{n-1}(2m+1) \ , \tag{8.13}$$

for some m, so that any odd-ℓ components vanish on the first itera-

tion, and any even ℓ must be 2^n times an odd number for some n. Thus any initial $W_0(x)$ does indeed iterate to equilibrium.

Equation (8.11) for $W_n(x)$ resembles the "rate equation" for a random walk process (steps to x from x/2 and (x+1)/2), and we now show that the Baker's transformation (8.7) does indeed have a stochastic character. Let x_0 and y_0 each be represented by a binary "decimal":

$$x_0 = .a_1a_2a_3a_4 \cdots \qquad \text{(a's and b's all 0 or 1).}$$
$$y_0 = .b_1b_2b_3b_4 \cdots \qquad (8.14)$$

Put these "back to back":

$$\{\cdots\cdots b_4b_3b_2b_1 \cdot a_1a_2a_3a_4 \cdots\cdots\} . \qquad (8.15)$$

The Baker's transformation corresponds to a shift of the decimal point one place to the right! This is because such a shift doubles x and halves y, and automatically takes care of the conditions arising if $x_0 \gtrless 1/2$. Let us agree to label the orbit of (x_0,y_0) a sequence of 0's and 1's according to whether the iterated points have $x<1/2$ or $x>1/2$. Thus the sequence of numbers is just the sequence of first binary digits of the x-values of the iterated points, a doubly infinite sequence $-\infty < n < +\infty$. Because the Baker's transformation is isomorphic to the shift of decimal point in (8.15), and the first binary digit of x is the number immediately to the right of the decimal point, the sought-for sequence is simply

$$\{\cdots\cdots b_4b_3b_2b_1a_1a_2a_3a_4 \cdots\cdots\} . \qquad (8.16)$$

Now, "almost all" initial points (x_0,y_0) are *irrational*, so that the decimals (8.14) are nonterminating, nonrepeating sequences that could have been obtained by tossing a coin (0 = heads, 1 = tails).

Therefore almost all orbits in the Baker's transformation, although perfectly deterministic, can be made to generate a set of "random" numbers. (The exceptional orbits are the set-of-measure-zero closed orbits generated by rational initial points (x_0,y_0).)

The central mathematical tool that is used here is the correspondence between the system considered (Baker's transformation) and the so-called *Bernouilli shift on infinitely many symbols* (moving the · in 8.15). In recent years a number of such correspondences have been found, and it seems as if this idea goes right to the heart of the problem of finding randomness in deterministic systems. Most important, it has been shown that *near any homoclinic point of a mapping* another mapping can be found which corresponds to a Bernouilli shift. To describe this map, refer to fig. 59. In any

region R (e.g. the shaded quadrilateral) there will be a dense set of points P that eventually map back into R. The map $\tilde{T}$ in question is from P to its point of first return to R, $\tilde{T}P$.

Such homoclinic points, we learned, occur for generic Hamiltonian systems and not just for abstract algebraic mappings. Therefore, in real mechanical systems there are orbits describable by random sequences of integers, and we end this section with three examples of such systems. All involve a change in the unperturbed motion as energy varies, from bounded to unbounded.

The first example is *Sitnikov's case of the three-body problem.* Two equal "primary" masses M move in ellipses about their centre of mass O. The test mass, $m \to 0$, in whose motion we are interested, moves along the line OZ perpendicular to the plane in which the primaries move (fig. 78). Its orbit is z(t). The perturbation ε is the eccentricity of the primaries' ellipse. With suitable scaling (G=1, M=1/2, stretching of t coordinate) we have the distance r(t) of either primary from O as

$$r_\varepsilon(t) = \frac{1}{2}(1 - \varepsilon \cos 2t) + O(\varepsilon^2) \ . \qquad (8.17)$$

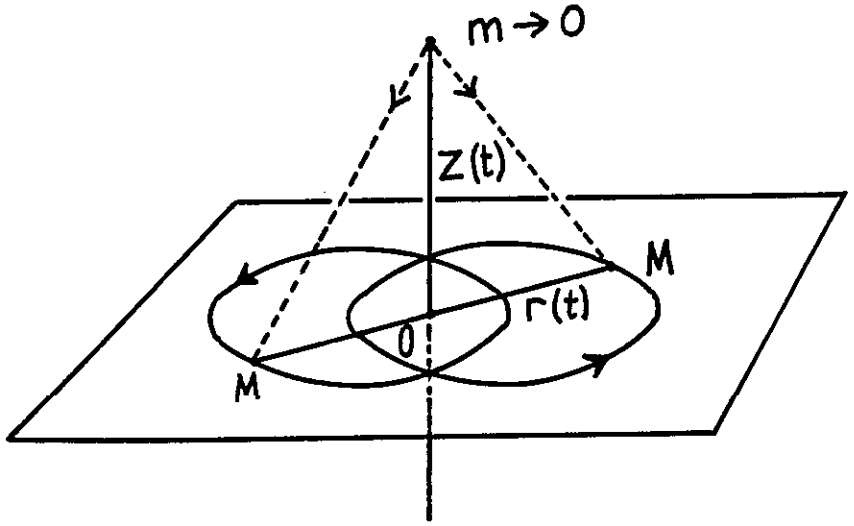

Fig. 78

Under the primaries' gravitation m's equation is

$$\frac{d^2z}{dt^2} = -\frac{z}{(z^2+r_\varepsilon^2(t))^{3/2}} , \qquad (8.18)$$

which comes from a Hamiltonian

$$H = \frac{p^2}{2} - \frac{1}{\sqrt{z^2+r_\varepsilon^2(t)}} . \qquad (8.19)$$

For the unperturbed motion ($r_\varepsilon \to r_0 = 1/2$), H(=E) is a constant of motion, and the phase plane z,p for this one-dimensional system is as shown in fig. 79.

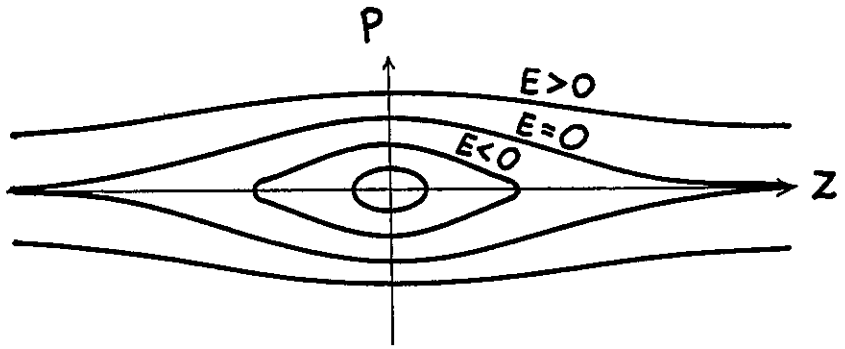

Fig. 79

E=0 separates bounded motion (E<0), in which m oscillates between the primaries with period (fig. 80)

$$T(E) = \frac{2\pi}{\omega(E)} = 4 \int_0^{(1/E^2-1/4)^{1/2}} \frac{dz}{\{2(E+(z^2+1/4)^{-1/2}\}^{1/2}} \quad -2<E<0 , \qquad (8.20)$$

from unbounded motion (E>0) in which m moves from $z = \pm\infty$ to $z = \mp\infty$. We can define a discrete mapping on $S = (z,p)$ by plotting the position and momentum of m at the discrete times

$$t_n = \{.....2,-1,0,1,2,3, ...\} , \qquad (8.21)$$

that correspond to periods of the primaries.

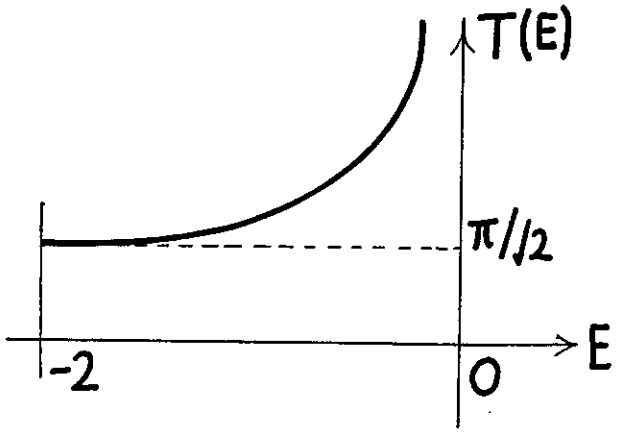

Fig. 30

For $\varepsilon=0$ the iterates of any point $X = (z,p)$ move around one of the E-invariant curves (fig. 81), making ever smaller fractions of a revolution as $E \to 0$ from below. The line $E=0$ is an invariant curve joining two unstable fixed points at $|z| = \infty$, $p=0$, each of which is a degenerate kind of hyperbolic point. When the eccentricity ε is switched on, H is no longer a constant of the motion, but the KAM theorem tells us that closed invariant curves fill most of the region near the origin $p=0$, $z=0$, and we also know that there will be small irregular regions near unperturbed orbits with rational period T (remember the perturbation has period unity). These irregular orbits are bounded however - the resonance between M's and m's motion can never catapult m to infinity - because the irregular motion is trapped (on S) between smooth KAM curves.

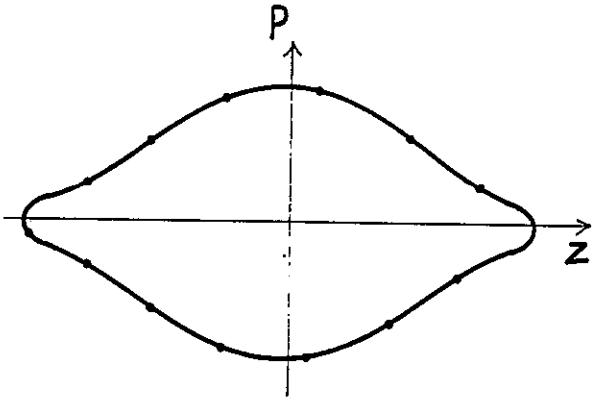

Fig. 81

The situation is however very different near E=0, where the unperturbed motion is itself unstable. We define an integer sequence from our mapping as follows: let t_k be the times of zeroes of any solution z(t) (i.e. times when m crosses the primaries' plane). Without loss of generality we can take $0 < t_0 < 1$. Then we define the doubly infinite integer sequence $\{S_k\}$

$$S_k \equiv \text{integer part of } t_{k+1} - t_k,\ z(t_k) = 0\ . \qquad (8.22)$$

Thus S_k measures the number of iterations of the mapping between successive zero-crossings of z(t). What Sitnikov and Alexseev showed was this: given any small ε, a motion z(t) can be found that corresponds to *any* sequence $\{S_k\}$ provided all S_k exceed some number $m(\varepsilon)$. As $\varepsilon \to 0$, $m(\varepsilon) \to \infty$ so that the erratic orbits (random $\{S_k\}$) whose existence this result implies (fig. 82) are concentrated in narrow regions near E=0.

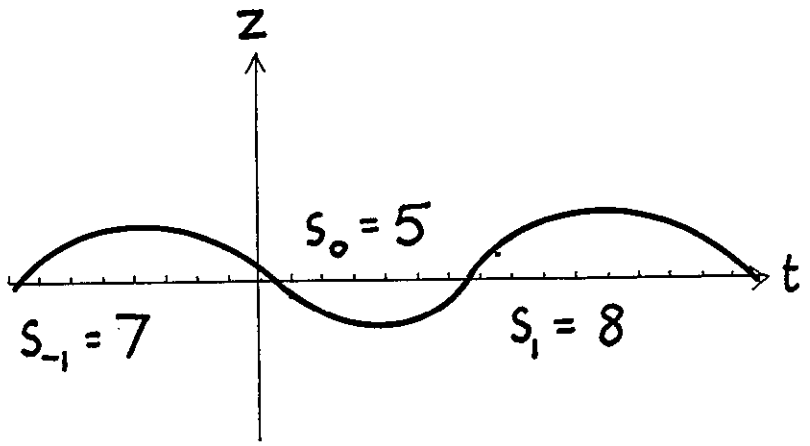

Fig. 82

An important feature of this result follows from the existence of sequences $\{S_k\}$ with one or two S_k equal to infinity. These correspond to "escape" orbits, which oscillate infinitely often before z becomes infinite (fig. 83),

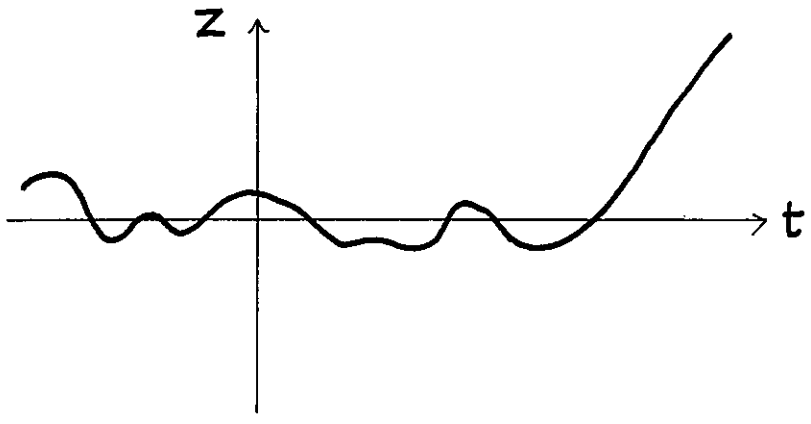

Fig. 83

or "capture" orbits, which fall in from infinity and then oscillate infinitely often (fig. 84),

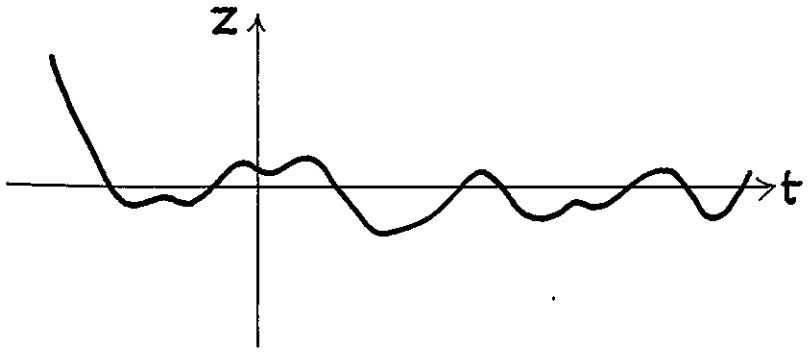

Fig. 84

or "capture and escape" orbits, where m falls in from infinity, oscillates arbitrarily often and then escapes (fig. 85).

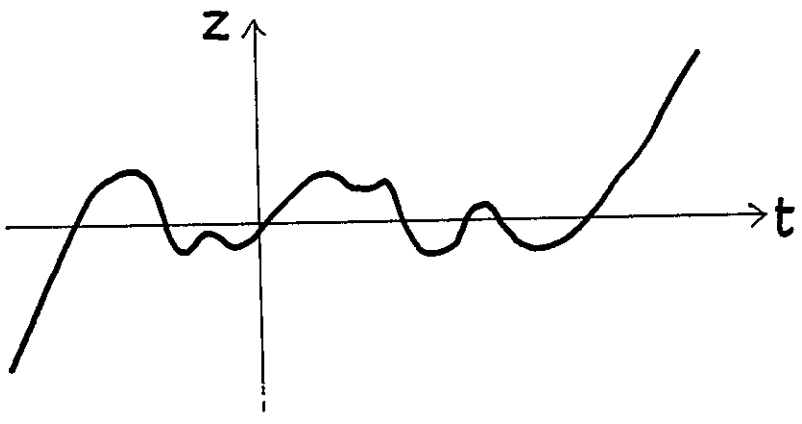

Fig. 85

Of course, the S_k can be totally *random* (provided $S_k > m(\varepsilon)$), so once again we have "stochasticity within determinism". These results apply also for large perturbations ε.

Our second example is the *swing*. The unperturbed case, and associated invariant curves, was considered in section 2. The perturbed case has the swing periodically excited by varying the length ℓ with period unity:

$$\ell \to \ell_0(1 + \varepsilon \cos 2\pi t) \ . \tag{8.23}$$

The map on the plane $S = \{q,p\}$ is defined by the p and q at integer times t. When $\varepsilon \neq 0$ the Hamiltonian (2.20) is no longer a constant of the motion and the system is nonintegrable. Nevertheless, invariant curves still exist except where the period

$$T = 2R\ell \int_{-\pi}^{\pi} \frac{dq}{\sqrt{\frac{2}{m\ell^2}(E+mg\ell \cos q)}} \ , \ E < mg\ell \ , \tag{8.24}$$

is nearly rational. The irregular motions in these "gaps" are limited in amplitude except near $E=mg\ell$ which corresponds to the unperturbed orbit with a hyperbolic fixed point at $q=\pm\pi$ (fig. 86). Here it is possible to define arbitrary sequences $\{S_k\}$ as in (8.22) with q replacing z. Thus S_k measures the integral part of the time in-

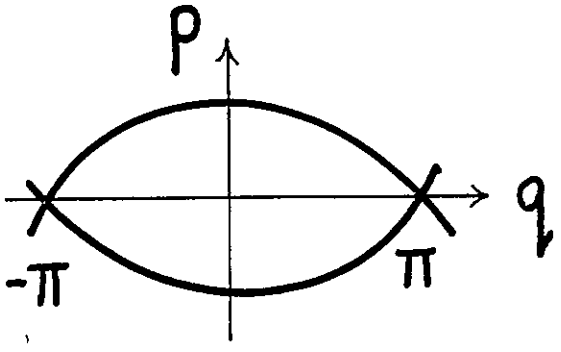

Fig. 86

terval between t_k and t_{k+1} when the swing is momentarily at rest. By analogy with the previous case it is likely that any sequence $\{S_k\}$ with $S_k > m(\varepsilon)$ corresponds to an orbit. In this problem, however, the topology of motion is different and suggests defining a new sequence $\{r_k\}$ by

$$r_k = \text{integer part of } |q(t_{k+1})-q(t_k)|/2\pi \ ; \qquad (8.25)$$

then r_k gives the number of rotations per libration. For the unperturbed swing $r_k = 0$ if $E < mg\ell$ and $r_k = \infty$ if $E > mg\ell$; it would be interesting to know whether r_k can take on a "stochastic" range of values when $\varepsilon \neq 0$, for energies near $mg\ell$.

These strongly irregular motions occur for E near $mg\ell$ - the unstable case. It is amusing to look at the perturbed swing motion *near equilibrium* ($E = -mg\ell$), where the unperturbed motion of q(t) is like a harmonic oscillator. Then (2.22) becomes, when linearized

$$\ddot{q}(t) + \frac{g}{\ell_0}(1-\varepsilon \cos 2\pi t)q(t) = 0. \qquad (8.26)$$

This is Mathieu's equation, better known to physicists as Schrödinger's equation for an electron in a one-dimensional solid with sinusoidal potential with unit spatial period. The "wave function" is

$$q(t) = e^{ikt} \times \text{periodic function of } t,$$

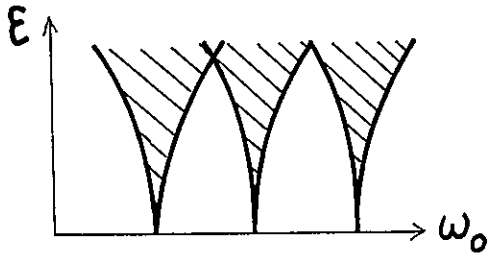

Fig. 87

where k is real except for "energies" g/ℓ_0 in the nearly-free-electron "band gaps" (fig. 87) centered on

$$\frac{g}{\ell_0} \equiv \omega_0^2 = \left(\frac{n}{2} \times 2\pi\right)^2 . \qquad (8.28)$$

In these gaps, k is imaginary and e^{ikt} can grow exponentially - the swing's equilibrium is *unstable* and its deflection grows exponentially. What has happened is that for these unperturbed equilibrium frequencies ω_0 the elliptic fixed point at the origin of (q,p) has eigenvalues near ± 1, i.e. is nearly *parabolic*, and so is easily converted into a hyperbolic fixed point. For small ε the real, nonlinear problem has invariant curves near q=p=0 so that the exponential instability is soon quenched - the swing's frequency is no longer ω_0 and the resonance is lost. Children don't know this, but they automatically adjust the frequency (of altering the length ℓ) to suit the "local" unperturbed frequency, and this nongeneric perturbation beats the KAM theorem! A dramatic example of this "adaptive pumping" occurs at the shrine of Santiago de Campostella in Spain, where according to H. Pomerance, pilgrims get incense to burn by swinging a brazier hanging from the ceiling, increasing the amplitude to about 180° by shortening and lengthening the supporting rope (fig. 88).

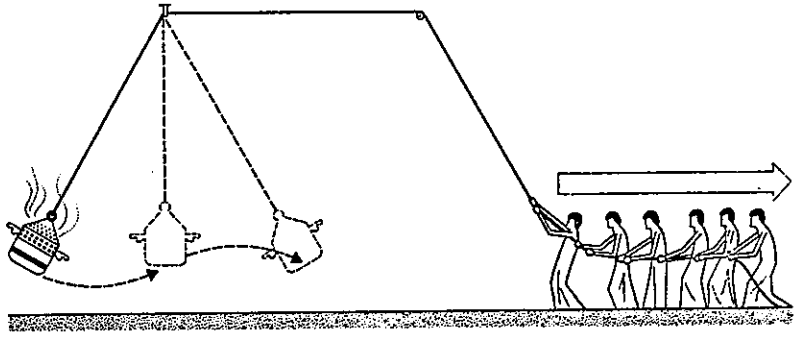

Fig. 88

Our final example is the *collision of a rigid-rotor molecule with a surface*. The molecule is a dumbbell with length d and two equal masses m/2, with centre of mass at height z above the surface, with which each mass interacts according to a Lennard-Jones type of potential U(z) (fig. 89).

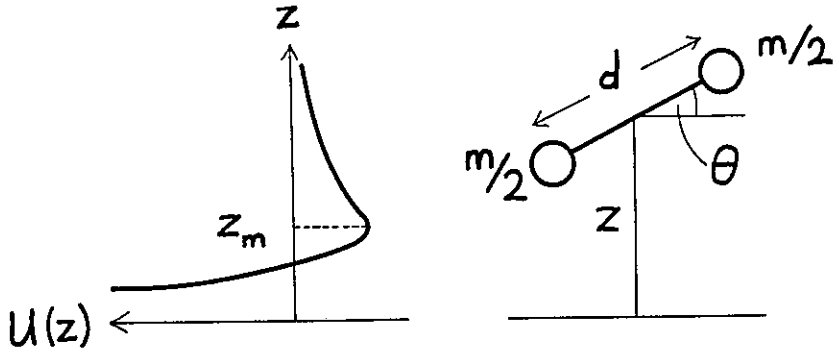

Fig. 89

This problem has two degrees of freedom, z and the dumbell's angle θ. Consideration of the forces and torques acting leads to the following Hamiltonian for small d:

$$H = \frac{p_z^2}{2m} + 2U(z) + \frac{2p_\Theta^2}{md^2} + \varepsilon \frac{U''(z)d^2}{4} \sin^2\Theta \,. \qquad (8.29)$$

The last term is the perturbation, describing the torque exerted by the surface. $\varepsilon \to 0$ describes the gradual switching-off of this torque (e.g. by sphericising the dumbbell). We take the surface of section as $S_z = \{a, p_z\}$ defined by $\Theta = 0$ (molecule parallel to the reflecting surface). H(=E) is always a constant of the motion, fixed on S_z.

When $\varepsilon = 0$ (unperturbed case), p_Θ is a constant of the motion too (unhindered rotation), and S_z is covered by invariant curves whose

equation is

$$P_z = \pm \{(E - 2U(z) - 2P_\Theta^2/md^2)2m\}^{1/2} , \qquad (8.30)$$

sketched in fig. 90 for some positive E.

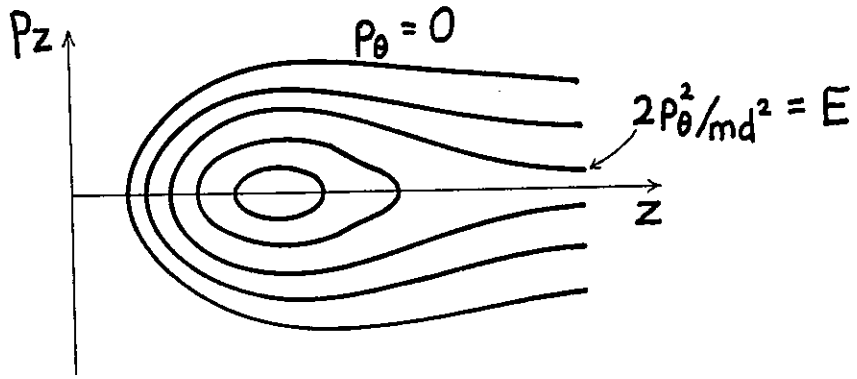

Fig. 90

Once again there is a quasi-hyperbolic fixed point at infinity (cf. Sitnikov's problem), when $2p_\Theta^2/md^2 = E$. The "rotation number" $\alpha(P_\Theta)$ of this mapping is (cf. 7.3)

$$\alpha(P_\Theta) = \frac{\omega_z}{\omega_\Theta} = \frac{\pi\, md^2}{2p_\Theta \mathrm{Re} \int_0^\infty dz/\{\frac{2}{m}(E - 2U(z) - 2p_\Theta^2/md^2)\}^{1/2}} , \qquad (8.31)$$

which vanishes at the "escape" critical angular momentum $|p_\Theta| = d\sqrt{mE/2}$ (fig. 91).

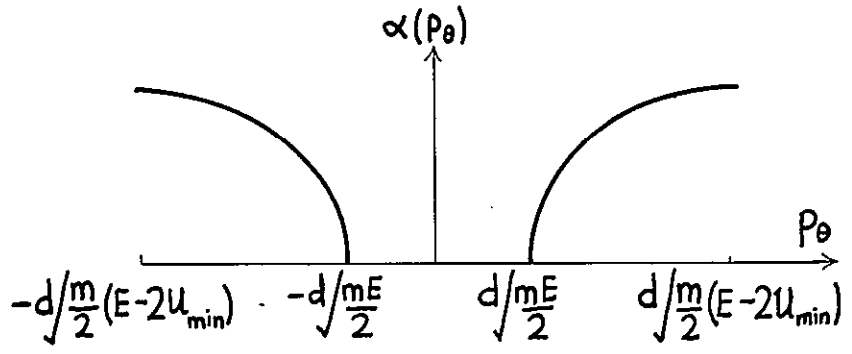

Fig. 91

When $\varepsilon \neq 0$ we once again expect strongly irregular behavior near the p_Θ corresponding to escape for the given E. An interesting integer sequence is again $\{r_k\}$ of (8.25), with q replaced by θ and t_k denoting the k'th crossing of the potential minimum z_m by the molecule. Then an infinity in the sequence $\{r_k\}$ would correspond to escape (capture) of the molecule by the surface, preceded (succeeded) by oscillatory trapping in the well of U(z). Rigorous statements about $\{r_k\}$ and similar sequences would be very useful in surface physics, where questions of capture and escape are studied largely by computations which, in view of the probably pathological dependence on initial conditions, are difficult to interpret.

Perhaps the most striking aspect of these modern developments in mechanics is the detailed understanding of the way in which stochastic elements enter into the motion of systems governed by causal equations. It is instructive to end this section by quoting from an essay written by Maxwell in 1873, showing how sophisticated was his philosophical thinking on these matters.

"It is a metaphysical doctrine that from the same antecedents follow the same consequents. No one can gainsay this. But it is not of much use in a world like this, in which the same antecedents never again concur, and nothing ever happens twice...

The physical axiom which has a somewhat similar aspect is 'that from like antecedents follow like consequents.' But here we have passed from sameness to likeness, from absolute accuracy to a more or less rough approximation. There are certain classes of phenomena

... in which a small error in the data only introduces a small error in the result ... The course of events in these cases is stable.

"There are other classes of phenomena which are more complicated, and in which cases of instability may occur, the number of such cases increasing, in an extremely rapid manner, as the number of variables increases...

"....Every existence above a certain rank has its singular points: the higher the rank, the more of them. At these points, influences whose physical magnitude is too small to be taken account of by a finite being, may produce results of the highest importance ...

"If, therefore, those cultivators of physical science from whom the intelligent public deduce their conception of the physicist... are led in pursuit of the arcana of science to the study of the singularities and instabilities, rather than the continuities and stabilities of things, the promotion of natural knowledge may tend to remove that prejudice in favor of determinism which seems to arise from assuming that the physical science of the future is a mere magnified image of that of the past."

9. SEMICLASSICAL QUANTUM THEORY FOR NONINTEGRABLE SYSTEMS

In a general context, all of the complicated classical behavior that we have described must be regarded as the limiting behavior of the corresponding quantal system when Planck's constant $\hbar$ is negligible. Now in this last section we shall discuss some of the largely unsolved problems arising when $\hbar$ is not negligible but is small enough (in comparison with classical quantities of the same physical dimension) for us to hope that the quantal behavior can be understood in terms of the classical behavior. In other words we intend to discuss "semiclassical mechanics". For simplicity the treatment here will be restricted to *bound* quantum and classical systems, where the main problem is the determination of semi-classical energy levels. This is not a problem that can easily be left to a computer, because of the interaction between numerical noise and the increasingly fine scale of oscillation of wave functions as $\hbar \to 0$.

For *integrable systems* the problem is well understood and the levels are given explicitly by a quantum condition best expressed with the action-angle formalism explained in Section 2, as follows. Let the energy levels in an N-dimensional system be labelled by N quantum numbers $\underline{m} \equiv (m_1 \ldots m_N)$. Then the $\underline{m}$'th bound state is associated with a *particular torus* $\underline{I}_{\underline{m}}$, and its energy $E_{\underline{m}}$ is given by the Hamiltonian (2.14) expressed in action variables:

$$E_{\underline{m}} = H(\underline{I}_{\underline{m}}) \ . \tag{9.1}$$

The quantized tori $\underline{I}_{\underline{m}}$ lie on the points of a lattice in the N-dimensional $\underline{I}$ space whose unit cells have side length $\hbar$. The only subt-

lety is that the origin of the lattice is usually not at the origin of $\underline{I}$ space, so that

$$\underline{I}_{\underline{m}} = (\underline{m} + \underline{\alpha}/4)\hbar \ , \tag{9.2}$$

where $\alpha \equiv (\alpha_1..\alpha_1...\alpha_N)$ describes this displacement. The numbers α_i are integers equal to the number of "turning points" of the projection onto $\underset{\sim}{q}$ space of the i-th irreducible circuit γ_i of the torus $\underline{I}_{\underline{m}}$, i.e. the number of places on γ_i where the torus is "normal" to the $\underline{q}$ space. On the schematic fig. 92, for example, $\alpha_1 = 0$ ("rotation") and $\alpha_2 = 2$ ("libration").

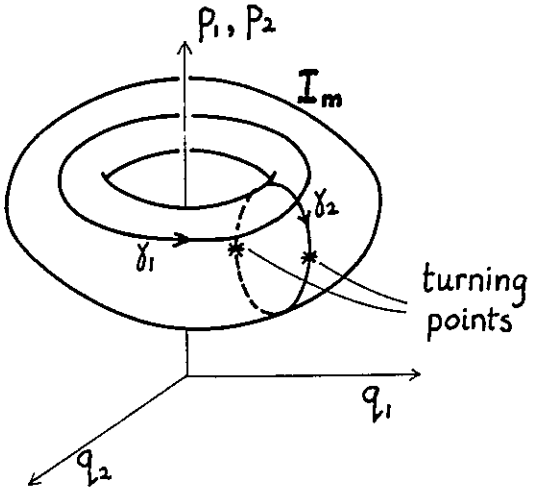

Fig. 92

The quantum condition (9.1)-(9.2) generalizes the old rules of Bohr and Sommerfeld. Perhaps the easiest way to obtain it is by demanding single-valuedness of the simplest W.K.B. wave function obtained by solving the time-independent Schrödinger equation to lowest orders in $\hbar$. This gives a travelling wave at any point q and hence corresponds to just one of the possible intersections in phase space of the manifold $\underline{q}$=constant with the torus $\underline{I}$ to which the wave function corresponds. This "local" W.K.B. wave is

$$\psi(\underline{q},\underline{I}) = C(\det \frac{\partial^2 S(\underline{q},\underline{I})}{\partial q_i \partial I_j})^{1/2} \ e^{\frac{i}{\hbar} S(\underline{q},\underline{I})} \tag{9.3}$$

where $S(\underline{q},\underline{I})$ is the action integral (2.6) with the constants $\underline{f}$ chosen as $\underline{I}$, and C is a constant. After going around γ_i the action S in (9.3) has acquired an increment of $2\pi I_i$ (cf. equation 2.13). However this is not the only source of change in ψ, because the determinant becomes infinite at turning points on γ_i. To see this, realize that (2.15) implies

$$\det \frac{\partial^2 S}{\partial q_i \partial I_j} \sim [\text{Jacobian}(\frac{\partial \underline{q}}{\partial \underline{\theta}})]^{-1} \tag{9.4}$$

The Jacobian vanishes at turning points on γ_i, and if the α_i such zeroes are simple each contributes a factor $e^{i\pi}$, so that the total phase increment of ψ round γ_i is

$$\frac{2\pi I_i}{\hbar} - \frac{\alpha_i \pi}{2} . \tag{9.5}$$

For ψ to be single valued this must equal $2\pi m_i$, where m_i is an integer, and (9.2) follows at once.

It must be emphasized that the frequencies $\underline{\omega}$ (equation 2.36) play no part in the quantum conditions. In particular, *closed orbits*, corresponding to tori $\underline{I}$ for which the ω_i are commensurable, will in general not be selected by equation 9.2. Therefore it is false (at least for integrable systems) to claim as some authors have done that quantum states are associated with closed orbits around which the action is an integer times $\hbar$. However, the closed orbits do play a most interesting role in determining the density of states function

$$n(E) \equiv \sum_{\underline{m}} \delta(E-E_{\underline{m}}) . \tag{9.6}$$

This can be transformed, using the quantum condition, into a representation of n(E) as a sum over all topologically different closed orbits (i.e. all "rational" tori). But each closed orbit gives not a set of levels but an oscillatory contribution to n(E); the more complicated closed orbits (high-order rational tori) give faster oscillations. As more and more closed orbits are included in this "topological sum" sharp peaks begin to appear and eventually turn into the delta functions corresponding to the energy levels.

What if the quantum system is classically *nonintegrable*? There will of course still be energy levels, and it is not hard to show that on the average, each level occupies a volume h^N in phase space, so that the average density of states $\bar{n}(E)$ is

$$\bar{n}(E) \equiv \lim(\Delta E\to 0)\lim(\hbar\to 0) \int_{\frac{-\Delta E}{2}}^{\Delta E/2} dE' n(E+E') = \frac{1}{h^N} \int\int d\underline{q}\, d\underline{p}\, \delta(E-H(\underline{q},\underline{p})). \tag{9.7}$$

But the levels can no longer be located by (9.1) and (9.2) because in nonintegrable systems the whole basis of the quantum conditions breaks down. This is because in the "irregular" regions of phase space, near unstable closed orbits, tori $\underline{I}$ do not exist, and therefore the quantum numbers $\underline{m}$ cannot be defined. As long ago as 1917 Einstein realized that semiclassical quantum mechanics must be very different for integrable and nonintegrable systems. He saw a contradiction in theoretical physics as it then existed, that the (integrable) systems which could be quantized at that time, and the (nonintegrable) systems to which statistical mechanics could be applied, fell into two mutually exclusive classes. He expressed the hope, soon to be justified, that a properly formulated quantum mechanics would remove this contradiction. These prescient remarks seem to have been ignored until 1973, when Percival pointed out that in the light of the much deeper understanding of classical mechanics provided by the KAM theorem etc. it was time to return to the problem recognized by Einstein.

Percival's suggestion was that the quantum levels in the regions of phase space occupied by irregular trajectories will form an *irregular spectrum*, with properties very different from the *regular spectrum* arising from those regions of phase space filled with KAM tori providing a basis for quantization according to (9.2). The two sorts of spectra would be distinguished by their behavior under perturbation - for example by an electromagnetic wave if the system is a nonsymmetrical molecule. Such a perturbation strongly couples together levels of the regular spectrum with similar quantum numbers $\underline{m}$; these coupled levels have energy differences of order $\hbar$. By contrast, under perturbation *all* levels in a given irregular region would be weakly coupled; these have the much smaller energy spacing h^N, so that the irregular spectrum is much more sensitive to perturbation than the regular spectrum, and under poor resolution might be confused with a continuous spectrum.

Apart from some exploratory computations indicating that nonintegrable systems do indeed have some energy levels that are very sensitive to perturbation, practically nothing is known about the irregular spectrum. However, it is possible on the basis of the KAM theorem to arrive at what seem to be reasonable conjectures about the way that regular and irregular regions are distributed in systems whose departure from integrability is described by a perturbation parameter ε. Let us confine the discussion to two degrees of freedom, and recall the arguments of Sections 2, 3 and 4, especially the crucial equation (4.12) giving the widths of the resonance zones, near rational tori, in which irregular orbits exist. Figure 93 illustrates the lowest-order resonance zones in the "unperturbed" $\underline{I}$ space which has been quantized according to equation (9.2) [the $\overline{1}/1$ tori for example, inhabit the locus of points in $\underline{I}$ space where the normals to the contours $H(\underline{I})=E$ lie at 45° to the $\overline{I}_1$ axis].

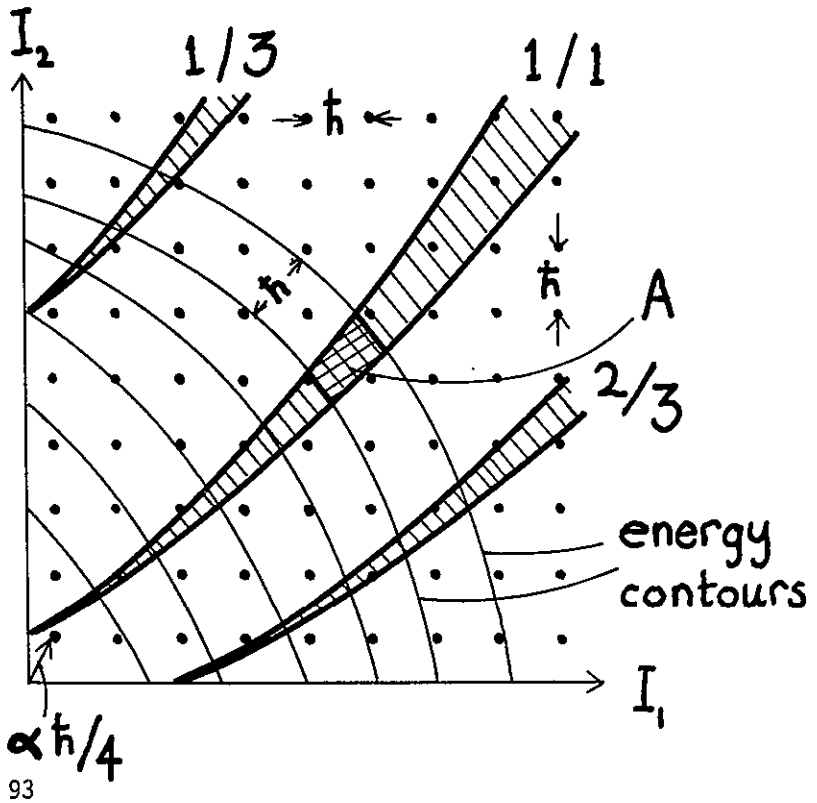

Fig. 93

I claim that the approach to the classical limit is non-uniform in ε. For fixed (small) ε there appear to be *three semi-classical regimes* as $\hbar \to 0$: These regimes are distinguished by values of a parameter β that will now be defined. Surrounding any point $\underline{I}$ is the area $\hbar^2$ corresponding to a quantum state. This area will be crossed (fig. 93) by infinitely many resonance zones, the widest of which has the frequency ratio r/s with smallest s (equation 4.12). Between two energy contours whose perpendicular separation $|\Delta \underline{I}|$ is $\hbar$ this widest resonance will occupy an action area A (fig. 93). Then β is defined as

$$\beta \equiv A/\hbar^2 \ . \qquad (9.8)$$

When β is small it is a measure of the proportion of the quantum area $\hbar^2$ occupied by irregular trajectories. Large β indicates that resonant zones near $\underline{I}$ contain many quantum states. Elementary geometry and use of (4.12) give the estimate

$$\beta \simeq \frac{\hbar \times \text{width of widest resonance}}{\bar{h}^2}$$

$$\sim \frac{\hbar \times |\underline{I}| \times \text{angular width of widest-resonance}}{\bar{h}^2}$$

$$\sim K(\epsilon)\ |\underline{I}|/\hbar s^{2.5} \ . \qquad (9.9)$$

Therefore β is large in the semiclassical limit ($\hbar$ small), and also for large perturbations ϵ, low order resonances (s small) and high excited states ($|\underline{I}|$ large).

In the *first semiclassical regime* $\hbar$ is small enough for a semiclassical treatment of the unperturbed system to be valid, but ϵ is so small that $\beta \ll 1$ for all $\underline{I}$ in the energy region of interest, even those crossed by lowest order resonances (s=1). The irregular regions occupy only a small fraction of the quantum area $\bar{h}^2$ and so do not affect the form of the quantum states $|\psi\rangle$. In effect Planck's constant $\hbar$ blurs all the pathology of the classical orbit structure. Under these circumstances quantization by tori based on equations (9.1) and (9.2) can be employed to locate the perturbed quantum levels $E_{\underline{m}}$, the actions $\underline{I}$ being approximately calculated by means of a perturbation scheme such as that discussed in Section 2.

Marking $\hbar$ smaller leads to the *second semiclassical regime*, in which β is of order unity for states whose actions $\underline{I}$ lie in the lowest resonance zones. Then there will be a few states whose quantum area is dominated by irregular trajectories. The energies of these states will still be given approximately by (9.1) with $\underline{I}$ obtained by interpolation from tori near the irregular region. However, the wave function $\psi(\underline{q})$ will no longer be given by the WKB expression (9.3) because the torus on which it is based no longer exists.

So what does such an "irregular state" look like? Since it is in phase space rather than in real space that the irregularity associated with nonintegrability manifests itself, it seems sensible to study a quantum object defined on phase space. Such an object is the Wigner function $\psi(\underline{q},\underline{p})$, defined as

$$\psi(\underline{q},\underline{p}) \equiv \frac{1}{h^{2N}} \int d\underline{q} \int d\underline{\Pi} e^{\frac{-i}{\hbar}(\underline{p}\cdot\underline{Q}+\underline{q}\cdot\underline{\Pi})} \langle\psi| e^{\frac{i}{\hbar}(\hat{\underline{q}}\cdot\underline{\Pi}+\hat{\underline{p}}\cdot\underline{Q})} |\psi\rangle \ , \qquad (9.10)$$

where $\hat{}$ denotes an operator. It is well known that this can be written in the following unsymmetrical form involving the wave function $\psi(\underline{q})$:

$$\Psi(\underline{q},\underline{p}) = \frac{1}{(\pi\hbar)^N} \int d\underline{X}\ e^{-2i\underline{p}\cdot\underline{X}/\hbar}\ \psi(\underline{q}+\underline{X})\psi^*(\underline{q}-\underline{X}) \ . \qquad (9.11)$$

For states in the "integrable" parts of phase space filled with tori the WKB wave function can be employed to take the classical limit of Ψ, with the pleasant result that the Wigner function for such a state with quantum number $\underline{m}$ condenses as $\hbar \to 0$ onto a delta function on the torus $\underline{I}_{\underline{m}}$, i.e.

$$\Psi_{\underline{m}}(\underline{q},\underline{p}) \xrightarrow{\hbar \to 0} \frac{(\underline{I}(\underline{q},\underline{p})-\underline{I}_{\underline{m}})}{(2\pi)^N} . \qquad (9.12)$$

(When $\hbar$ increases from zero $\Psi_{\underline{m}}$ develops "fringes" about the torus $\underline{I}_{\underline{m}}$ that have a characteristic "Airy function" form).

This makes it natural to conjecture that the Wigner function for an "irregular state" spreads over the corresponding irregular region in phase space, and a surface of section for the energy E of the quantum state might show a series of *randomly distributed maxima and minima* of Ψ. Figure 94 is a sketch of this conjectured behavior, to be compared with say, the inner irregular region on fig. 60. At this state we can only guess what sort of randomness

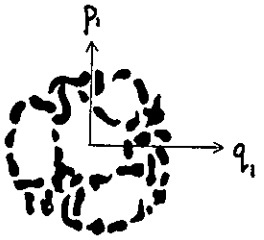

Fig. 94

Ψ will display. Probably it will be the "Gaussian" randomness studied in noise theory. It is also likely that the wave function $\Psi(\underline{q})$ in coordinate space is also of Gaussian random type for irregular states, with the mean intensity falling to zero at 'anticaustics' on the boundary of the region in $\underline{q}$ space explored by the orbit. This morphology of Ψ contrasts strongly with that for regular states, which have strong patterns of maxima and minima near intense caustics at the classical boundaries.

Further diminishing $\hbar$ leads to the *third semiclassical regime* which is the semiclassical limit proper. Now β is large for $\underline{I}$ in all lower-order resonance zones. The corresponding irregular regions in phase space will be densely populated with quantum states; in other words the lattice spacing in fig. 93 gets so small that each zone contains many lattice points. The group of states in each irregular region cannot now be individually labelled with quantum numbers although they may be said to share a "vague quantum number" corresponding to the destroyed region $\underline{I}$ in unperturbed action space.

Quantization by tori cannot now be applied in any sense. The Wigner function Ψ for any single state will presumably spread over the whole irregular region of the energy shell, and the surface of section is conjectured to resemble fig. 94 but with a much finer granularity in the randomness.

This does not exhaust the description of the generic structure of the third semiclassical regime, because there will be points $\underline{I}$ in high-order resonance zones where β is of order unity, and points $\underline{\underline{I}}$ in still higher-order zones where β is small. Therefore along with the groups of "irregular states" just described there will also be states of the type described for the first and second regimes. What seems to be happening is that the smaller values of $\bar{h}$ expose more of the *infinite heterogeneity of the classical orbit structure* so that the quantum states become more varied in nature as well as more numerous.

When ε is zero this heterogeneity of structure is absent, because the system is integrable and there are no irregular regions; Wigner's function Ψ for every state is a "fringed torus". When ε is large this heterogeneity is also absent, because the resonant zones have expanded and eaten away all the tori and all motions are irregular; Wigner's function for every state should now be disordered and spread all over the energy shell in phase space. Fig. 95 summarizes this picture of the generic structure of the semiclassical limit.

My opinion is that the full elucidation of the nature of irregular states and of the mingling of regular and irregular states as ε and $\bar{h}$ vary will require the development of new conceptual and mathematical tools. Perhaps Wilson's celebrated "renormalization group" technique recently developed to study disorder on all scales in statistical mechanics might play some part.

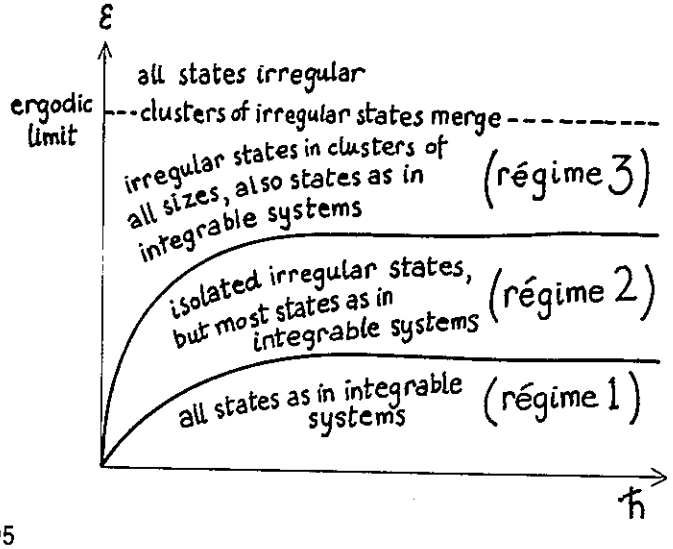

Fig. 95

REFERENCES

1. ARNOL'D, V. I., Russian-Mathematical Surveys 18, No. 6, 85-191 (1963), "Small Denominators and Problems of Stability of Motion in Classical and Celestial Mechanics".
2. ARNOL'D, V. I. and AVEZ, A., Ergodic Problems of Classical Mechanics (Benjamin, W., (1968)).
3. BERRY, M. V., Phil. Trans. Roy. Soc. (London), A287, 237-71 (1977), "Semiclassical Mechanics in Phase Space: a Study of Wigner's Function" J. Phys. A10, 2083-2091 (1977) "Regular and Irregular Semiclassical Wave Functions".
4. BORN, M., The Mechanics of the Atom (Ungar, New York, 1960).
5. BRILLOUIN, L., Scientific Uncertainty, and Information Theory, Part 2 (Academic Press, New York (1964)).
6. CAMPBELL, L. and GARNETT, W., The Life of James Clerk Maxwell (Macmillan Co., London, 1882).
7. CHIRIKOV, B. V., "Research Concerning the Theory of Non-linear Resonances and Stochasticity", Translation 71-40 CERN, Geneva, (1971).
8. EINSTEIN, A., Verh. Dt. Phys. Ges. 19, 82-92, (1917), "Zum Quantensatz von Sommerfeld und Epstein".
9. EMINHIZER, C. R., HELLEMAN, R. H. G. and MONTROLL, E. W., J. Math. Phys., 17, 121-140, (1976), "On a Convergent Nonlinear Perturbation Theory Without Small Denominators or Secular Terms".
10. FORD, J., "The Statistical Mechanics of Classical Analytic Dynamics" in Fundamental Problems in Statistical Mechanics III', edited by Cohen (North-Holland, Amsterdam 1975), 215-255.
11. FRANKLIN, F., in "The Rings of Saturn", Palluconi and Pettengill, Eds., NASA SP-343 (1974).
12. HÉNON, M., Quarterly of Applied Math. 27, 291-312, (1969), "Numerical Study of Quadratic Area-Preserving Mappings".
13. HÉNON, M. and HEILES, C., Astronomical Journal 69, 73-79 (1964), "The Applicability of the Third Integral of Motion: Some Numerical Experiments".
14. KHINCHIN, A. Ya., "Continued Fractions" (Univ. of Chicago Press, 1964).
15. MOLCHANOV, A. M., Icarus 8, 203-215, (1968), (see also, 11, 88-113) "The Resonant Structure of the Solar System".
16. MOSER, J., Mem. Am. Math. Soc. 81, 1-60 (1968), "Lectures on Hamiltonian Systems".
17. MOSER, J., "Stable and Random Motions in Dynamical Systems", Princeton University Press, (1973).
18. PERCIVAL, I. C., J. Phys. B. 6, L229-232 (1973), "Regular and Irregular Spectra".
19. PERCIVAL, I. C., Adv. Chem. Phys., 36, 1-61 (1977), "Semiclassical Theory of Bound States".

N. B. In most cases works by Soviet authors appeared earlier in Russian.